# MODELING THE CIRCADIAN REGULATION OF HPA AXIS ACTIVITY

By

ROHIT T. RAO

A dissertation submitted to the:

School of Graduate Studies

Rutgers, The State University of New Jersey

In partial fulfillment of the requirements

For the degree of

Doctor of Philosophy

Graduate Program in Chemical and Biochemical Engineering

Written under the direction of

Ioannis P. Androulakis, Ph. D.

And approved by:

_____

_____

_____

_____

New Brunswick, New Jersey

October, 2018

# ABSTRACT OF THE DISSERTATION

Modeling the Circadian Regulation of HPA Axis Activity

By ROHIT T. RAO

Dissertation Director:

Ioannis P. Androulakis

The hypothalamic-pituitary-adrenal (HPA) axis constitutes the primary physiological stress response mechanism, with cortisol (corticosterone in rodents) being the major effector molecule of the HPA axis, mediating an array of metabolic and immune-modulatory functions. The circadian dynamics of the mediators of HPA axis are considered to significantly modulate their functional characteristics and demonstrate remarkable plasticity. This is observed in pathological conditions where circadian disruption is often associated with disease etiology, as in the case of chronic inflammatory conditions such as rheumatoid arthritis, as well as in physiological conditions, where the presence of significant sex differences in numerous aspects of the HPA axis, including both basal circadian activity as well as in its response to physiological stressors is well established. It is widely suggested that the mechanisms that dictate the rhythmic properties of the HPA network might also contribute to its functioning in both physiological and pathological conditions. For example, the sex differences in the circadian dynamics of the HPA axis are thought to contribute to the observed sex disparity in the development of a variety of autoimmune and infectious diseases. Moreover, an understanding of these underlying mechanisms is critical to development of pharmacological approaches that can appropriately treat HPA axis

disorders. Mathematical modeling provides a promising approach to study physiological feedback systems such as the HPA axis, and enables the evaluation of the feasibility of hypotheses, by providing a phenomenological framework for explaining empirical observations as well as making testable predictions. In this work we develop semi-mechanistic mathematical models of the HPA axis to understand the critical regulatory mechanisms that contribute to its functioning in health and disease. In the first aim we develop a mathematical model for the progression of collagen-induced arthritis that evaluates the effect of chronic elevation on the proinflammatory cytokines on the circadian dynamics of corticosterone and important markers of disease activity such as paw edema, thus emphasizing the importance of accounting for circadian rhythms in models of chronic inflammation. Subsequently, we study how differences in the regulatory features of the HPA network might lead to basal variability, with a focus on sex-specific and individual differences in its activity. In doing so, we predict that the host can employ diverse regulatory mechanisms to maintain glucocorticoid circadian rhythms within strict physiological bounds, ultimately resulting in the existence of trade-offs between multiple functional characteristics of the HPA axis. Furthermore, we characterize specific chronic stress-induced allostatic adaptations in the regulatory dynamics of the HPA axis. Finally, through mathematical modeling, we determine how an understanding of the circadian dynamics of the HPA axis could be leveraged for the design of chronotherapeutic dosing regimens to minimize the incidence of adverse effects associated with chronic glucocorticoid therapy.

# Acknowledgements

I am grateful to my advisor Ioannis P. Androulakis for his guidance, encouragement, and patience. I could not have completed this work without his unwavering support. I thank my thesis committee for their continued support. I thank Alison, Seul-A, Megerle, Kamau and Clara for being the most supportive friends and colleagues one could wish for. I thank Sanjana and my family for their abiding support and encouragement; I dedicate this work to you.

# Table of Contents

# List of Illustrations

# CHAPTER 1:Background and Motivation

## 1.1 HPA Axis Rhythms

Despite phylogenetic diversity, nearly all organisms are equipped with elaborate intrinsic timing mechanisms, which enable them to optimally adapt to cyclical changes in their environment brought about by earth's continual periodic revolution around the sun (1). Circadian clocks have been found in both single-cell prokaryotes such as cyanobacteria as well as in eukaryotes and multicellular organisms ranging in complexity from drosophila and zebrafish to mammals (2). While there are differences between the phyla in the specific genes constituting the circadian clock, all circadian clocks seem to have a related genetic architecture composed of an autoregulatory feedback loop consisting of positive and negative elements. Importantly, the circadian clock network results in self-sustained, cell-autonomous oscillations (3,4). It is widely believed that this enables organisms to optimize their physiology and behavior in order to anticipate periodic changes in environment, which is expected to confer improved fitness in comparison to passively reacting to environmental changes. Additionally, the circadian oscillators optimize the activation of physiological networks so as to enable the temporal separation of chemically and energetically incompatible pathways (5).

Since, light can penetrate and directly influence cellular gene expression in single-cell organisms such as algae and fungi, as well as in all the tissues of simple animals such as drosophila and zebrafish, these organisms have evolved largely decentralized circadian clock mechanisms (6). However, more complex species have evolved a more centralized, hierarchical circadian system (6). In mammals, including humans, the seat of the central circadian clock is localized to the central nervous system (CNS), specifically, the

hypothalamic suprachiasmatic nucleus (SCN). While nearly all mammalian cells harbor their own cell-autonomous circadian clocks, current evidence suggests that it is the central circadian pacemaker located in the SCN that synchronizes these numerous "peripheral" clocks to environmental signals (3). The SCN, comprised of approximately 20,000 neurons, receives photic input from the retina via the retinohypothalamic tract, which results in the activation of cAMP-responsive element binding protein, (CREB) leading to subsequent activation of the canonical circadian gene Period, thereby modulating the phase of the molecular clock in the SCN neurons (3). The SCN then relays this photic phase information to the peripheral clocks by modulating the activity of systemic neuronal, and humoral signaling cues (3).

The glucocorticoid (GC) hormones released by the hypothalamic-pituitary-adrenal axis, constitute one of the primary routes by which circadian information from the SCN in distributed to the peripheral clocks (1). Adrenal glucocorticoids have a diverse array of effects, from modulating metabolic and immune signaling, to influencing host behavior. For example, GCs promote the breakdown of carbohydrates, inhibit gluconeogenesis, limit subsequent energy storage by modulating lipid deposition and storage, and inhibit the production of a number of immune processes, including the production of proinflammatory cytokines (7). Moreover, GCs are able to modulate blood pressure, bone resorption, and regulate progression through mitotic cycle. The basal concentrations of GCs vary in a predictable time-of-day dependent manner across the light/dark cycle (8). In humans and other diurnal species, basal circadian profiles of ACTH and cortisol exhibit a peak in activity in the early morning hours, while the opposite is true in nocturnal animals, which exhibit a peak just before the onset of the

nocturnal active phase. These rhythms are generally very robust in humans as well as nocturnal rodents, with the nadir levels of GC nearing the detection limits of most assays. The circadian rhythmicity of GCs is considered to play an important role in the optimal fuel allocation of energetically intensive processes, with high GC levels during the active phase, facilitating energy allocation to the brain, muscles, and immunosurveillance, while the nadir levels during the inactive phase, results in decreased immune inhibition, facilitating the activation of the immune system (7,9).

Additionally, the HPA along with the sympathetic branch of the autonomic nervous system constitutes the primary stress response mechanism of the host. The basal and stress responsive activity of the HPA axis are regulated by a carefully balanced signaling network, composed of feed-forward and feedback mechanisms (6). The stress response, initiated via several afferent neural pathways including those from the limbic and brain-stem structures, results in release of corticotrophin-releasing hormone (CRH) and arginine vasopressin from the neurons in paraventricular nucleus (PVN) into portal circulation. Through the portal vessels, CRH and AVP reach the pituitary and bind to their specific receptors, CRH receptor 1, (CRHR1) and AVP 1B binding receptor (V1bR) respectively, which results in the release of ACTH. The binding of ACTH melanocortin-type 2 receptor, which activates a signaling cascade that ultimately results in the release of the GCs, primarily cortisol in humans and corticosterone in rodents. Unlike the peptide hormones, CRH, AVP and ACTH, which are released upon receptor-dependent activation, GCs are synthesized de novo in the pituitary upon activation of the signaling cascade by ACTH. Finally, the GC released from the pituitary, in addition to mediating

their physiological effects, also negatively feedback on the HPA axis, by inhibiting the release of ACTH and CRH from the pituitary and PVN respectively (10).

## 1.2 Differences in the Basal Activity of the HPA Axis

GC circadian rhythms and HPA axis activity in general, exhibit remarkable plasticity in a variety of physiological conditions such as pregnancy and across the menstrual cycle as well as exhibit significant inter-individual variability. There are conspicuous sex differences in basal GC secretion. Basal corticosterone secretion in female rats is significantly enhanced in comparison to male rats (11,12). Moreover, female rats also release greater amounts of corticosterone in response to psychological and immune stressors. Gonadal steroids have major effects on the circadian and ultradian rhythmicity of the HPA axis. Gonadectomy in pre-pubertal and adult male rats, which results in a sharp decrease in circulating testosterone levels, leads to an increased secretion of basal ACTH and corticosterone levels (13). In contrast, gonadectomy in female rats leads to a decrease in overall corticosterone to levels observed in male rats (12). Furthermore, corticosterone levels in females vary with the stages of the estrous cycle (14). Rats in the diestrous phase of the estrous cycle, when estrogen levels are at their lowest, have corticosterone levels that are comparable to those in male rats, whereas rats in the proestrous phase when estrogen levels peak, have corticosterone circadian rhythms that are almost twice as pronounced as those in male rats. Given these observations, it is generally hypothesized that estrogen and testosterone mediate their influence on the HPA axis by modulating the strength of negative feedback and sensitivity of the HPA signaling network.

Furthermore, the mechanisms by which gonadal steroids contribute to sex differences in the basal activity of the HPA axis might also contribute to the observed sex differences in its response to stress. GC circadian dynamics are important determinants of the stress response. The relationships between the time of stress exposure and the extent of the HPA axis response have received much attention. Experimental and modeling results both suggest that there is a facilitated corticosterone stress response during the rising phase of the GC circadian rhythm in comparison to the declining phase, where the stress response in relatively inhibited. Gonadal steroids also manipulate the stress-responsiveness of the HPA axis (15). Female rats have a much more pronounced corticosterone response to immunological challenges as well psychological stressors, such as noise stress. Additionally, ovariectomy blunts the stress response in female rats, resulting in a stress response that is similar to that of male rats (11,16). Elucidation of the feedback processes contributing to such differences in basal circadian activity could provide insight into the mechanisms contributing to the observed disparity in a number of stress-related and immune disorders between males and females.

In addition to the substantial sex differences in HPA axis activity, there is significant within-sex inter-individual variation in the regulation and stress-responsive functioning of the HPA axis. This inter-individual variation is not simply a result of a noisy system, but is considered to arise from underlying differences in the regulatory mechanisms of the HPA axis (17). These differences in regulation of the HPA axis are also thought to contribute to the apparent inter-individual differences in susceptibility and resilience to the development of neuropsychiatric disorders in response to chronic stress exposure (18,19). Therefore, insight into the regulatory differences between the male and

female HPA axis in the context of inter-individual variability might result in an improved understanding of its functioning and dysregulation and might suggest a rationale for better diagnostic criteria and the development of personalized therapeutic interventions.

## 1.3 Significance of the Circadian Dynamics of the HPA Axis in Pathology and in Devising Pharmacological Interventions

### 1.3.1 Chronic Activation of the HPA Axis

GC circadian dynamics are often disrupted due to behavioral and pathophysiological factors, such as shift work, chronic stress conditions, Cushing's syndrome and ageing. For example, ageing is commonly accompanied by a decrease in HPA axis amplitude, and reduced responsiveness to stressors (20,21). Similarly, chronic inflammation, a model of chronic stress, with much clinical relevance, is associated with significant disruptions in circadian activity. These disruptions have been well documented in diseases such as rheumatoid arthritis (RA), where patients with high disease severity often have a blunted cortisol circadian rhythm. Such a blunted circadian rhythm has also been observed in animal models of arthritis such as collagen- and adjuvant-induced arthritis (22). Disease symptoms in chronic inflammatory disease, especially in the case of RA, often exhibit a circadian variation, with an increase in disease severity before the onset of the active phase, which is correlated to the circadian maxima in proinflammatory cytokines levels. It is generally believed that in addition to the disrupted cortisol circadian rhythm, there is an inadequate secretion of cortisol in comparison to the ongoing inflammation, a phenomenon termed adrenal insufficiency. Therefore, there are complex interactions between the chronically elevated

proinflammatory cytokines and the HPA axis, the dynamics of which are yet to be elucidated (23,24).

On the other hand, as mentioned above, HPA axis activity is highly dynamic in nature, and exposure to low-level chronic stressors can also result in habituation or adaption to chronic stress regimen (25). Habituation to the chronic stress regimen involves a return to basal HPA axis activity upon repeated exposure to the same stressor. Such a habituating response is often deemed physiologically beneficial, as prolonged increases in the activity of the HPA axis can be deleterious to the survival of the host. However, a stress-habituated state does not indicate a return to normal physiological functioning of the HPA axis, and often a novel stressor induces a disproportionately large adrenal response. This phenomenon, termed chronic stress sensitization, has been observed in a number of investigations, studying the habituation to a variety of different stressors. Evidence suggests that there is an alteration in the HPA feedback network in response to the chronic stressor, with some studies suggesting a decrease in the glucocorticoid receptor negative feedback, while others suggest an increase in adrenal sensitivity of the HPA axis (26).

### 1.3.2 Pharmacological Manipulation of GC Circadian Rhythms

Exogenous administration of synthetic GCs is used to treat a variety of inflammatory and autoimmune disorders, such as rheumatoid arthritis. The key consideration in the administration of synthetic GCs has been to use an efficacious dose and duration of exposure that is as low as possible, in order to limit side effects of GC therapy. Excessive plasma GC levels concentrations over prolonged period of time can result in a number of side effects including weight gain, osteoporosis and hyperglycemia

(21). Furthermore, administration of synthetic GCs at supraphysiological doses often results in adrenal suppression, a reduction in endogenous cortisol production, due to the inhibitory feedback effects of GCs. Due to the temporal dynamics of the HPA axis, a time-of-day dependent response of the HPA axis to the administration of synthetic GCs has been considered. Studies investigating the chronotherapeutic administration of GCs, have revealed that administration of GCs before the onset of the rising phase, results in lower suppression of the adrenal GC production in comparison to administration during the end of the active phase (27). Clinical trials studying the effects of low-dose modified release (MR) prednisolone on RA symptoms have revealed that administration of MR prednisolone at 10 PM such that it is released at 2:00 AM results in an improvement in self-reported joint pain and early morning stiffness. In fact, a study by Kirwan et al. has shown that HPA axis activity might even be enhanced with late night low-dose MR prednisone administration resulting a higher early morning peak and lower evening minima (28).

## 1.4 Outline of Dissertation

It is evident that the circadian dynamics of the HPA axis are critical determinants of HPA axis activity and of much physiological significance. Mathematical modeling enables the development and testing of hypotheses within a quantitative framework that can provide mechanistic insight and a systems-level understanding into complex biological phenomena (29). In subsequent chapters, we will use semi-mechanistic ODE models to investigate the circadian dynamics of the HPA axis with the aim of providing an improved understanding of the possible mechanisms contributing to the observed differences in pathological and basal HPA axis activity. Chapter 2 discusses the

development of a mathematical model with the aim of identifying the types of regulation in a signaling network that can yield results that qualitatively represent the important circadian pathophysiological features of experimentally induced models of arthritis. Chapter 3 addresses the hypothesis that differential sensitivity and negative feedback within the HPA axis network lead to the observed sex differences glucocorticoid circadian rhythms. Moreover, we aim to predict specific functionally relevant adaptations that might occur in the HPA network upon exposure to chronic stress. Finally, in Chapter 4 we used a semi-mechanistic mathematical model of the HPA axis to study the influence of chronic chronopharmacological intervention on endogenous HPA axis activity.

# CHAPTER 2: Mathematical Modeling the Circadian Dynamics of the Neuroendocrine-Immune Network in Experimentally-Induced Arthritis

## 2.1 Background

Rheumatoid arthritis (RA) is a systemic, chronic inflammatory disease that is characterized by elevated proinflammatory cytokine levels, synovial inflammation and cartilage and bone loss (30). The mechanisms by which the disease is triggered are yet to be elucidated. More work has however, been done in characterizing the disease pathophysiology and understanding the mechanisms of disease progression. It has been well documented that clinical symptoms in RA patients exhibit pronounced circadian rhythms with increased pain and stiffness in the early morning hours coinciding with the start of active phase (31). This variation in disease severity is correlated with the circadian rhythms of proinflammatory cytokines. Furthermore, the hypothalamic-pituitary-adrenal (HPA) axis, a critical component of the neuroendocrine system, has been shown to modulate the secretion of proinflammatory cytokines and is thought to be an important regulator of disease activity (32). A number of investigators have hypothesized that adrenal insufficiency; the inability of the HPA axis to mount an adequate anti-inflammatory in response to ongoing chronic inflammation in RA might contribute to disease pathophysiology (33). Moreover, a disruption in the circadian rhythms of cortisol has been observed in patients with high disease activity (31). A mechanistic understanding of the complex interactions between the hypothalamic-pituitary-adrenal (HPA) axis and the proinflammatory cytokines of the immune system can provide important insights into RA pathophysiology and the optimization of

treatment regimens. In this regard, mathematical modeling has been used to support systems-level investigations aimed at understanding how circadian dynamics arising due to interactions between multiple physiological systems contribute towards overall disease pathophysiology(34).

## 2.2 Approach

In this work we discuss the development of a mathematical model in order to evaluate the dynamic interactions between the HPA axis and pro-inflammatory cytokines, and their downstream effects on paw edema, a key disease end-point in CIA. In particular, we investigate the changes in circadian rhythms of key HPA axis mediators, such corticosterone (CORT) and pro-inflammatory cytokines after induction of CIA, that ultimately result in circadian variability in paw edema. Moreover, we simulate the phenomenon of adrenal insufficiency that has been observed in both CIA as well as RA patients (33).

The model accounts for circadian variability in the expression of primary mediators of the HPA axis, proinflammatory cytokines and a critical disease endpoint in characterizing severity of experimental arthritis; paw edema. Furthermore, we account for the light-mediated entrainment of the autonomous oscillations of these neuroendocrine-immune mediators. The model builds on our previous work (35-38) and is essentially composed of three components; a central oscillatory compartment that simulates the circadian secretion of corticosterone (CORT) (37) in the HPA axis, a peripheral compartment that captures the downstream effects of secreted CORT on proinflammatory cytokine expression, and finally, a compartment that accounts for the

disease endpoints, specifically, paw edema. A schematic illustrating the various glucocorticoid and cytokine signaling pathways considered in our model is shown in Figure 1.

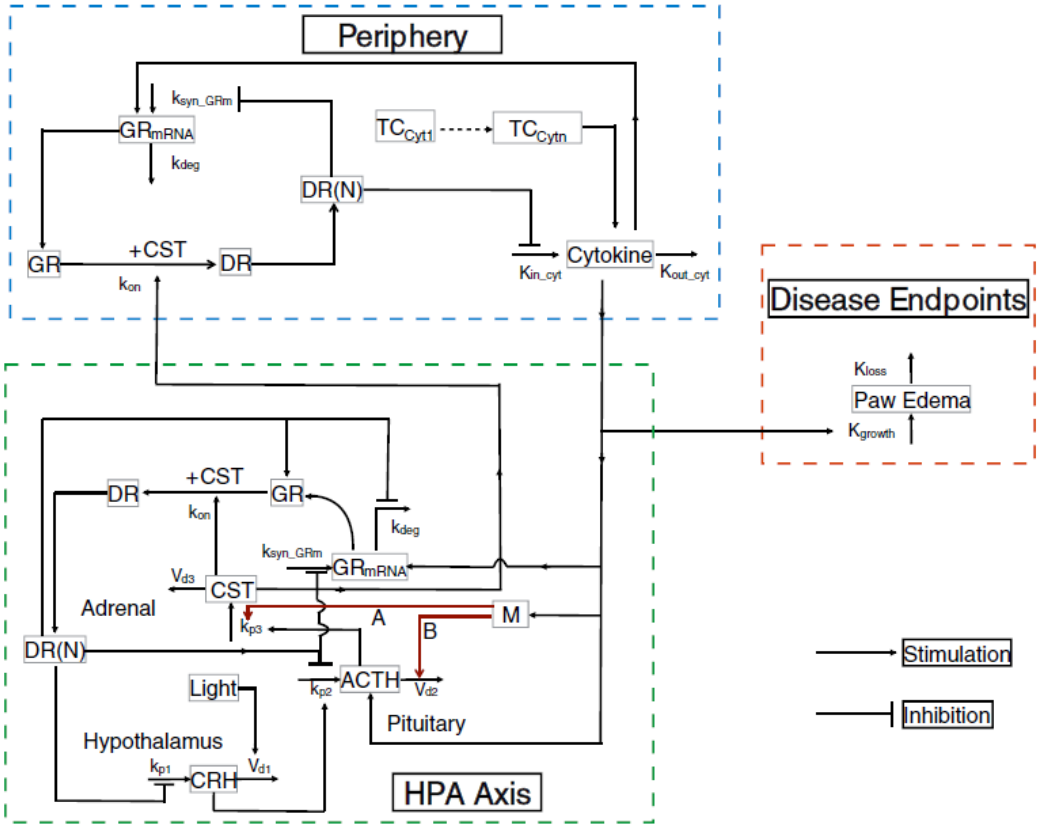


Figure 1: Model schematic for glucocorticoid and cytokine inter-regulation during arthritis progression (corticosterone is labeled CST). The two tolerance mechanisms are depicted in red.

### 2.2.1 HPA axis and Glucocorticoid Receptor Dynamics

The central compartment describes the self-sustaining circadian release of CORT from the HPA axis, as a result of the negative feedback loop formed between corticotrophin releasing hormone (CRH), adrenocorticotropic hormone (ACTH), and CORT itself. This central signaling pathway is approximated mathematically by **Equations 1-4**, which represent a Goodwin oscillator modified to include Michaelis-Menten degradation kinetics in the hypothalamic, pituitary and adrenal regions in order to

avoid the use of unrealistically high Hill coefficients (39). Briefly, CRH production in the hypothalamus is described by a zero-order synthesis term and results in the production of ACTH in the pituitary **[Equation 3]** ACTH is released into systemic circulation and eventually stimulates the secretion of CORT from the adrenals. This is accounted for by the first-order synthesis term for CORT **[Equation 4]**. Finally, the glucocorticoid receptor-mediated effects of CORT result in inhibition of ACTH and CRH secretion, thus closing the negative feedback loop. There is evidence that the basal dynamics of the HPA axis are characterized by both a circadian as well as a pulsatile ultradian rhythm (8). However, for simplicity, our model approximates the true dynamics by accounting for only the circadian rhythmicity of the HPA axis.

Furthermore, the free-running circadian rhythms of the HPA axis are entrained by the hypothalamic suprachiasmatic nucleus (SCN) to a 24-hour period. The SCN integrates photic signals from the environment and functions as the central endogenous pacemaker of the physiological circadian clock (2). Arginine vasopressin (AVP) release, which is induced by light, has been shown to strongly inhibit the release of CRH and consequently adrenal CORT in rats (40), while it is shown to have a stimulatory effect on HPA axis activity in humans (41). Therefore, vasopressin release is responsible for low levels of circulating CORT levels in the inactive phase of nocturnal animals. These observations suggest that inhibitory and excitatory effects of vasopressin release in rats and humans respectively, is not due to the direct action of vasopressin on CRH neurons but due to activation of inhibitory or excitatory neuronal pathways regulating the release of CRH (8). Therefore, we hypothesize that light entrains the rhythm of corticosterone to a 24-hour period by regulating the degradation of CRH (38) [**Equation 1**].

We use a pharmacodynamic glucocorticoid model previously developed by our group to describe the dynamics of glucocorticoid receptor signaling in both the HPA axis as well as in the peripheral cells (36). The model simulates the transcription of GR mRNA ($GR_{mRNA}$) and the subsequent translation of GR protein ($GR$) **[Equations 8, 9, 13, and 14]**. Briefly, CORT binds to cytoplasmic GR to form a complex, ($DR$), after which a fraction of the complex is eventually translocated to the nucleus, $DR(N)$. Once in the nucleus the hormone-receptor complex binds to multiple downstream glucocorticoid responsive elements (GREs) to mediate its regulatory effects.

$$\frac{dCRH}{dt} = \frac{k_{p1}}{K_{p1} + DR(N)_{HPA}} - V_{d1}.\frac{CRH \cdot \left(1 + \frac{light}{1 + light}\right)}{K_{d1} + CRH} \qquad \textbf{Eq. 1}$$

$$light = 1 \quad from \ \ 6{:}00\ AM < t < 6{:}00\ PM \qquad \textbf{Eq. 2}$$

$$else, light = 0$$

**Mechanism A**

$$\frac{dACTH}{dt} = \frac{k_{p2}.CRH}{{K_{p2}}^{\gamma 1} + DR(N)^{\gamma 1}{}_{HPA}} + \frac{k_{pcyt\_ACTH} Cyt_{HPA}}{{K_{pcyt}}^{\gamma 2} + DR(N)^{\gamma 2}{}_{HPA}} \qquad \textbf{Eq. 3}$$

$$- V_{d2}.\frac{ACTH}{K_{d2} + ACTH} \times \left(1 + \frac{V_{dm} \cdot M^{\gamma m}}{{K_{dm}}^{\gamma m} + M^{\gamma m}}\right)$$

$$\frac{dCORT_{HPA}}{dt} = k_{p3}.ACTH - V_{d3}.\frac{CORT_{HPA}}{K_{d3} + CORT_{HPA}} \quad \textbf{Eq. 4}$$

**Mechanism B**

$$\frac{dACTH}{dt} = \frac{k_{p2}.CRH}{K_{p2} + DR(N)^{\gamma 1}{}_{HPA}} + \frac{k_{pcyt\_ACTH}Cyt_{HPA}}{K_{pcyt} + DR(N)^{\gamma 2}{}_{HPA}} - V_{d2}.\frac{ACTH}{K_{d2} + ACTH} \quad \textbf{Eq. 5}$$

$$\frac{dCST_{HPA}}{dt} = k_{p3}.ACTH \times \left(1 + \frac{V_{dm} \cdot M^{\gamma m}}{K_{dm}{}^{\gamma m} + M^{\gamma m}}\right) - V_{d3}.\frac{CORT_{HPA}}{K_{d3} + CORT_{HPA}} \quad \textbf{Eq. 6}$$

$$\frac{dM}{dt} = k_{m1} \cdot \frac{Cyt^{\gamma cyt}{}_{HPA}}{k_{pm}^{\gamma cyt} + Cyt^{\gamma cyt}{}_{HPA}} - k_{out}M \quad \textbf{Eq. 7}$$

$$\frac{dGR_{mRNA,HPA}}{dt} = k_{syn_{GRm}}.\left(1 - \frac{DR(N)_{HPA}}{IC_{50_{GRm}} + DR(N)_{HPA}}\right) - k_{deg}.GR_{mRNA,HPA} + k_G \cdot \frac{Cyt^{\gamma 3}{}_{HPA}}{k_{p\_GRcyt}^{\gamma 3} + Cyt^{\gamma 3}{}_{HPA}} \quad \textbf{Eq. 8}$$

$$\frac{dGR_{HPA}}{dt} = k_{syn,GR}.GR_{mRNA,HPA} + r_f.k_{re}.DR(N)_{HPA} - k_{on}.(CORT_{HPA}).GR_{HPA} - k_{deg,GR}.GR_{HPA} \quad \textbf{Eq. 9}$$

$$\frac{dDR_{HPA}}{dt} = k_{on}.(CORT_{HPA}).GR_{HPA} - k_T.DR_{HPA} \quad \textbf{Eq. 10}$$

$$\frac{dDR(N)_{HPA}}{dt} = k_T.DR_{HPA} - k_{re}.DR(N)_{HPA} \quad \textbf{Eq. 11}$$

$$\frac{dCST_{per}}{dt} = \frac{1}{\tau_{HPA}}.\left(CORT_{HPA} - CORT_{per}\right) \quad \textbf{Eq. 12}$$

$$\frac{dGR_{mRNA,per}}{dt} = k_{syn,GRm}.\left(1 - \frac{DR(N)_{per}}{IC_{50,GRm} + DR(N)_{per}}\right) - k_{deg}.GR_{mRNA,per} + k_{GR\_cyt2} \cdot \frac{Cyt^{\gamma 3}{}_{per}}{k^{\gamma 3}_{pGR_{cyt}} + Cyt^{\gamma 3}{}_{per}} \quad \textbf{Eq. 13}$$

$$\frac{dGR_{per}}{dt} = k_{syn,GR_{per}}.GR_{mRNA,per} + r_f k_{re} DR(N)_{per} - k_{on}.\left(CORT_{per}\right).GR_{per} - k_{deg}.GR_{per} \quad \textbf{Eq. 14}$$

$$\frac{dDR_{per}}{dt} = k_{on}.\left(CORT_{per}\right).GR_{per} - k_T.DR_{per} \quad \textbf{Eq. 15}$$

$$\frac{dDR(N)_{per}}{dt} = k_T DR_{per} - k_{re} DR(N)_{per} \quad \textbf{Eq. 16}$$

### 2.2.2 Cytokine Activation of Glucocorticoid Signaling

It has been well established that proinflammatory cytokines such as interleukin -1β (IL-1β), interleukin-6 (IL-6), and tumor necrosis factor (TNF-α) are potent activators of the HPA axis (42). *In vivo* evidence strongly suggests that the activation of the HPA in response to acute inflammatory stress is strongly dependent on pituitary and hypothalamic CRH expression (42). However, a number of studies demonstrate that in spite of elevated CORT levels there is decreased CRH expression at the onset of inflammation in response to chronic inflammatory adjuvant-induced arthritis, with minimum CRH expression being reached at peak disease severity (43-45). This paradoxical decrease has been observed in Lewis (46), Wistar (47) and Piebald-Viral-Glaxo (43) strains of rat and is thus, thought to be a common mechanism in the pathogenesis of adjuvant-induced arthritis.-Taking these observations in to consideration, we postulated that proinflammatory cytokines activate the HPA axis independently of CRH. This is mathematically represented by the proinflammatory cytokine term in **Equation 3**.

In developing our model, we also consider the effects of chronic inflammation on glucocorticoid receptor (GR) signaling dynamics. It has been established that the proinflammatory cytokines TNF-α, IL-1β and IL-6 upregulate the expression of the GR mRNA (48). Studies by Earp et al. have demonstrated increased GR mRNA expression in collagen-induced arthritis (49), suggesting that proinflammatory cytokines upregulate GR

mNRA expression. We represent this positive regulation by the cytokine dependent synthesis term in GR mRNA equations in both central and peripheral cells **[Equations 8 and 13]**.

### 2.2.3 Proinflammatory Cytokine Dynamics

Cytokines are considered to be the most important molecular mediators in the pathogenesis of RA. For instance, it is thought that the deterioration of articular cartilage and the surrounding bone is largely facilitated by proinflammatory cytokines, such as IL-1β, IL-6, and TNF-α, both in human RA as well as in animal models of the disease. For simplicity, we consider a single lumped cytokine term in order to describe the time-course of proinflammatory cytokines after induction of the disease. We model the transcription of cytokine mRNA in peripheral cells, and the subsequent translation of the protein in **[Equations 17 and 18]**. Peripheral CORT inhibits the production of the cytokine mRNA through a GR mediated indirect response mechanism and in our model is also assumed to be responsible for the generating the cytokine circadian rhythm. Moreover, the peripheral cytokine protein is also transported to the HPA where it can stimulate neuroendocrine activity. The delay in cytokine signal to the HPA axis is applied by using a single transit compartment with a mean transit time of about 10 minutes **[Equation 21]**. This is in agreement with experimental observations where IL-1β administration *in vivo* results in increased ACTH secretion with about 5-10 minutes (48).

In general, a delay is observed in the onset of cytokine upregulation once the animals are inoculated. We model this delay by simple transduction using a sequence of transit compartments. The number of transit compartments can be adjusted to fit an experimentally observed time delay, as was done in our previous work (37,49). However,

since we are interested in a qualitative model of disease progression we choose a number of transit compartments that is representative of the experimentally observed delay **[Equation 19 and 20]**. In order to simulate the induction of the disease, the value of $k_{dis}$ in **Equation 19** is increased to a new disease steady-state value, while in simulations of healthy animals, $k_{dis} = 0$.

Finally, we attempt to simulate the phenomenon of adrenal insufficiency, which refers to perceived inability of the HPA axis to mount an effective anti-inflammatory response to the elevated cytokine levels observed in chronic RA and animal models of the disease. A number of theories have been proposed to explain the onset of adrenal insufficiency in chronic inflammatory diseases. Straub et al. suggest that in contrast to the situation in acute inflammation, chronically elevated proinflammatory cytokine levels inhibit HPA axis activity resulting in the low HPA axis response relative to ongoing inflammation (50). On the other hand, Edwards has recently proposed that proinflammatory cytokines stimulate 11β-hydroxy steroid dehydrogenase (51), an enzyme that catalyzes the conversion of inactive cortisone to cortisol (52). This results in increased cortisol levels which negatively feedback to the HPA axis and inhibit further cortisol secretion. Ultimately, these theories suggest that the apparent adrenal insufficiency is due to downstream effects of proinflammatory cytokine signaling in chronic inflammation. Recent work by Wolff et al. demonstrated that CORT shows an initial increase in response to elevated proinflammatory cytokines in CIA rats followed by an eventual decline suggesting the onset of tolerance as the disease progresses. Thus, we postulate an indirect response tolerance mechanism to model this phenomenon. Indirect response models are frequently used in pharmacokinetic/pharmacodynamic

models and were originally used to capture a delay in the response of a measured variable of interest in response to a stimulus of interest especially, when the intermediate events between the onset of the stimulus and the response of the measured variable cannot be explicitly stated (53). Since, the complex regulatory mechanisms involved in the onset of adrenal insufficiency are yet to be elucidated, we find indirect response modeling particularly appealing in capturing the possible implicit interactions between variables of interest (54), which in our case are the interactions between CORT and proinflammatory cytokines. Therefore, we use an indirect response tolerance mechanism where chronically elevated cytokine levels lead to the stimulation of a hypersensitive tolerance mediator, M **[Equation 7]** We consider two hypothetical mechanisms by which this tolerance mediator might act on the HPA axis to reduce corticosterone secretion relative to ongoing inflammation under chronic conditions. In the first, Mechanism A, we assume that activated tolerance mediator inhibits HPA axis signaling. This is represented in **Equation 3 and 4,** where M effectively acts to decrease ACTH concentrations, by increasing the clearance of ACTH in arthritic conditions, and thereby reducing corticosterone secretion. In the second mechanism (Mechanism B), the activated tolerance mediator instead further increases corticosterone concentrations [**Equation 5 and 6**] in response to chronically elevated proinflammatory cytokine levels. We hypothesize that the increased corticosterone levels would result in greater negative feedback to the HPA via a GR-mediated mechanism [**Equation 8**] leading to the eventual desensitization of the HPA under conditions of chronic inflammation. Due to the hypersensitive response of M, homeostatic levels of cytokines, like those present in healthy controls, do not activate the

tolerance mechanism. Parameter values for both mechanisms are presented in **Table A1** (Appendix).

$$\frac{dCyt_{mRNA}}{dt} = k_{\ TC_{Cyt}} TC_{Cyt_{n-1}} + k_{in_{Cyt\_mRNA}} \times \left(1 - \frac{DR(N)_{per}}{IC_{50_{Cyt}} + DR(N)_{per}}\right) - k_{out_{Cyt\_mRNA}} Cyt_{mRNA} \quad \textbf{Eq. 17}$$

$$\frac{dCyt_{per}}{dt} = k_{in_{Cyt\_per}} Cyt_{mRNA} - k_{out_{Cyt_{per}}} Cyt_{per} \quad \textbf{Eq. 18}$$

$$\frac{dTC\_Cyt_1}{dt} = k_{t_{Cyt}} \times \left(k_{dis\_Cyt} - TC\_Cyt_1\right) \quad \textbf{Eq. 19}$$

$$\frac{dTC\_Cyt_n}{dt} = k_{t_{Cyt}} \times (TC\_Cyt_{n-1} - TC\_Cyt_n) \quad \textbf{Eq. 20}$$

$$where\ n = 15$$

$$\frac{dCyt_{HPA}}{dt} = {}^{1}/_{\tau_{cyt}} \cdot \left(Cyt_{per} - Cyt_{HPA}\right) \quad \textbf{Eq. 21}$$

### 2.2.4 Paw Edema Dynamics

We consider paw edema as an indicator of disease severity in arthritic conditions. Paw edema progression is modeled as a result of the stimulation by proinflammatory cytokines and loss of the produced edema through a first order decay term. We hypothesize that a slight delay exists between the onset of increased proinflammatory cytokine expression and onset of the rise in paw edema. For instance, it has been observed that levels of cytokines, chemokines, and cytokine receptors were significantly higher before disease onset in individuals who subsequently developed RA in comparison to control subjects who did not develop RA (55). This delay is incorporated by making the rate constant for paw edema generation dependent on the final cytokine transit compartment, $TC\_Cyt_n$. Moreover, this enables us to avoid circadian variation in the paw size during healthy conditions.

$$\frac{dPAW}{dt} = k_{growth} + k_{cyt\_in} \times TC\_Cyt_n \times Cyt_{per} - \frac{(PAW - PAW_0)}{PAW_0} \qquad \textbf{Eq. 22}$$

### 2.2.5 Cosinor Rhythmometry Analysis

Cosinor rhythmometry is a commonly used technique in the analysis of both experimental and simulated circadian data. We employed cosinor analysis to estimate characteristic parameters of the circadian rhythms of the neuroendocrine-immune mediators. This enabled us to quantitatively evaluate changes in circadian rhythm of various model species in our simulations of chronic inflammation.

Briefly, cosinor analysis involves the fitting of a sinusoid to the dataset using non-linear regression. Depending on the nature of the data, one can attempt to fit a single component sinusoid, or multiple sinusoids. For the purposes of our simulation, we were able to achieve sufficient resolution with a single-component sinusoid.

Thus, the regression model can be represented as

$$Y(t) = M + A \cdot cos\left(\frac{2\pi(t-\Phi)}{\tau}\right) + \varepsilon \quad \textbf{Eq. 23}$$

Where,

1. M is the MESOR (Midline Estimating Statistic Of Rhythm): The MESOR is a rhythm adjusted mean
2. 2A is the measure of the predictable change within the data (the amplitude)
3. $\Phi$ is the acrophase of the rhythm.
4. $\tau$ is an estimate of the period of oscillation
5. ε are the errors accounting for the difference between model predictions and data observations.

*Sensitivity Analysis:* A local sensitivity analysis is performed to gain insight into the corticosterone dynamics predicted by our model both in the nominal healthy state and in response to the elevated cytokine levels in the arthritic state. As in previous studies by our group (56) and others (35) we use a relative sensitivity coefficient computed as the product of the absolute sensitivity function (the partial derivative of the of the response variable to changes in the parameter of interest) and the ratio of the nominal value of the parameter to the nominal output of the signal.

$$\frac{1}{NM}\sum_{j=1}^{NM}\frac{p_k}{y_{ij}}\left(\frac{\partial y}{\partial p_k}\right)_{y=y(t_{ij},p)} \quad \textbf{Eq. 24}$$

Where

$NM\ are\ the\ number\ of\ measures$

$y\ is\ the\ state\ variable\ whose\ response\ is\ being\ studied$

$p_k\ are\ the\ parameters\ of\ interest$

Since, we were primarily interested in the dynamics of CORT predicted by the model, we use its profile as the response variable in calculating the sensitivity coefficients. Parameters are individually varied by 1% and the sensitivity coefficients are calculated for each parameter accordingly. For the simulated arthritic state of the model, parameters are perturbed before the simulated onset of the disease to determine the change in response of the system to elevated disease state proinflammatory cytokine levels.

## 2.3 Results

Our model aims to characterize the effects of chronic inflammation on the circadian dynamics of proinflammatory cytokines and HPA axis hormones. **Figure 2**, shows the time course of cytokines both in simulated healthy control conditions as well as in arthritic conditions. The disease was induced at an arbitrarily selected time, $t_{ind} >$

0, in order enable visual comparison of changes in cytokine levels before and after disease induction. A noticeable delay is observed in the upregulation of proinflammatory cytokines after disease induction together with a marked loss in circadian rhythm. Furthermore, cytokine levels remain elevated over the entire time course of the simulated experiment, thus indicating a state of chronic inflammation. These features are in qualitative agreement with results from experimental models of rheumatoid arthritis (49).

**Figure 2** also shows the corresponding time-course of CORT, while **Figure 3** shows that time-course for CRH and ACTH, for both mechanisms of adrenal insufficiency. Cosinor analysis **[Table A2** (Appendix)**]** demonstrates that the circadian rhythm of the HPA axis hormones is entrained by light to a steady state 24-hour period over the entire time-course of the simulated experiment. Interestingly, both postulated mechanisms of the adrenal insufficiency (Mechanisms A and B) yield qualitatively similar profiles of HPA axis mediators. Model simulations predict a marked increase in the CORT levels corresponding to the upregulation of proinflammatory cytokine levels after disease induction **[Figure 2C and 2D].** This increase in CORT levels is accompanied by a slight decrease in the amplitude of CORT oscillations. However, these CORT levels are not maintained, and there is an eventual decrease in mean CORT release in response to chronically elevated cytokine levels, due to the activation of the postulated tolerance mechanism. Moreover, this decrease is accompanied by a further loss in circadian rhythmicity of CORT. Cosinor analysis reveals that although mean CORT levels decrease, they do not return to the levels present in healthy controls and remain slightly elevated for the entire duration of the simulated experiment.

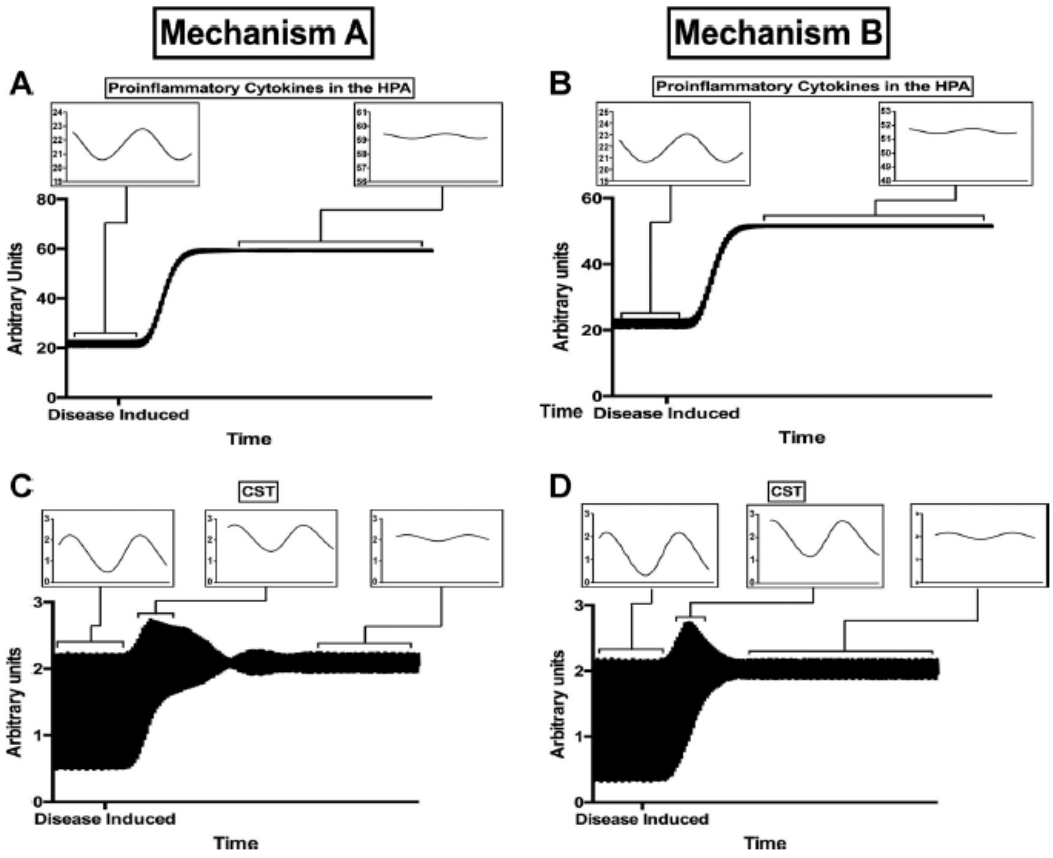


Figure 2: Time-course of proinflammatory cytokine protein when onset of tolerance is due to a) mechanism A and b) mechanism B, respectively. Time-course of CORT when onset of tolerance is due to c) mechanism A and d) mechanism B, respectively. Inset images depict the circadian profile in indicated regions of the time-course profiles of the respective mediator.

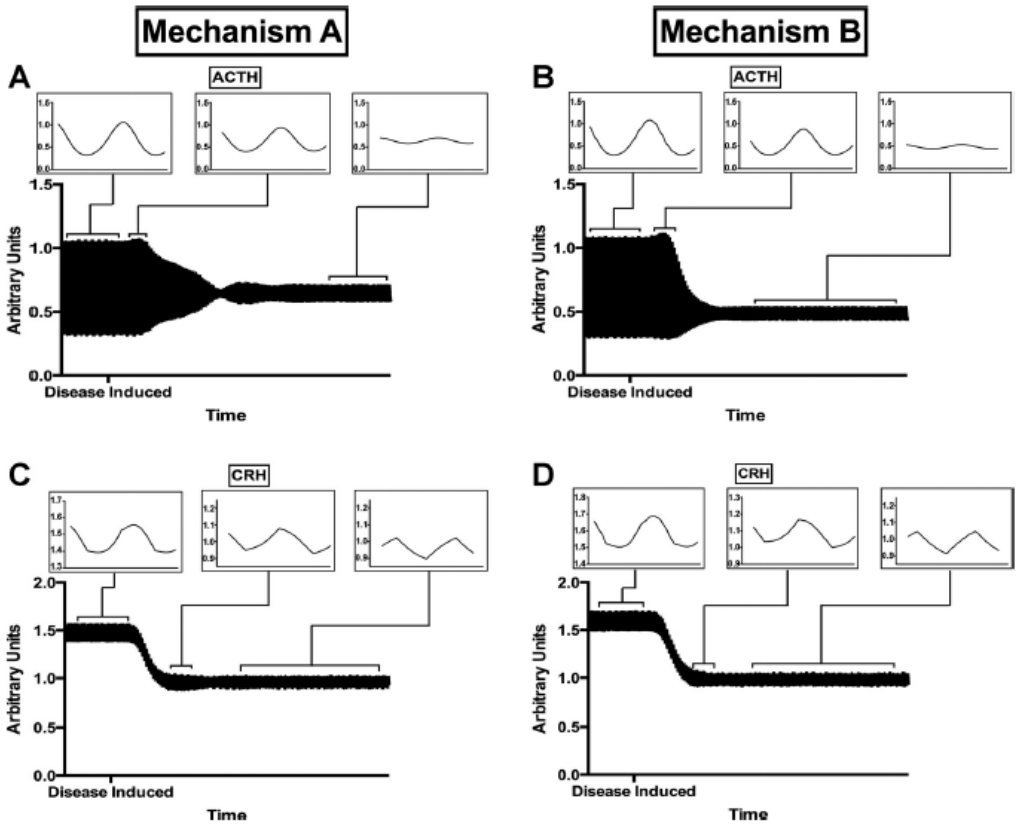


Figure 3: Time-course of CRH when onset of tolerance is due to a) mechanism A and b) mechanism B, respectively. Time-course of ACTH when onset of tolerance is due to c) mechanism A and d) mechanism B, respectively. Inset images depict the circadian profile in indicated regions of the time-course profiles of the respective mediator.

On the other hand, there is a significant decrease in the mean expression of CRH **[Figure 3C and 3D]**, in spite of the increase in CORT levels. Although CRH levels increase slightly after the activation of tolerance mediator, they remain distinctly lower when compared to levels in healthy controls. Similar to the other HPA axis hormones, ACTH **[Figure 3A and 3B]** also shows a discernable decrease in amplitude of oscillation after induction of the disease. There is a substantial decrease in diurnal ACTH maxima and a slight increase in its diurnal minima. Interestingly, model simulations predict that maximum CORT levels show a relatively small decrease in spite of the marked decrease

in maximum ACTH levels, as revealed by respective time-course profiles **[Figure 3A and 3B]** as well as the cosinor analysis.

We further consider glucocorticoid receptor dynamics in response to changes in CORT and cytokine levels. We find that both GR protein and mRNA initially show a sharp decrease in expression corresponding to transient increase in CORT levels and onset of increased proinflammatory cytokine levels **[Figure 4]**. However, there is an eventual increase in both GR mRNA and protein levels after the onset of tolerance in comparison to those observed in the healthy state accompanied by a decrease in amplitude of oscillation.

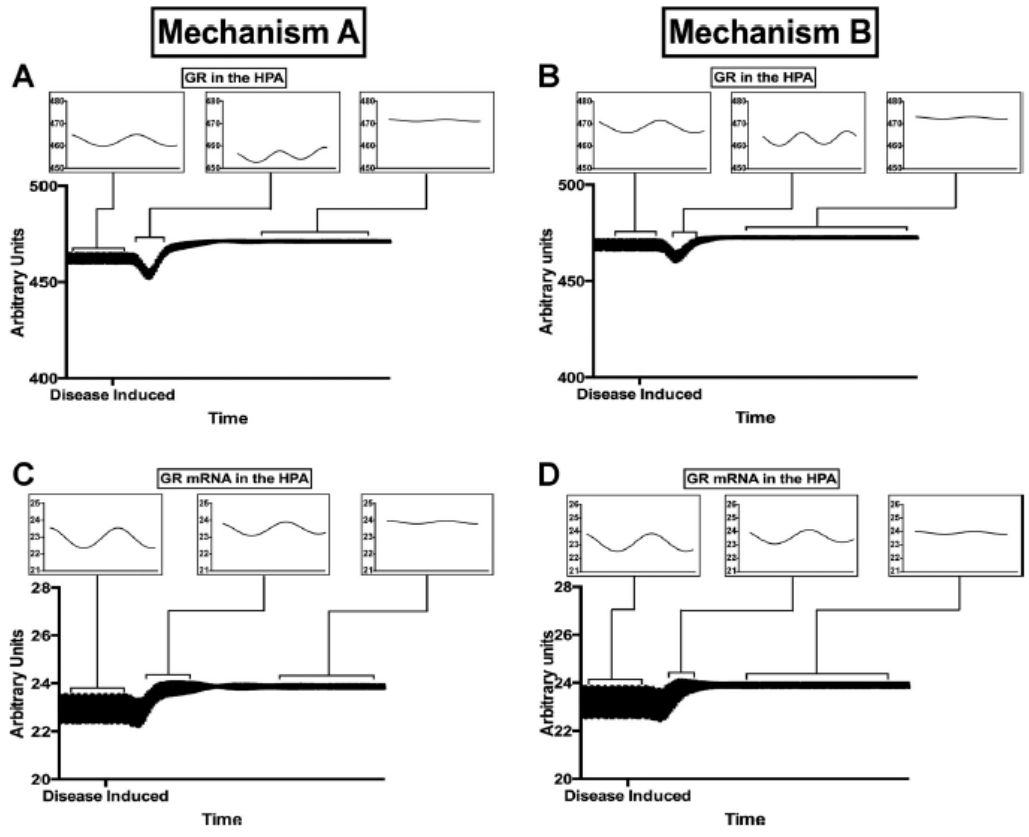


Figure 4: Time-course of GR mRNA when onset of tolerance is due to a) mechanism A and b) mechanism B, respectively. Time-course of GR when onset of tolerance is due to c) mechanism A and d) mechanism B, respectively. Inset images depict the circadian profile in indicated regions of the time-course profiles of the respective mediator.

**Figures 5 and 6** compare the circadian profile of the HPA axis hormones, proinflammatory cytokines and glucocorticoid receptor expression over a 48-hour time period representative of the rhythm in healthy controls and after the onset of tolerance for both mechanisms, respectively. It can be seen that the CRH and ACTH profiles peak slightly earlier than the CORT profile accounting for the time required for the signal transduction along the HPA axis. Moreover, it can be seen from the cosinor analysis that CORT profiles peaks just before the onset of the dark period. A number of experimental studies have established that CORT levels peak slightly before the start of the active phase, which is during the dark period for nocturnal animals, such as rats considered in our model (57). The decrease in amplitude and change in mean value of oscillation are clearly discernible in these profiles. Furthermore, there is a noticeable shift in the phase of oscillation towards earlier time points in the circadian profiles for ACTH, CORT, proinflammatory cytokines as well as glucocorticoid receptor mRNA and protein. Using

cosinor analysis we estimated this change in phase to be approximately 10 hours

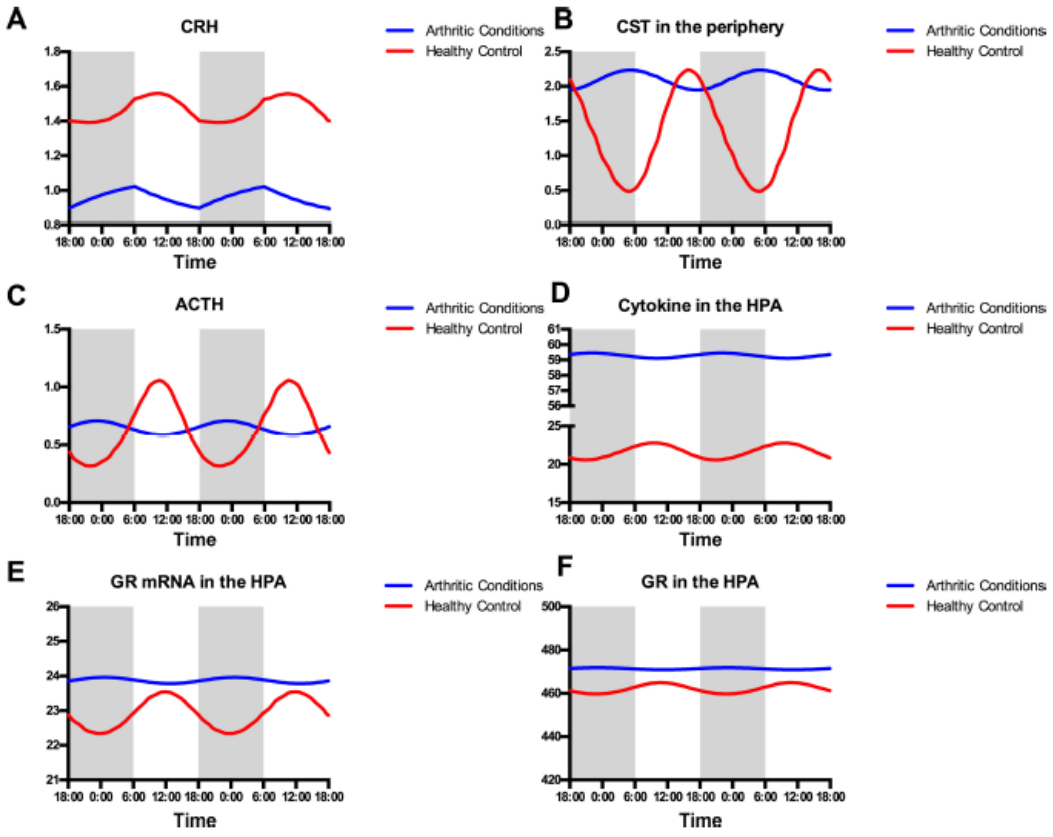


Figure 5: Circadian profile over a 48-hour period in healthy controls (blue) and arthritic conditions (red) when onset of tolerance is due to mechanism A for a) CRH, b) CORT, c) ACTH, d) Peripheral cytokine protein, e) GR

mRNA in the HPA, f) GR protein in the HPA. Note the change in y-axis scale in d).

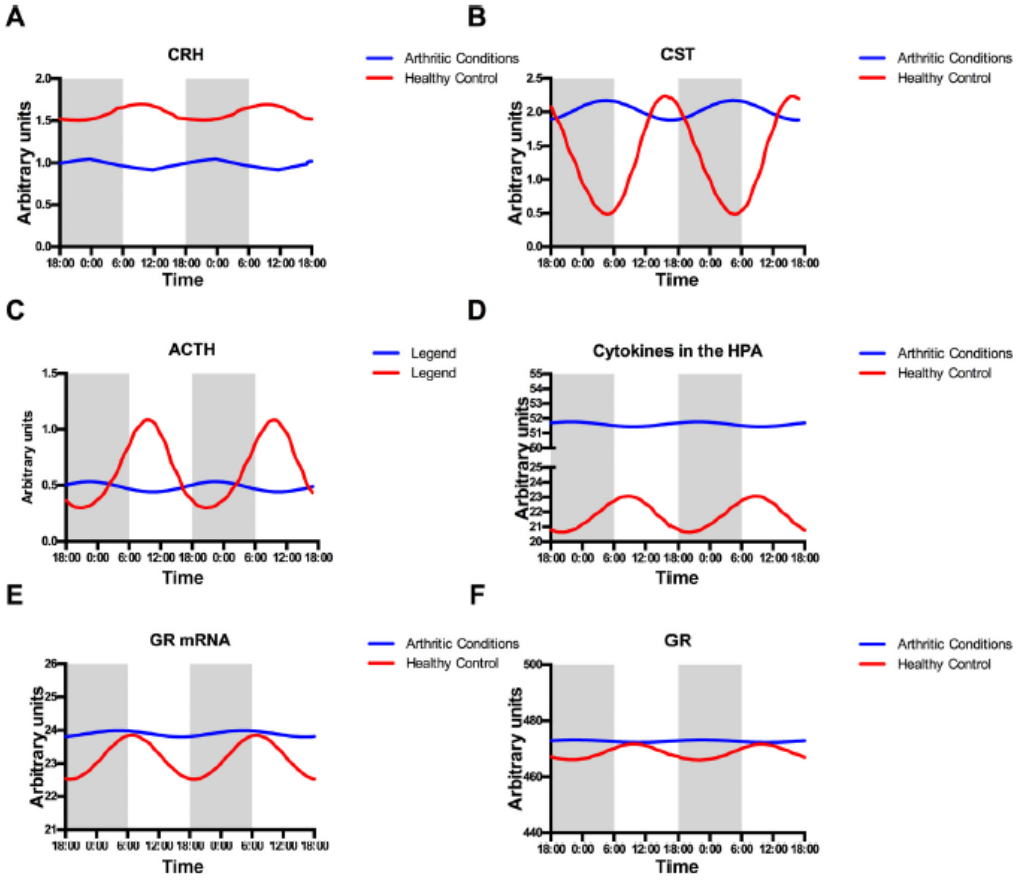


Figure 6: Circadian profile over a 48-hour period in healthy controls (blue) and arthritic conditions (red) when onset of tolerance is due to mechanism B for a) CRH, b) CORT, c) ACTH, d) Peripheral cytokine protein, e) GR mRNA in the HPA, f) GR protein in the HPA. Note the change in y-axis scale in d).

Model simulations predict a constant steady-state paw size for healthy control simulations. However, there is almost a three-fold increase in paw size due to the formation of paw edema as a result of the chronically elevated proinflammatory cytokines **[Figure 7A and 7B]**. A diurnal variation in paw edema is evident in the simulated arthritic state **[Figure 7C and 7D]**. Moreover, comparing the circadian rhythms of proinflammatory cytokines and paw edema **[Figure 7E and 7F]**, it can be observed that this rhythmic variation in the disease end-point is well correlated to the circadian rhythm exhibited by the proinflammatory cytokines in the arthritic state.

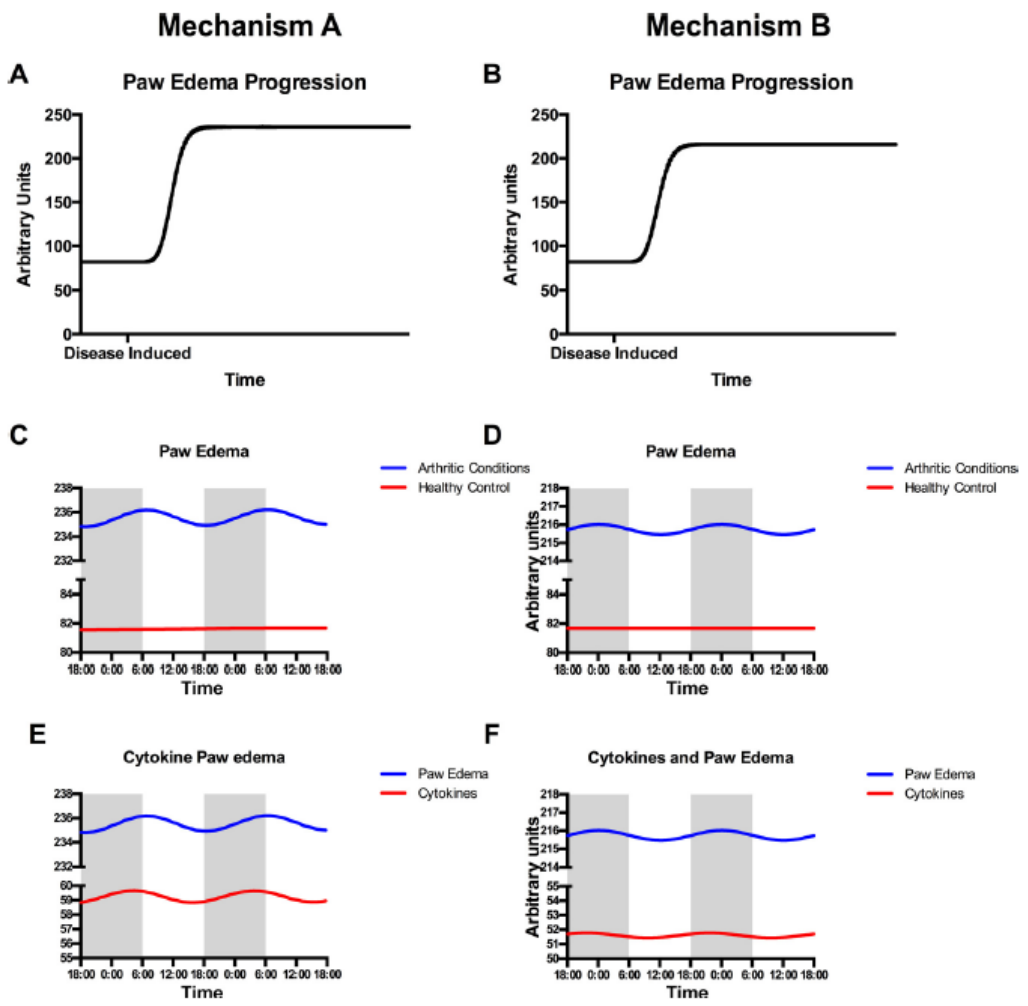


Figure 7: Paw edema progression over time course of simulation when onset of tolerance is due to a) mechanism A and b) mechanism B, respectively. Circadian variation of paw edema in arthritic conditions when onset of tolerance is due to c) mechanism A and d) mechanism B, respectively. Paw size in healthy controls is maintained at a constant value in healthy controls. Comparison of circadian rhythm of proinflammatory cytokines and circadian rhythm in paw edema in arthritic conditions when onset of tolerance is due to e) mechanism A and f) mechanism B, respectively. Note the change in y-axis scale in c), d), e) and f).

Sensitivity coefficients for each parameter are calculated as shown in **Equation 24**. The results of the sensitivity analysis are shown in **Figures 8A** and **8B** for both the mechanisms respectively. The magnitude of the sensitivity coefficients are comparable to models that we have previously developed (56). The analysis reveals that in the healthy state, which is considered to be the nominal state of the system, the model output is most sensitive to perturbations in estimated parameters associated with Goodwin

oscillator of the HPA axis (i.e. **Equations 1-6**). Furthermore, the sensitivity coefficients for most of the parameters are lower in the arthritic state of the model than in the healthy state of the model.

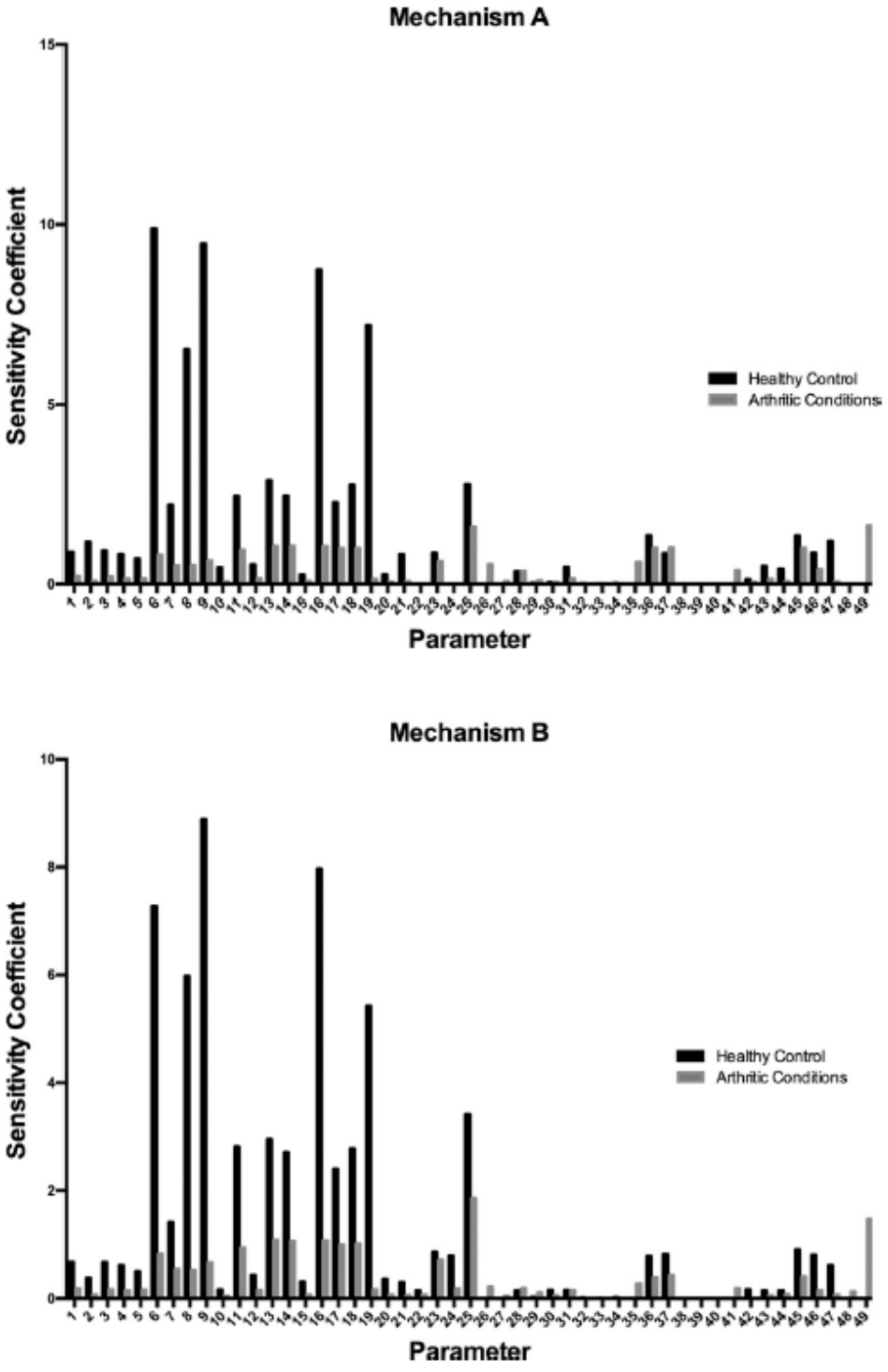


Figure 8: Sensitivity coefficients calculated as per Equation 24. for a) mechanism A and b) mechanism B in the simulated healthy state and in response to elevated cytokine levels in the arthritic state, respectively.

## 2.4 Discussion

The neuroendocrine hormonal regulation of the immune system has received a great deal of research attention in relation to its importance in the pathophysiology of chronic inflammatory diseases. Rheumatologists routinely administer glucocorticoids in the treatment of RA due to their potent anti-inflammatory and anti-proliferative effects (58-60). Moreover, a number of studies have investigated the possibility of altered endogenous glucocorticoid regulation by the HPA axis in rheumatic diseases.

In general, increased glucocorticoid secretion is observed in studies on animal models of both adjuvant-induced and collagen-induced arthritis. Evidence suggests that cortisol levels in RA patients with low to moderate disease activity remain largely unchanged in comparison to healthy controls, while patients with severe RA show elevated cortisol levels (31). However, it is widely considered that the anti-inflammatory glucocorticoid response is inadequate in relation to the ongoing inflammation in both RA and animal models of the disease (61-65). This phenomenon, termed adrenal insufficiency, is generally evaluated by comparing the glucocorticoid hormone-proinflammatory cytokine ratio in arthritic conditions to that in healthy control conditions (33). In a recent study by Wolff et al. a marked increase CORT levels was observed on day 1 after induction of collagen-induced arthritis in rats. However, CORT concentrations returned to levels comparable to those in healthy controls by day 5, in spite of IL-1β levels showing a steady increase over the duration of the experiment (64). This behavior was also observed for ACTH expression in the same study. In agreement with the general pathological features exhibited in experimental studies, our model simulations reveal a transient rise in CORT levels due to the upregulation of

proinflammatory cytokines regardless of the mechanism of adrenal insufficiency. This transient increase is due to activation of the HPA axis as a result of upregulated cytokine levels soon after disease induction. Subsequently, the model predicts that this increase in CORT levels is quickly followed by the onset of tolerance. This results in a relative decrease in CORT levels, although they are still significantly elevated in comparison to CORT levels in healthy controls. Therefore, taken together, our simulations suggest that as in the phenomenon of adrenal insufficiency; the HPA axis cannot mount a sustained anti-inflammatory response in the presence of chronically elevated levels of proinflammatory cytokines.

Despite the increase in CORT levels our model simulations reveal that CRH expression decreases in arthritic conditions when compared to healthy controls. As discussed in previous sections, a number of studies report a paradoxical decrease in CRH levels despite of the increased HPA axis activity. Conversely, it has been observed that the decrease in CRH levels in adjuvant-induced arthritis is accompanied by an increase in the arginine vasopressin (AVP) expression. Therefore, it has been hypothesized that AVP may be the primary mediator responsible for the observed increase in HPA axis activity in response to chronic inflammatory conditions in adjuvant-induced arthritis (43,66). Furthermore, a number of studies demonstrate that vasopressin is an inhibitor of CRH secretion in nocturnal animals such as rats and mice, with increased vasopressin activity being correlated with decreased CRH expression (40). Evidence suggests that the observed CRH decrease as result of altered HPA axis activity is characteristic of the pathophysiology of a number of other experimental models of immune-mediated diseases

such as experimental allergic encephalomyelitis (67), eosinophilia-myalgia syndrome (46), and systemic lupus erythematosus (32,68).

It has been established that a multitude of biological processes, critical to the maintenance of homeostasis are under precise circadian regulation. Chronic circadian disruption has been implicated in increasing the susceptibility to a number of chronic inflammatory diseases including RA, diabetes, obesity and cancer (69-71). Furthermore, a number of studies report a disruption of neuroendocrine and immune circadian rhythms in human and experimental RA. A number of studies on animal model of adjuvant-induced arthritis have observed that elevated CORT levels have been associated with a blunted circadian rhythm (65,72,73). Interestingly, this has also been observed (61) (31,74) in patients with high RA activity. In a study by Sarlis et al., which studied HPA axis activity in adjuvant-induced arthritis, it was observed that CORT and ACTH levels were higher in the inactive phase when compared to healthy controls. Similar behavior was observed in salivary cortisol levels in patients with high disease activity, where cortisol levels did not significantly drop after the afternoon maximum (62). Model simulations seem to be in general agreement with these experimental observations. Our simulations describe a loss in CORT rhythm, as indicated by the decreased amplitude and furthermore, show that while the diurnal maxima for CORT is largely unchanged the diurnal minimum is markedly elevated.

On the other hand, in our simulations the diurnal peak of the ACTH circadian rhythm is clearly lower while its minima is elevated. Mean ACTH levels are slightly higher when the onset of tolerance is due to mechanism A, while they are lower when adrenal insufficiency is achieved by mechanism B as shown by the mesor value in the

cosinor analysis **[Table A2** (Appendix)**]**. Considering the striking decrease in the circadian peak of ACTH, it is interesting to note that the corresponding maximum for CORT is substantially unchanged. Although such a finding has not been corroborated by experimental studies with animal models of rheumatoid arthritis, Straub et al. observed that RA patients had a higher cortisol-ACTH ratio in comparison to healthy controls (75). Moreover, RA patients with a relatively lower cortisol-ACTH ratio were more likely to respond positively to anti-TNF-α therapy than patients with a high cortisol-ACTH ratio. Under healthy conditions it is considered that the cortisol-ACTH ratio is strictly regulated, however, under arthritic conditions it is hypothesized that this ratio increases due to alterations in regulatory network between the HPA axis and adrenals glands resulting in cortisol secretion being seemingly decoupled from the corresponding ACTH signal. A possible cause for this decoupling could be attributed to the ability of proinflammatory cytokines to stimulate the cortisol secretion from the adrenals independently of the HPA axis (75,76). Our model suggests that such an observation might be due to the increased negative feedback from the cytokine-induced increase in CORT levels to CRH and ACTH resulting in lower levels of these mediators.

Model simulations also predict an initial decrease in GR mRNA and protein expression followed by an eventual increase to a level higher than the corresponding expression levels in healthy controls. In agreement with our results, Earp et al. observed an increase in GR mRNA expression following induction of the disease in CIA rats (49).

IL-1β and TNF-α are widely considered to be the primary mediators of chronic inflammation in rheumatoid arthritis. Experimental evidence from both animal models and human patients seems to support this view (64,77). However, often IL-6 is used as a

marker for chronic inflammation in rheumatoid arthritis as it is the most easily measureable of the three primary proinflammatory cytokines (64). Cytokine levels in both animal models of the disease as well as RA patients are found to be up to 10 times as high as in healthy controls (49,78). The cytokines in our simulation results have a 3-fold increase in mean levels. Furthermore, Seres et al. report that the circadian rhythm of IL-1 is suppressed in adjuvant-induced arthritis, while the amplitude of IL-6 circadian expression increases. A suppression of cytokine rhythms has also been observed in fibroblasts isolated from synovium of RA patients, which showed weak rhythmic expression as compared synovial fibroblasts isolated from osteoarthritic patients, suggesting that there is damping of the circadian rhythm of cytokines in RA patients.

Furthermore, simulation results also show an advance in the phase of the circadian rhythm for both neuroendocrine hormones as well as the cytokines. This suggests that alterations in HPA axis signaling regulation in response to chronic inflammation might result in the observed phase advance. Our model simulations are in qualitative agreement with these findings from both animal models and human studies. Seres et al. report a phase advance in IL-1β circadian rhythm but a phase delay in the circadian rhythm of IL-6 in a model of adjuvant-induced arthritis (73). Further, Li et al. showed that rats with CIA exhibited a significantly earlier and higher IL-6 peak, with a nearly inverted CORT rhythm (79). Interestingly, Neeck et al. (61) also observed that in RA patients with low to moderate disease activity cortisol maxima and minima were shifter to earlier times of the day. Moreover as mentioned earlier, these patients also had higher cortisol levels with blunted amplitude. However, other studies report a broadening of the cytokine peak with a shift to later times of the day, resulting in an effective rise in

amplitude (80). It is well established that the expression of proinflammatory cytokines is regulated by the expression of components of the circadian clock, including Cry (70), Bmal1 (81) and Clock (82). However, in our model cytokine oscillations are driven only by CORT oscillations and we do not explicitly account for circadian clock control of cytokines. This might be able to explain some of the discrepancy between experimental findings and the cytokine phase relationships predicted by our model.

The sensitivity analysis reveals that the parameters associated with the Goodwin oscillator have the highest sensitivity coefficients of the estimated parameters (parameters 6, 8 and 9). This is expected considering that the dynamics of the model are largely determined by the equations representing the Goodwin oscillator [**Equations 1-6**]. Further, since we use the CORT profile as the primary response variable in calculating the sensitivity coefficients, it is not surprising that $k_{p3}$, the rate of CORT synthesis and $V_{d3}$, the rate of enzymatic degradation of CORT (parameters 8 and 9, respectively) are amongst the most sensitive parameters. Furthermore, the parameters associated with the dynamics between corticosterone and the glucocorticoid receptor (parameters 16 and 19, which were obtained from literature) also contribute significantly to model sensitivity. The model output is probably sensitive to perturbations in these parameters, since they directly influence the amount of $DR(N)$, which determine the extent of CORT feedback to CRH and ACTH. Interestingly, the sensitivity analysis of a similar model of the HPA axis by Sriram et al. also found that the model output was most sensitive to perturbations in parameters associated with glucocorticoid receptor dynamics. Notably, the model is much less sensitive to perturbations in parameters in the arthritic state than in the nominal healthy state as can be observed from the lower values of the sensitivity coefficients

(**Figures 8A** and **8B**). This is likely due to the relatively strong feedback term of the elevated cytokine levels to the HPA axis equations; forcing the system towards a more stable state. Such a response is applicable to experimental models of arthritis, such as adjuvant-induced arthritis and collagen-induced arthritis, which are generally used to model the severe late stage of the disease (83,84) primarily associated with high levels of monokines such as TNF-α, and IL-1β (85).

Finally, it is well established that disease related symptoms in patients of chronic inflammatory diseases, such as RA, exhibit distinct circadian rhythms (31,78,86-89). For instance patients report maximum severity of symptoms such as joint pain, stiffness and functional disability in the early morning hours (start of the active phase), with mild to moderate disease active in the evening (end of the active phase). Furthermore, it is observed that the diurnal variation in disease symptoms is well correlated with the circadian rise in the levels of proinflammatory cytokines and conversely, the circadian decrease in levels of CORT. Circadian rhythms have also been observed in rodent models of experimental inflammation such as carrageenan-induced paw edema (90,91) Our model simulations are in qualitative agreement with these experimental observations, where the paw edema peak is correlated to the cytokine peak.

In conclusion, our model qualitatively captures key features of RA pathophysiology. Through the model simulations we are able to relate chronic upregulation of proinflammatory cytokine with incidence of adrenal insufficiency and the circadian disruption of critical mediators of the neuroendocrine and immune systems. We also show that both postulated mechanisms of adrenal insufficiency result in qualitatively similar profiles of neuroendocrine and proinflammatory mediators. Furthermore, our

work highlights the importance of accounting for circadian dynamics while studying the interactions between the neuroendocrine and immune signaling pathways. It is interesting to note that loss in amplitude and change in phase of the rhythms resulted solely from the model dynamics and were not explicitly accounted for in the model equations. Our model suggests that the activation of the postulated tolerance mechanisms results in the manifestation of symptoms characteristic of chronic inflammation in RA, such as a significant loss in diurnal rhythm of the HPA axis hormones and the supposed decoupling of ACTH and CORT signaling. However, the model has some important limitations. The model assumes that circadian rhythm of the cytokines is generated only by the circadian oscillations of CORT from the Goodwin oscillator. However, it has been established that proinflammatory cytokines have their own intrinsic circadian rhythm and regulated by the peripheral circadian clocks, independently of the HPA axis. This limits the extent to which our model can capture the dynamics of the proinflammatory cytokines in the arthritic state. Moreover, we do not consider the interactions between the sympathetic nervous system mediator, norepinephrine, the other important stress response mechanism, and the HPA axis as well the proinflammatory cytokines.

Though our model predictions are largely qualitative in nature, we were able to identify regulatory structures of signaling networks that could qualitatively capture key pathophysiological features of the disease; such as the apparent adrenal insufficiency, loss of circadian amplitude in the arthritic state, and possible alterations in the phase of the rhythm of the HPA axis mediators. We consider two alternative hypothetical mechanisms for the onset of adrenal insufficiency, which yield qualitatively similar results. Future work could involve further incorporating the mechanisms by which

regulatory intermediates (such as 11-βHSD) involved in the feedback of cytokines to the HPA axis might result in its altered signaling in both animal model of arthritis as well as in the human disease. Thus, the model developed here provides a foundation for further work on the significance of circadian rhythms in neuroendocrine-immune signaling in chronic inflammatory diseases.

# CHAPTER 3: Modeling the Sex Differences and Individual Variability in the Activity & Stress Response of the Hypothalamic-Pituitary-Adrenal Axis

## 3.1 Background

### 3.1.1 Sex Differences in HPA Axis Regulation

Numerous studies have documented the existence of sex differences in the secretion of CORT under both basal conditions as well as in response to precursors of CORT, and a variety of psychological and physiological stressors (11). It is generally thought that these sex differences are primarily mediated by the differential influence of the circulating gonadal hormones on the HPA axis during both development and in adult life (12,92). Studies show that in general estrogens sensitize the HPA axis response to stressors and increases basal HPA axis activity, while testosterone has the opposite effects (11). Evidence suggests that ovarian steroids also impair GR-mediated negative feedback with studies showing higher levels of corticosterone at the end of stress application in rats receiving estradiol (93,94). Furthermore, GR agonists suppress stress-induced corticosterone and ACTH responses to a greater extent in ovariectomized female rats in comparison to rats treated with estradiol (95). Accordingly, a number of studies have shown that gonadectomy in rats, results in the dampening of HPA axis activity in female rodents, while it increases basal HPA axis activity in males (12). Studies have also shown that HPA axis activity varies with the estrous cycle in rodents, with females showing higher CORT levels during the proestrous phase of the estrous cycle, when circulating levels of estrogen are at their highest (14).

Atkinson and Wadell (23), using chronobiological assays and standard cosinor models, found prominent sex differences in CORT circadian rhythms, with female rats exhibiting more pronounced rhythms than male rats. The extent of these differences varied with the stage of the estrous cycle, with the highest mean levels of CORT being found in females in the proestrous phase. Furthermore, no significant differences were found in ACTH levels between males and females during the course of the estrous cycle. Such studies have led investigators to hypothesize that the development and expression of sex differences in the HPA axis emerge predominantly due to differences in the sensitivity and negative feedback within the HPA axis caused by the influence of the gonadal steroids.

### 3.1.2 Allostasis & the Exposure to Chronic Stress

Glucocorticoid circadian rhythms enable the host to adjust its behavior and physiology in anticipation of regular periodic changes in environment, such as the daily variability in light, temperature, food availability and environment stressors (96-98). Therefore, the maintenance of appropriate circadian rhythmicity has important functional implications and preserves host homeostasis by appropriately synchronizing a multitude of internal physiological processes to the external environment (21). Disruptions in glucocorticoids rhythmicity are associated with the incidence of many complex diseases such as rheumatoid arthritis, diabetes, and breast cancer(99). Even short periods of misalignment of homeostatic cortisol rhythms in human subjects participating in controlled forced de-synchronization experiments are associated with the signs of insulin resistance (100). Additionally, the HPA axis also occupies a central role in responding to unpredictable and threatening environmental stressors (101). The stress-responsive

behavior of the HPA axis is further tuned by the circadian activity of its mediators. Exposure to an acute stressor results in the stimulation of the HPA axis and the sympathetic nervous system leading to the production and release of stress hormones such as, norepinephrine and glucocorticoids as well as other mediators such as cytokines, which interact within a vast physiological network and enable the host to actively re-establish homeostasis (102).

The concept of allostasis was introduced as an alternative hypothesis to explain the process by which the host actively maintains physiological stability (homeostasis) through appropriate deviations in critical physiological mediators from their basal activity levels in the face of both predictable and unpredictable environmental demands(103,104). Defined as the "maintenance of stability through change", allostasis, as proposed by Mcewen, offers a more precise and integrated description of the regulation of host fitness, physiological stressors, and the stress response than offered within the framework of homeostasis (105). While homeostasis is conventionally thought to be based on negative feedback architectures that restore physiological variables to their basal states upon their deviation by stressors (106-108), allostasis describes a labile equilibrium by which critical physiological mediators actively deviate from basal levels to trigger adaptive mechanisms that enable the host to cope with perceived stressors and subsequently re-establish homeostasis. Thus, within the allostatic framework, transient deviations in cortisol and other stress hormones from their basal predictive activity levels in response to stressors followed by their gradual return to pre-stress levels is considered to be beneficial by promoting host survival through the appropriate activation of immune processes and channeling of energetic resources (109,110).

However, chronic deviation of regulatory mediators from their basal levels through prolonged activation results in a physiological cost, termed "allostatic load"(111). Thus, chronic physiological stress resulting in sustained stimulation of the HPA axis leads to the accumulation of allostatic load and is associated with detrimental health outcomes, including depression, post-traumatic stress disorder (PTSD) and cardiovascular and metabolic disorders (111-113). Given that glucocorticoid mediated signaling effects have profound implications for host survival and fitness, it has been suggested that there is considerable selective pressure for the precise coordination of the mechanisms regulating HPA axis activity such that they maintain cortisol levels within an optimal operating regime. In such a context habituation of the HPA axis, such that glucocorticoid levels return to pre-stress levels in response to repeated or chronic exposure to the same stressor can provide the host with fitness advantages by allowing it to optimize energetic resources and prevent the persistent pathological dysregulation of downstream glucocorticoid-responsive signaling mechanisms as a result of the chronically disrupted glucocorticoid levels (114-116). However, successful habituation to chronic stress regimens requires the activation of further adaptive allostatic regulatory mechanisms, which might alter the homeostatic functioning of physiological systems when the host is exposed to novel environments or stressors. Certainly, habituation to chronic stress does not necessarily imply a removal of the allostatic load, and failure to resolve the chronic stressor might eventually result in the long-term disruption of glucocorticoid rhythms, further compromising homeostasis.

Such chronic accumulation of allostatic load is ultimately thought to result in an altered energetic state of the host (103,117). Considering the practical difficulty in

measuring changes in energetic expenditure and intake in a variable environment, it is suggested that monitoring changes in the concentrations of the physiological mediators of energy balance such as glucocorticoids can be indicative of allostatic state of the host (111). However, in the case of a habituating allostatic adaptation to chronic exposure of stress, when little discernible change in the levels of glucocorticoids occurs, it becomes increasingly difficult to characterize the allostatic state of the system. In such cases, a modeling-based approach can be a particularly useful tool for generating and evaluating experimentally verifiable hypotheses(118).

In the present work, we use a semi-mechanistic light-entrainable model of the HPA axis that accounts for circadian rhythmicity in the expression of its primary mediators in order to address the hypothesis that differential sensitivity and negative feedback within the HPA axis network lead to the observed sex differences CORT circadian rhythms. Moreover, we aim to predict specific functionally relevant adaptations that might occur upon its habituation to chronic stress (119).

## 3.2 Approach

We consider sex differences in the circadian rhythms of the activity of HPA axis hormones, since it provides a more complete representation of sexually dimorphic activity in comparison to studies including only a single time-point. To evaluate the above-mentioned hypothesis, we use three tunable parameters; one representing the adrenal sensitivity of CORT to ACTH, and two parameters representing the strength of GR-mediated negative feedback to CRH and ACTH respectively.

A schematic description of the primary interactions included in the model is depicted in **Figure 9**. The model captures both the sequential feed-forward induction of CORT whereby; CRH induces pituitary ACTH release, which stimulates the release of CORT from the adrenals, as well as the GR-mediated negative feedback of CORT on its precursors. A key assumption in our work is that the topological representation of the male and female HPA network is identical and does not explicitly account for any differences in biochemical signaling pathways that might result in sex differences in CORT circadian rhythms. Therefore, any differences between males and females will only be as a result of a difference in parameters of interest in the model. The processes represented by the parameters central to our hypothesis [**Figure 9**] include adrenal sensitivity, and the GR-mediated negative feedback, (labeled in green and black, respectively), while the remaining processes are defined by parameters common to both sexes. Thus, as depicted schematically in **Figure 9**, we assume that the gonadal hormones facilitate the expression of sex differences in the HPA axis through biochemical mechanisms that ultimately modulate processes represented by the three tunable parameters.

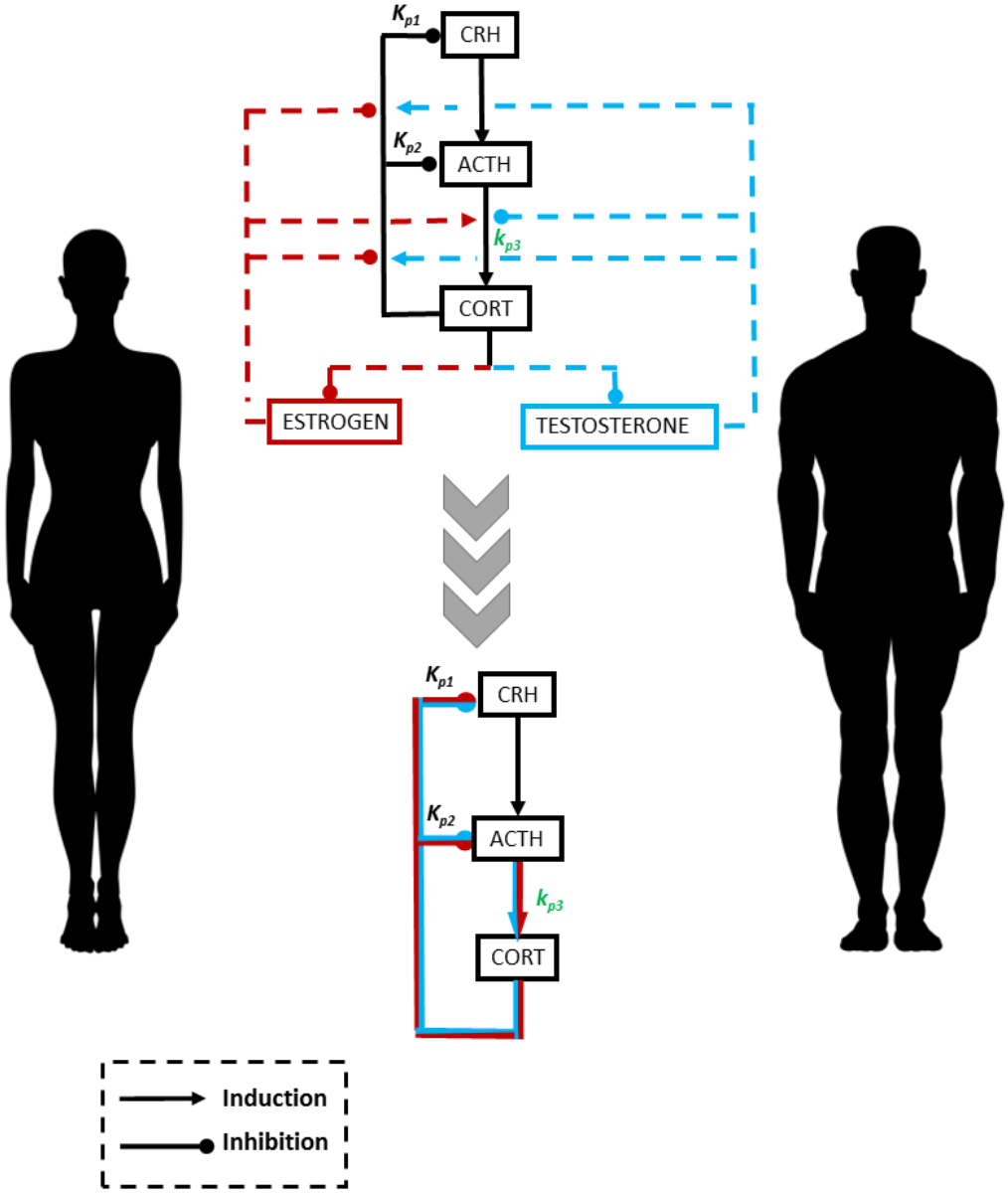


Figure 9: Schematic of the primary interactions modeled in the HPA axis. The influence of gonadal steroids, estrogen and testosterone, on the HPA axis is lumped into three tunable parameters representing the strength of glucocorticoid-mediated negative feedback and adrenal sensitivity within the HPA network.

Each of the primary mediators of the HPA axis, CRH, ACTH and CORT are represented by separate dynamical variables [**Equations 31-33**]. CORT negative feedback is captured by a pharmacodynamic model for glucocorticoid receptor dynamics [**Equations 35-37**], developed by Ramakrishnan et al. (36) and accounts for the

contributions of the free, bound fractions of cytoplasmic and nuclear glucocorticoid receptor (GR) species as well as GR mRNA. For simplicity, we only account for negative feedback through GR-mediated mechanisms and do not consider MR-mediated mechanisms in our model.

As in SA 1, hypothalamic CRH, which is described by zero-order synthesis and Michaelis Menten degradation kinetics **[Equation 31]**, proportionately stimulates the release of ACTH at the pituitary [**Equation 32]**, which subsequently stimulates the synthesis of CORT [**Equation 33]**. Finally, **Equations 31** and **33** also capture the ability of CORT to inhibit the synthesis of its precursors through a glucocorticoid receptor-mediated mechanism, where $K_i$ determines the strength of inhibition by CORT. In doing so, CORT binds to the cytoplasmic glucocorticoid receptor, which is determined by a second-order rate constant. The transcriptional and translational dynamics of the glucocorticoid receptor are also accounted for in **Equations 34 and 35**. Upon binding of CORT the cytoplasmic receptor-glucocorticoid complex translocates to the nucleus [**Equation 37**] to facilitate glucocorticoid-mediated gene expression, which for our purposes is limited to the negative feedback of CORT on its precursors as well as the synthesis of the glucocorticoid receptor mRNA.

In modeling the circadian rhythms of nocturnal rodents in our study we assume that light indirectly induces the degradation of CRH based on the mechanism suggested by Kalsbeek et al. whereby the light-mediated release of vasopressin inhibits CRH expression in the neurons of the hypothalamic PVN in nocturnal animals (120). Furthermore, a number of studies have shown a delay of approximately ~1-2 hours has been observed in the effect of light exposure on plasma cortisol (and CORT) levels (121).

However, the exact phase relationship between the onset of light and peak of the CORT circadian rhythms depends on both the time-scale of signal transduction as well the ability of light to synchronize the intrinsic CORT circadian rhythm via SCN-mediated signaling pathways. Since the exact photosensitive and neural signaling mechanisms by which light synchronizes the CORT circadian rhythm are yet to be elucidated and are too complex to model currently, we use a simple transit compartment model [**Equation 26-29**] to capture the approximately 1-2 hour delay between the light onset and its indirect effect (denoted by the term $light_{effect}$) on the production of CRH. While a simple step function is used to model the onset of light and dark phases [**Equation 25**], we use a Hill function to model the production of $light_{effect}$ [**Equation 30**] in order to reflect the photosensitive response of the light-mediated signaling pathways represented by our transduction model.

Given the experimental observations summarized in the previous section, we use our mathematical model of the HPA axis to evaluate the hypothesis that differences in male and female corticosterone rhythms are a result of two factors: (i) differences in adrenal sensitivity to circulating ACTH levels and, (ii) differential negative feedback inhibition of CORT precursors. In our model, the parameters $K_{p1}$ and $K_{p2}$ mathematically represent the biochemical processes responsible for the glucocorticoid-receptor mediated negative feedback of CORT on ACTH and CRH, respectively, while $k_{p3}$ represents the sensitivity of adrenal CORT secretion to ACTH. While it is quite possible that more parameters could be different between the male and the female HPA axis, we constrain our analysis to the three parameters mentioned above in order to evaluate our hypothesis. Importantly, as a first approximation, we assume that the parameters in our model

implicitly account for any physiological influence the sex hormones; estrogen and testosterone might have in determining the sexual dimorphism in the circadian rhythms of the HPA axis. Additionally, we make a further simplification by not explicitly accounting for possible sexual dimorphism in the modulation of the HPA axis by stress mediators such as the proinflammatory cytokines or any other stress-responsive elements such as the sympathetic nervous system.

**HPA Axis Mediators**

$$light = \begin{cases} 1 & 7{:}00 \le t \le 21{:}00 \\ 0 & 21{:}00 < t < 7{:}00 \end{cases} \quad \textbf{Eq. 25}$$

$$\frac{dlight_{TCsynth1}}{dt} = k_t\left(light - light_{TCsynth1}\right) \quad \textbf{Eq. 26}$$

$$\frac{dlight_{TCsynth1\,i}}{dt} = k_t\left(light_{TCsynth\,i-1} - light_{TCsynth\,i}\right), i = 3 \quad \textbf{Eq. 27}$$

$$\frac{dlight_{TCdeg1}}{dt} = k_t\left(light_{deg} - light_{TCdeg1}\right) \quad \textbf{Eq. 28}$$

$$\frac{dlight_{TCdeg\,i}}{dt} = k_t\left(light_{TCdeg\,i-1} - light_{TCdeg\,i}\right); i = 3 \quad \textbf{Eq. 29}$$

$$\frac{dlight_{effect}}{dt} = k_{us}\frac{light^n_{TCsynth\,i}}{K^n_{M,us} + light^n_{TCsynth\,i}} - k_{deg,us}light_{effect}(1 + k_{eff}light_{TCdeg\,i}) \quad \textbf{Eq. 30}$$

$$\frac{dCRH}{dt} = \frac{k_{p1}.K_{p1}}{K_{p1} + DR(N)} - V_{d1}.\frac{CRH \cdot \left(1 + \frac{light_{effect}}{1 + light_{effect}}\right)}{K_{d1} + CRH} \quad \textbf{Eq. 31}$$

$$\frac{dACTH}{dt} = \frac{k_{p2}.K_{p2}CRH}{K_{p2} + DR(N)} - V_{d2}.\frac{ACTH}{K_{d2} + ACTH} \quad \textbf{Eq. 32}$$

$$\frac{dCORT}{dt} = k_{p3}.ACTH - V_{d3}.\frac{CORT}{K_{d3} + CORT} \quad \textbf{Eq. 33}$$

$$\frac{dGR_{mRNA}}{dt} = k_{syn_{GRm}}.\left(1 - \frac{DR(N)}{IC_{50_{GRm}} + DR(N)}\right) - k_{deg}.GR_{mRNA} \quad \textbf{Eq. 34}$$

**Glucocorticoid Receptor Pharmacodynamics**

$$\frac{dGR}{dt} = k_{syn,GR}.GR_{mRNA} + r_f.k_{re}.DR(N) - k_{on}.(CORT).GR - k_{deg,GR}.GR \quad \textbf{Eq. 35}$$

$$\frac{dDR}{dt} = k_{on}.(CORT).GR - k_T.DR \quad \textbf{Eq. 36}$$

$$\frac{dDR(N)}{dt} = k_T.DR - r_f.k_{re}.DR(N) \quad \textbf{Eq. 37}$$

### 3.2.1 Calibrating the Model for Male and Female CORT Rhythms

We are primarily concerned with rodent studies, due to the greater reproducibility in observations in comparison to results from studies in humans, which are less consistent due to methodological issues arising from a difficulty to control for confounding factors

such as age, phase of menstrual cycle, circadian rhythmicity, and use of oral contraceptives. Experimental data on sex differences in the circadian rhythms of the Wistar rat HPA axis was obtained from Atkinson et al. (14). The study compared the plasma corticosterone and immunoreactive (I-) ACTH levels in males and females at each stage of estrous cycle using a serial blood-sampling technique that allowed for continual measurement of the HPA axis hormones throughout the 24-hour circadian cycle. All rats in this study were entrained to a 14-hour light/10-hour dark lighting schedule. We use an identical light schedule to entrain the HPA axis in our model. Atkinson et al. used cosinor analysis to characterize and compare the circadian rhythms of male and female rats across the estrous cycle.

As discussed earlier, we hypothesize that the negative feedback and adrenal sensitivity components define the focal points of convergence of the intrinsic sex-dependent differences; $K_{p1}$, $K_{p2}$ and $k_{p3}$ and therefore the analysis will focus on those. The parameters that account for the glucocorticoid receptor pharmacodynamics are obtained from previous work by Ramakrishnan et al. (36). Thus, of the parameters that are common to both sexes, we are primarily concerned with estimating the 8 that describe the behavior of the primary HPA axis mediators, CRH, ACTH and CORT **[Equations 31-33]**. Given that the model equations are non-linear and include feedback, multiple sets of sex-specific parameters might yield sexually dimorphic circadian profiles, therefore a sampling-based approach was undertaken. More importantly, a sampling-based approach is appropriate for our purposes since we are primarily interested in a sex-specific parametrization of the model by efficiently identifying possible parameter sub-spaces that can qualitatively replicate male and female CORT circadian rhythms. This enables us to

parametrically characterize both sex-specific differences in the HPA axis as well as the possible systematic variation in parameters that might account for inter-individual differences within each sex. Finally, this enables us to infer the properties of the system from a range of parameter sets, rather than just a single pair of parameter sets that optimally fit the average male and female experimental profiles, respectively (122) . Investigators have previously used such a sampling approach to determine multiple parametric solutions in calibrating their model (123,124).

In constructing the sample space, we used a method based on Sobol sequences (125). Sobol sequences belong to the class of quasi-random number generators, used to produce highly uniform samples of a unit hypercube. Quasi-random number generators aim to minimize the discrepancy between the distribution of generated points and a distribution of points equally-proportioned across each of the sub-cubes formed by a uniform partition of the unit hypercube (126). The algorithms generating Sobol sequences form successively finer partitions of the unit interval using a base of 2 and subsequently, reorder the generated coordinates in each dimension. We used the implementation provided in MATLAB 2016a with the commands `sobolset` and `net`, to generate an initial quasi-random Sobol point set (127,128). In order to decrease the probability of undesired correlations in the initial segments of sequence, we applied a random linear scrambling algorithm combined with a random digital shift (129,130) to the initial Sobol point-set to generate the final sample space used for each stage of our sampling protocol.

Briefly, the 14-parameter space is decomposed into two sets: the 8 parameter-set common to both sexes and two sets of the 3 sex-specific parameters($K_{p1}$, $K_{p2}$ and $k_{p3}$) encapsulating sex-dependent influences in adrenal sensitivity. We used the optimized

parameter values from our previous work as a nominal parameter set and varied them within ±50%, to generate a set of 50,000 Sobol samples (38). Using the male and female CORT profiles from Atkinson and Wadell (14), we first identify a representative set of parameter values. Subsequently, a targeted sampling of the sex-specific parameters $K_{p1}$, $K_{p2}$ and $k_{p3}$ was performed. By using such an approach, we try to avoid biasing our model behavior in favor of generating profiles matching those of one sex over the other; which might have been possible, were the set of common parameters selected arbitrarily. Sriram et al. have adopted an analogous parameter estimation approach in their model of the HPA axis for patients with PTSD and depression, where they first determine a shared set of parameters following which they estimate parameters central to their hypothesis (35). The three sex-specific parameters [**Table A3**, Appendix] were sampled over a wide range of values, while still allowing for a sample size that can be evaluated in a computationally reasonable amount of time.

In order to keep our analysis consistent with that in the study by Atkinson et al., we characterize the mean, amplitude and phase of our simulated circadian profiles using cosinors fitted to our simulated profiles. We scale all the cosinor parameters from the experimental study by the mean of the male cosinor and subsequently calibrate our model to the scaled circadian rhythms (54,56). Therefore, we calibrate our model by comparing the cosinors fitted to our simulated circadian profiles to the cosinors obtained by Atkinson et al in their experiments. The simulated circadian profiles generated by these samples were accordingly, selected and classified as “male” or “female” circadian profiles if their cosinor parameters were within ±1 standard deviation of the scaled experimental cosinor parameters obtained by Atkinson et al. These error criteria are listed

in **Table A3** (Appendix). Using these criteria enables us to characterize inter-individual variability in the HPA axis, while still selecting for parameters that capture the qualitative differences between the male and female CORT profiles observed in the experiments. A similar procedure to classify model responses has been used in prior work (123).

### 3.2.2 Response to Bolus Injection of ACTH

We studied the CORT response to in-silico ACTH stimulation in order to determine whether the systems specified by the putative sex-specific parameter spaces differ in their responsiveness. A bolus injection of ACTH was simulated as a single pulse perturbation in the ACTH rhythm **[Equation 32]**. A pulse perturbation in ACTH was adopted since it simulates a bolus injection of ACTH, a procedure used by number of experimental studies in order to determine sex differences in the HPA axis sensitivity (11,131). The pulse perturbation was simulated by pausing the integrator at the desired time-point for the pulse administration, increasing the concentration of the mediator by a constant amount, while keeping the value of all other dynamical variables constant and subsequently continuing the integration. This protocol has also been used to simulate pulse perturbations in previous in-silico models of the HPA axis (132). We quantify the CORT response to ACTH injection by calculating the difference in area under curve (AUC) between the stimulated and nominal conditions for 4 hours from the application of pulse perturbation for the systems described by male and female parameters sets, respectively. Finally, we administer the pulse at multiple time points in order to determine whether the model exhibits a time-of-day dependent response to ACTH stimulation. The Kruskal-Wallis test was applied to determine statistically significant differences between the male and female responses to acute ACTH injection.

### 3.2.3 Regulatory Adaptation to Chronic Stress

We aim to characterize putative adaptations occurring in the system by determining the possible changes in male and female parameter subspaces exhibited upon habituation to chronic stress. In order to simulate conditions of chronic stress, we adopt a method previously used by Sriram et al. where, $k_{p1}$, the zero-order rate of synthesis of CRH, is elevated to a chronically stressed value, thereby resulting in an increase in CRH drive within the HPA axis network. Following this, we resample the three sex-specific parameters, $K_{p1}$, $K_{p2}$ and $k_{p3}$, and repeat the classification procedure described previously to identify the "male" and "female" parameter sub-spaces in the chronically stressed condition. This process is carried out for two different values of $k_{p1}$.

Subsequently, we study the system response to an acute stressor for male and female parameter sub-spaces both in the case of the basal state of the system (a the nominal $k_{p1}$value, in the absence of chronic stress) as well as in the "chronically stressed" states described above. By doing so, we determine possible differences in HPA axis responsiveness as a result of the adaptations to chronic stress, and thus attempt to quantitatively characterize the cost to adaptation within a more physiologically relevant framework. The acute stressor is simulated as a transient increase in the rate of production CRH [**Equation 39-40**]. The response to the acute stressor is characterized by the difference in AUC between the respective stressed and nominal profiles for 4 hours from the in-silico administration of the acute stressor. As in the case of the ACTH injection, we simulate the stressor at various times during the circadian period of CORT to determine whether our model predicts the existence of a time-of-day dependent response to the acute stressor. The Kruskal-Wallis test was applied to determine

statistically significant differences in the acute stress response between the stressed and nominal conditions as well as between the sex-specific acute stress responses.

$$\frac{dstress}{dt} = -k_{stress.out} stress \quad \textbf{Eq. 39}$$

$$\frac{dCRH}{dt} = \frac{k_{p1}.(1 + k_s.stress).K_{p1}}{K_{p1} + DR(N)} - V_{d1}.\frac{CRH \cdot \left(1 + \frac{light_{effect}}{1 + light_{effect}}\right)}{K_{d1} + CRH} \quad \textbf{Eq. 40}$$

Finally, in order to study possible inter-individual variability in the adaption to acute chronic stress, we used a procedure developed by Lin et al. (133) to symbolically partition the acute stress response for the individual male and female parameter sets for each of the three cases (no chronic stress, intermediate chronic stress and high chronic stress). Briefly, the acute stress response at a specific time-point for the parameters sets comprising the three surfaces was pooled together for males and females, respectively, and subsequently z-scored. Following this, the z-scored values were partitioned into five equiprobable regions, and assigned symbols from 1-5, with 1 and 5 representing the z-scored values at the lower and upper tails of the normal distribution, respectively. For a more detailed review of the procedure the reader is referred to Lin et al (133).

### 3.2.4 Cosinor Analysis

Cosinor rhythmometry is a commonly used technique for the analysis of both experimental and simulated circadian data (134). We employed cosinor analysis to

estimate characteristic parameters of the circadian rhythms of the primary HPA axis mediators. This enabled us consistently compare the circadian characteristics of our simulated data with those obtained from experiment (14).

Cosinor analysis involves the fitting of a sinusoid to the dataset using nonlinear regression. Depending on the nature of the data, one can attempt to fit a single sinusoidal component, or multiple sinusoids. For the purposes of our simulation, we use a single sinusoid to fit our simulated rhythms in order to keep our analysis consistent with analysis carried out by Atkinson and Wadell (14), who, as mentioned above, also use a single sinusoid to quantify sex differences in the circadian rhythms of corticosterone and ACTH in their experiments.

The regression model is generally represented as shown in **Equation 41,** where $M$ is the MESOR (Midline Estimating Statistic Of Rhythm), a rhythm adjusted mean; $2A$ is the measure of the predictable change within the data (the amplitude); $\phi$ is the acrophase of the rhythm; $\tau$ is an estimate of the period of oscillation; and $\varepsilon$ are the errors accounting for the difference between model predictions and the data.

$$Y(t) = M + A \cdot cos\left(\frac{2\pi(t-\Phi)}{\tau}\right) + \varepsilon \qquad \textbf{Eq. 41}$$

## 3.3 Results

### 3.3.1 Distinct Male and Female Parameter Spaces

We first determined the most suitable parameter set for the 8 HPA axis parameters common to both sexes. Values for these parameters are listed in **Table A4 (Appendix)**. As detailed in the methods, we fix the values for these 8 common parameters along with the parameters for GR receptor dynamics, and subsequently

sample only the sex-specific parameters ($K_{p1}$, $K_{p2}$ and $k_{p3}$) to identify solutions that replicate experimental male and female CORT profiles to within ±1 SD of their cosinor parameters. The cosinor parameters (mean ± SD) for the simulated CORT profiles are presented in the Appendix. Following this procedure, we are able to identify two distinct, parameter sub-spaces, which correspond to male and female CORT solutions, respectively. The two parameter-spaces are represented as surfaces as shown in **Figure 10**. These surfaces are constructed from the Delaunay triangulation of the discrete points contained on the surface. Importantly, in agreement with experimental results the CORT profiles generated by the parameters sets within the male and female parameter spaces capture the significant differences in circadian amplitude between males and females and are in good qualitative agreement with experimentally observed CORT circadian rhythms [**Figure 11]**. Notably the parameter sub-spaces exclusively define either male or female CORT profiles. Furthermore, the male and female parameter spaces span a relatively wide range of parameter values. Interestingly, despite the wide range of values that the parameters can assume within each sex-specific sub-space, there appears to be a relationship between the three individual parameters, as defined by the surface, such that they generate qualitatively similar CORT profiles. Moreover, there is an inverse relationship between the parameter representing the strength of inhibition of CRH by CORT ($K_{p1}$), and the parameter representing the strength of inhibition of ACTH by CORT ($K_{p2}$) for both male and female parameter spaces. It is observed that on average the parameter sets that constitute the female parameter space have higher levels of adrenal sensitivity ($k_{p3}$) than the parameters sets constituting the male parameter space.

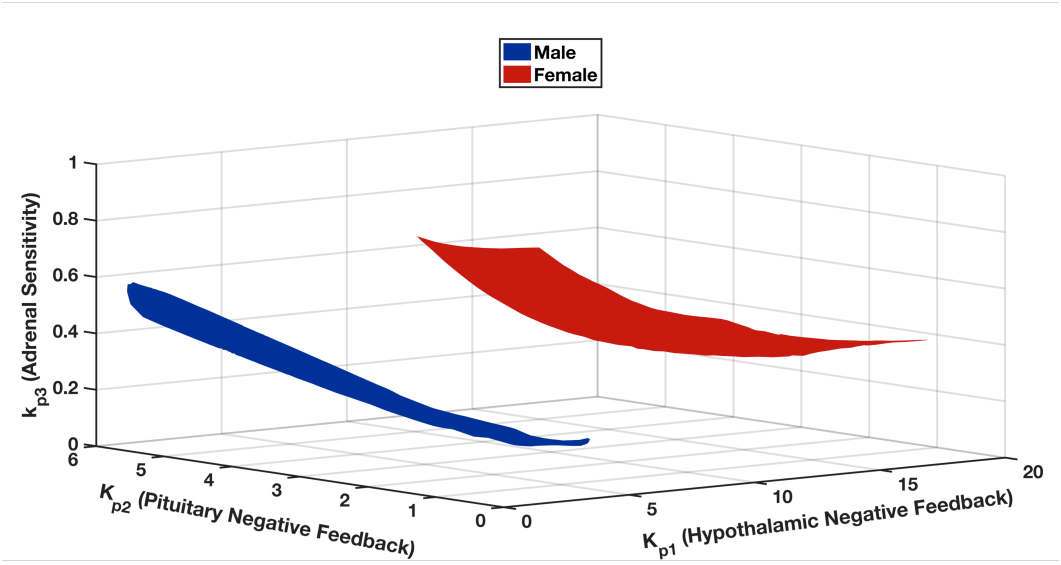


Figure 10: Distinct male (blue) and female (red) parameter spaces for putative sex-specific parameter in the model. The parameters sets within these regions satisfy the error criteria shown in Table A3, (Appendix).

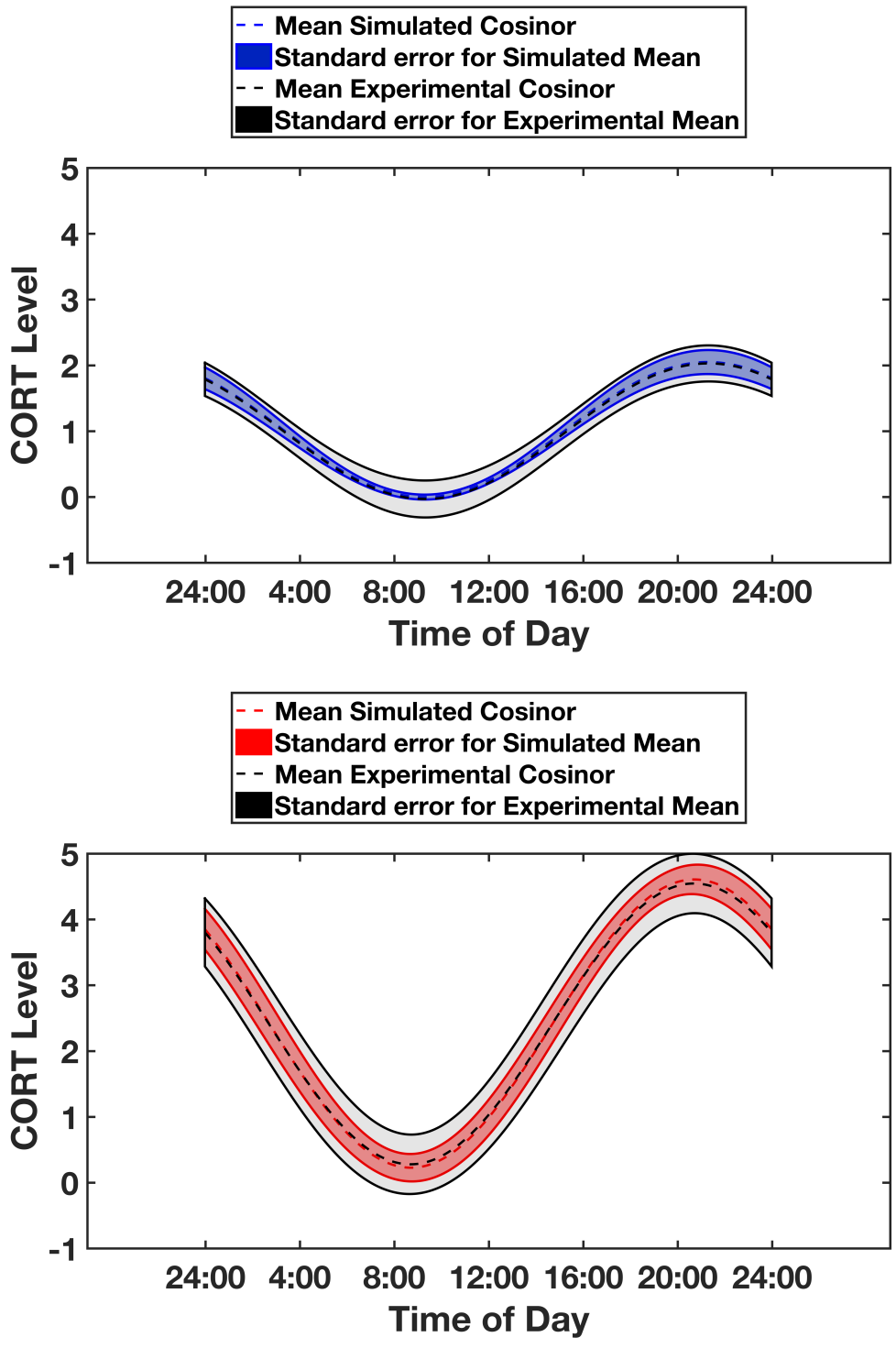


Figure 11: Representative circadian CORT profiles generated by the parameter sets within each parameter space shown in A. The blue dashed line (top) represents the mean of CORT circadian profiles generated by the male parameters, while the red dashed line (bottom) represents the mean of the CORT circadian profiles generated by the female parameters. The blue (top) and red (bottom) shaded areas represent the standard deviation of the male and female simulated CORT circadian profiles, respectively. The black dashed lines represent the experimental cosinors,

for male (top) and female (bottom) parameters, respectively. The gray shaded areas represent the standard deviation of the male (top) and female (bottom) experimental CORT cosinors, respectively.

The circadian characteristics of the remaining model variables, CRH, ACTH and translocated receptor bound CORT (described DR(N)) were determined to gain further insight of baseline system behavior. **Figure 12A** and **Figure 12B** depict the parameter sets composing the surfaces, with the color of the markers denoting the mean of ACTH circadian rhythms. We find that the mean value of ACTH remains nearly unchanged for a given value of adrenal sensitivity ($k_{p3}$).

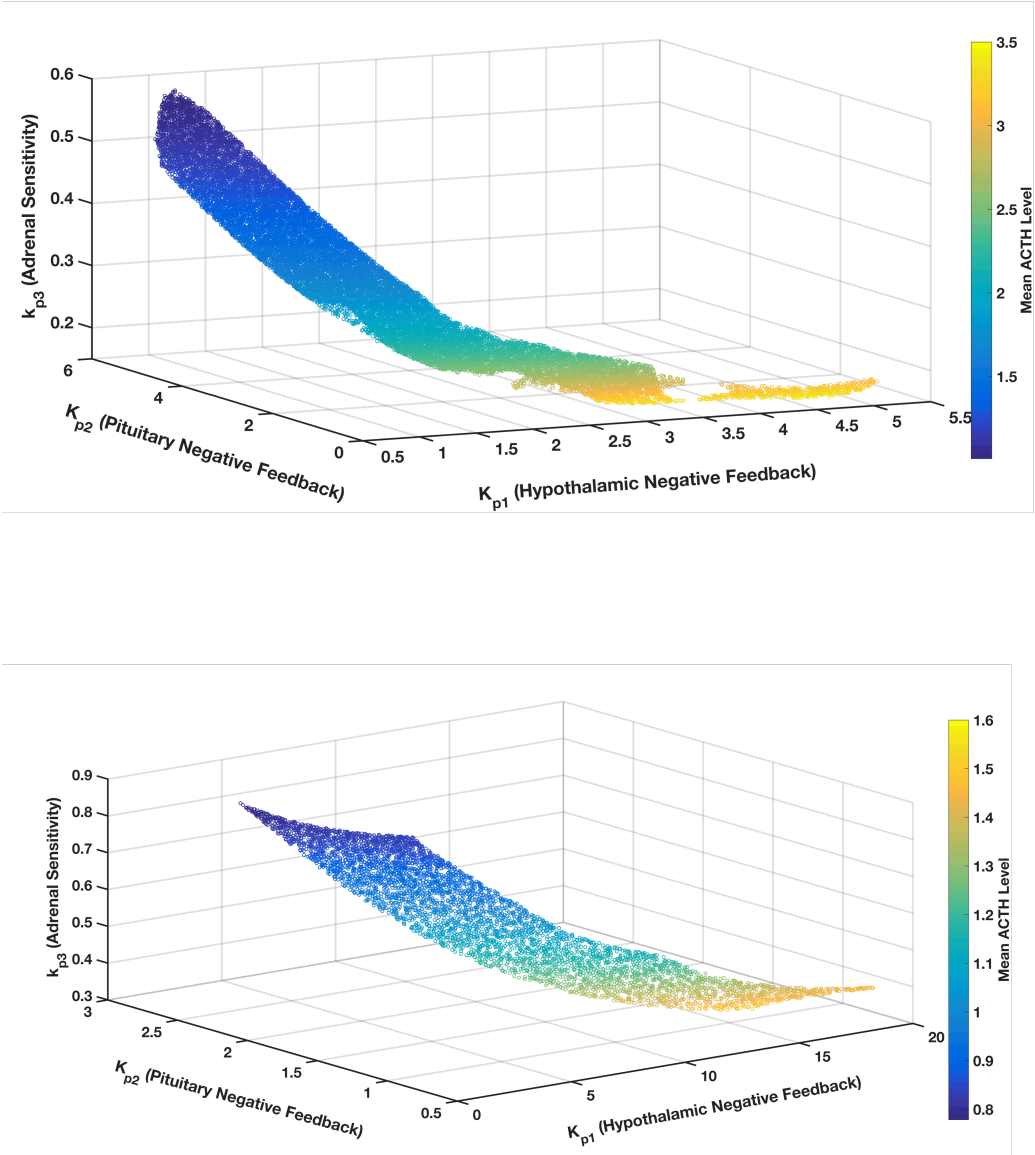


Figure 12: Mean levels of ACTH for both male (top) and female (bottom) parameters constituting the surfaces in Figure 10. Note the different scales on the color bars for male and female ACTH mean levels.

Furthermore, the mean value of ACTH generally increases with decreasing adrenal sensitivity ($k_{p3}$) for both in-silico male and female parameter spaces. **Figures 13** and **14** show that while the CORT circadian rhythms are constrained to a relatively narrow range of values, there is much more variability in the circadian rhythms of ACTH

and CRH, with CRH rhythms showing the greatest variability. This relationship is observed for both in-silico male and female solutions.

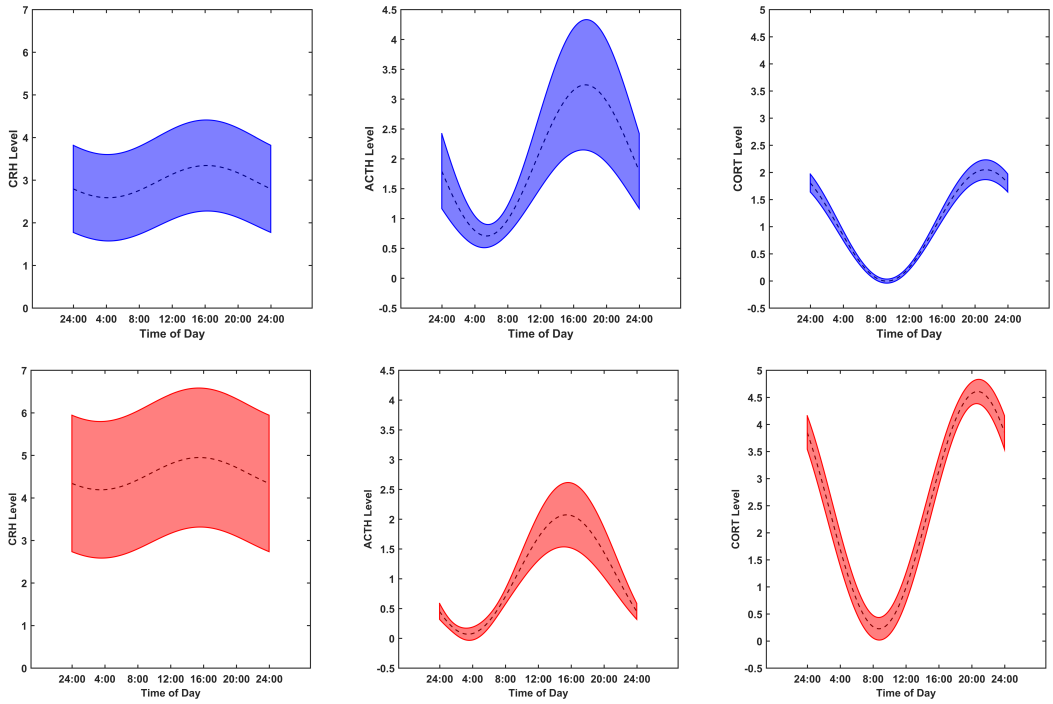


Figure 13: Representative circadian dynamics of the primary HPA axis mediators, CRH, ACTH and CORT, for both male (top, blue) and female (bottom, red) parameter sets. The black dashed lines represent the mean, while shaded areas represent the standard deviation of the cosinors for males and females, respectively.

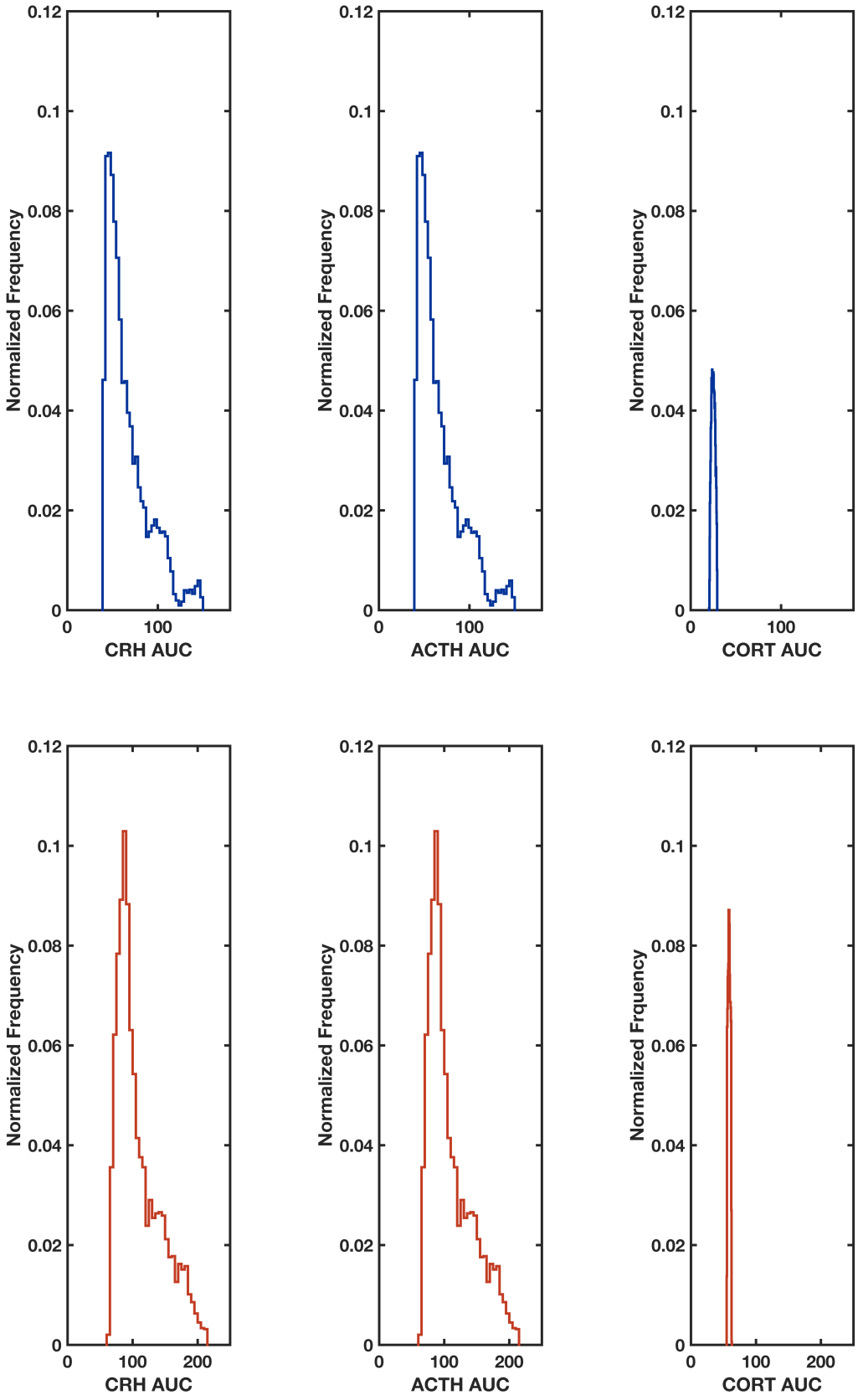
0.12
0.1
0.08
0.06
0.04
0.02
0
Normalized Frequency
0
100
CRH AUC
ACTH AUC
CORT AUC
200
Normalized Frqquency

Figure 14: Distribution of AUC indicating greater variability in CRH and ACTH activity in comparison to CORT activity for in-silico males (top, blue) and females (bottom, red).

Furthermore, our model predicts that on average the CRH levels are greater in in-silico females than in males, while, ACTH levels tend to have a higher peak in males than in females. Finally, as can be seen in **Figure 15** mean levels of nuclear translocated receptor bound CORT, DR(N) **[Equation 37]** are generally higher for in-silico females than males.

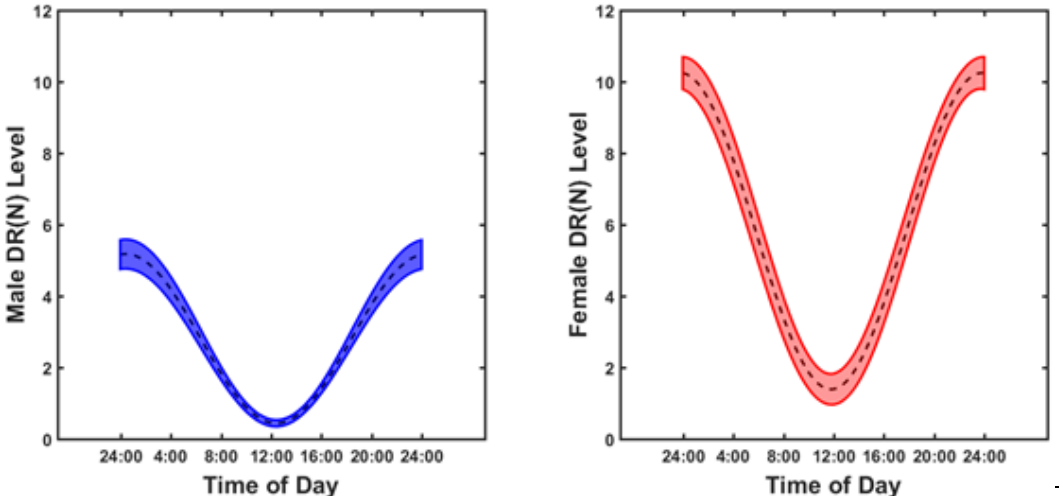


Figure 15: Representative circadian dynamics of nucleated receptor-bound CORT, DR(N), for both male (left) and female (right) parameter sets. The black dashed lines represent the mean, while shaded areas represent the standard deviation of the cosinors for males and females, respectively.

### 3.3.1.1 Response to Bolus ACTH Injection

Results presented in **Figure 16** were obtained by simulating an ACTH bolus injection at multiple time-points during the course of a 24-hour period for profiles defined by the male and female parameter sets shown in **Figure 10** and depicts the difference in AUC between stimulated and nominal conditions for in-silico males and females. Interestingly, CORT shows a significant time-of-day dependent response to ACTH stimulation. However, despite this significant variation in CORT response, in

silico-females, on average, consistently secrete greater amounts of CORT than do in-silico males.

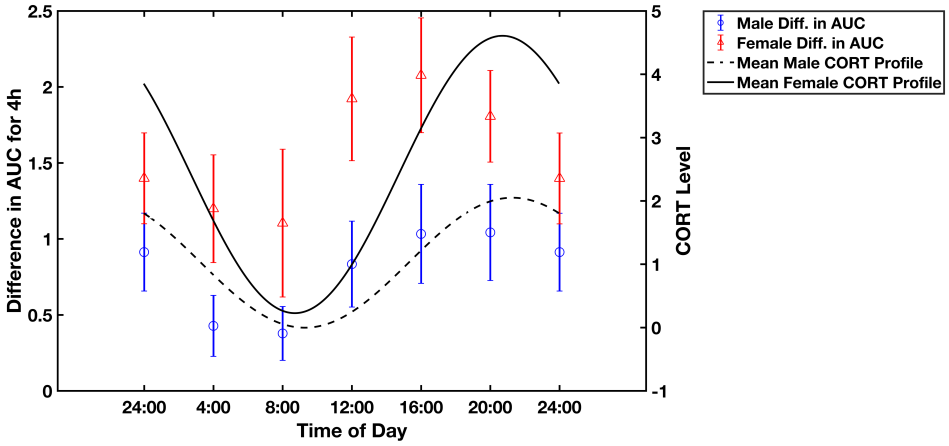


Figure 16: Time-of-day dependence of the CORT response to ACTH injection, characterized as the difference in AUC between stimulated and nominal profiles within the first 4 hours after stimulation. The mean female cosinor is depicted by the solid black line, while the mean male cosinor is depicted by the dashed black line. The blue circles and red triangles with error bars depict the difference in AUC for 4 hours from stimulation for males and females, respectively. In all cases the female response is statistically significantly greater than the male response at a given time point ($p<0.01$ using the Kruskal-Wallis test).

Finally, comparing the acute stress responses between nominal in-silico males and females (without exposure to chronic stress), [**Figure 17**] our model predicts that females have a more pronounced stress response at time-points closer to the transition from the dark (active) phase to light (inactive) phase. In all cases considered, our in-silico experiments indicate a strong time-of-day dependence in the stress response.

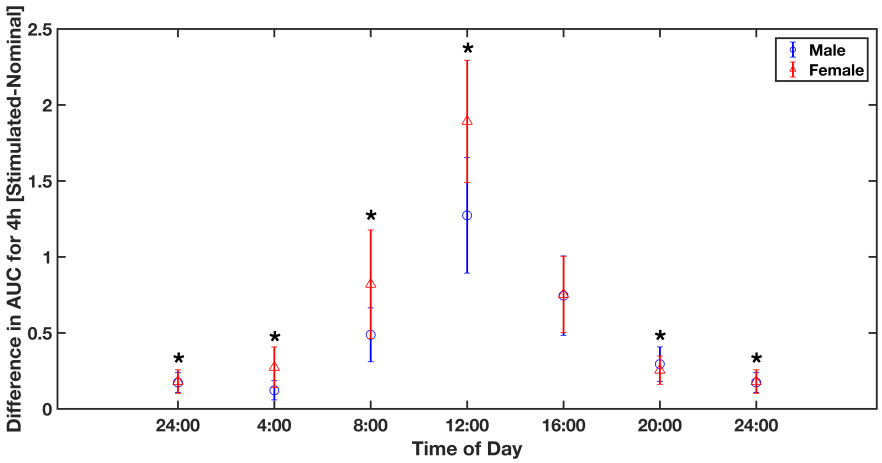


Figure 17: The difference in AUC for 4 hours from the application of acute stressor at the indicated time-points during the day for males (blue circles) and females (red triangles) with nominal kp1 levels (without chronic stress). Asterisks indicate a significant difference between males and females at that time-point, as determined by the Kruskal-Wallis Test ($p<0.01$).

### 3.3.1.2 Adaptation to Chronic Stress and Individual Variability

Within the framework of allostasis, adequate flexibility in glucocorticoid responsiveness enables the host to suitably adapt to transient environmental challenges (105,117). However, given the important regulatory role of glucocorticoids there is, at the same time, basal glucocorticoid activity must be constrained within reasonable physiological bounds such that compensatory downstream homeostatic processes necessary for host survival are optimally balanced (103). Thus, the physiological need for the system to conserve a primary phenotype, namely basal circadian activity, while also allowing for adequate stress responsiveness, permits the coexistence of a multitude of individually "customized" regulatory strategies (135).

While transient perturbations in the basal glucocorticoid rhythms in response to acute stressors is beneficial, chronic deviation from nominal rhythmicity results in dysregulated, potentially pathological, functioning (105). Therefore, to prevent persistent dysregulation of glucocorticoid responsive signaling mechanisms, the host can habituate

to an unresolved low-level chronic stressor, through adaptations in the relative strength of the regulatory arms, thereby enabling the maintenance of homeostatic glucocorticoid circadian rhythmicity. However, such adaptations are associated with a physiological cost, likely the result of allostatic load accumulation (136).

As discussed previously (35), chronic stress induced activation of the HPA axis is thought occur as a results of increased hypothalamic drive (represented in our model by persistently increased values of $k_{p1}$). Allostatic habituation to chronic stress results in adaptation of regulatory mechanisms so as to maintain basal circadian levels of glucocorticoids (in our case, CORT) [**Figure 18B, Supplementary Figures S1, S2**]. These adaptations imply an average increase in the adrenal sensitivity, $k_{p3}$of the system, while at the same time resulting in increased hypothalamic negative feedback and a slight decrease in pituitary negative feedback (increased $K_{p2}$ levels). Regulatory diversity is still observed upon allostatic habituation, as indicated by the ensemble of regulatory parameters, which maintain homeostatic rhythms. However, an overall loss of the flexibility of the system is also observed in order to maintain these rhythms, as indicated by the reduction in the overall area of the surfaces as the level of chronic stress increased. In other words, while the system still maintains its regulatory diversity even under conditions of chronic stress and allostatic habituation the regulatory flexibility of the system is reduced thus, rendering it more challenging to maintain homeostatic rhythms.

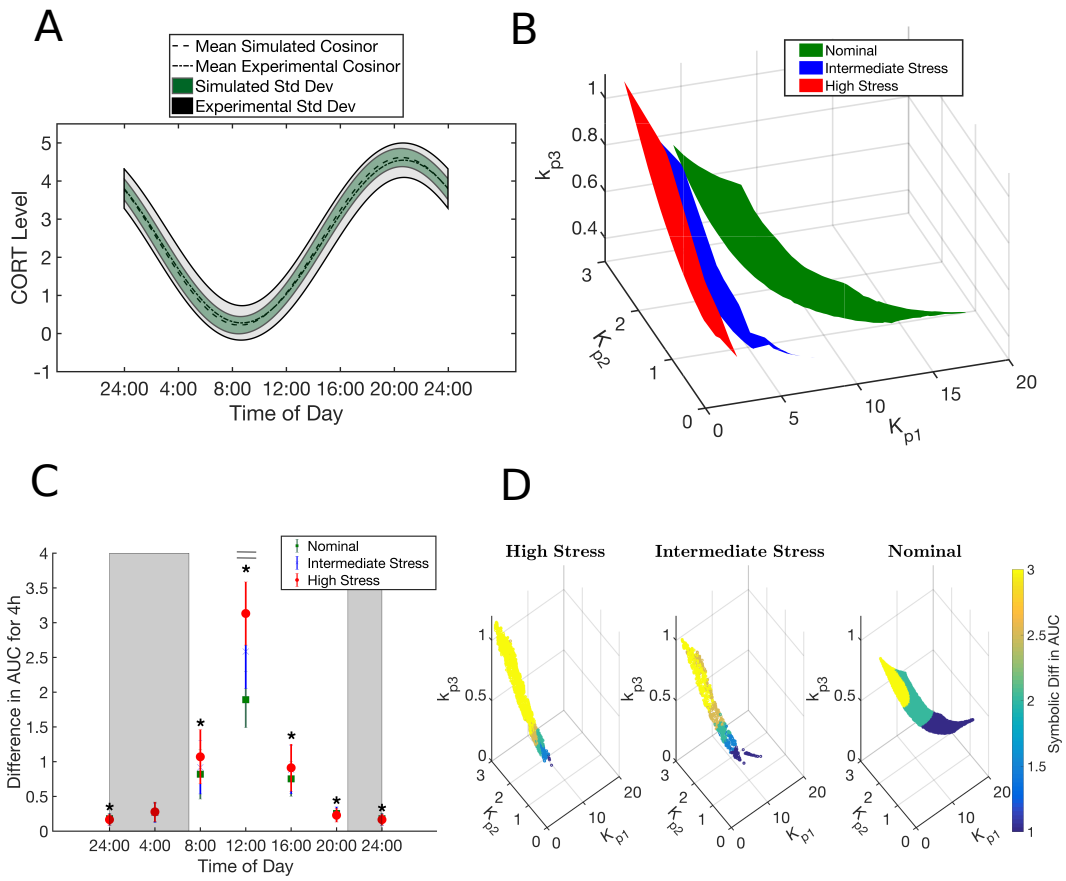


Figure 18: a) Simulated corticosterone cosinor rhythms that qualitatively match experimentally obtained cosinor rhythms as generated by the parameter sets constituting the b) nominal parameter space. There is a balance between the three regulatory mechanisms considered here such that they match the experimental rhythms. Upon habituation to chronic stress the nominal parameter space (green) allostatically adapts to increasing levels of chronic stress such that the system still produces nominal corticosterone rhythms. The allostatic adaptations include a substantial increase in the average strength of hypothalamic negative feedback decrease, accompanied by a sharp decrease in the range of the $K_{p1}$ values that the system can take. Furthermore, there is an increase in the average adrenal sensitivity and a slight decrease in the strength of pituitary negative feedback. These adaptations result in a decrease in the area of the surfaces with increasing chronic levels of chronic stress, which implies a decrease in underlying regulatory flexibility of the system. c) The acute stress response of the system is increased when exposed to a stressor in the middle of the inactive phase. (Bottom) We find that at the same level of adrenal sensitivity chronically stressed individuals respond more strongly to a subsequent stressor than individuals in the nominal case as shown by the increase in individuals with high (yellow) response with increasing levels of chronic stress. d) In both the nominal and chronically stressed conditions, the acute stress response increases with increasing adrenal sensitivity. Moreover, we find that there is a sensitization of the stress response upon habituation to chronic stress, with individuals with higher adrenal sensitivity more likely to exhibit stress sensitization as indicated by the increase in the proportion of parameters exhibiting the most robust acute stress response (denoted by the yellow region).

If the system, despite chronic stress and the associated allostatic load, is still able to maintain its homeostatic phenotype, it is natural to question whether the regulatory. In

order to better quantify the allostatic load and understand the implications of these regulatory changes for the functional characteristics of system, we characterize system's response to an acute stressor subsequent to allostatic habituation. The acute stressor is simulated by inducing a transient increase in CRH production, as would occur in response to a bolus injection of an HPA axis stimulant, such as bacterial lipopolysaccharide (137). The HPA response to acute stress is quantified by calculating the area under the curve (AUC) of CORT over a 24hr period following exposure to the (acute) stress (138). We determine that habituation to chronic stress results in time-of-day dependent alterations in the system's acute stress response. Specifically, after habituation to chronic stress, the acute stress response of the HPA axis is sensitized when experienced towards the middle of the inactive phase relative to the nominal homeostatic state [**Figure 18C**]. In studying the individual differences in acute stress response in the nominal case without exposure to chronic stress, we determined that individuals with higher adrenal sensitivity tend to have a more robust acute stress response [**Figure 18D**]. We hypothesized that chronic stress habituation would alter these individual differences in acute stress response during the inactive phase. We used a symbolic representation method to partition the acute stress responses in order to qualitatively differentiate between them(133). We find that chronic stress habituation results in a sensitization of the response such that, individuals with same adrenal sensitivity responds more strongly in the chronically stressed state [**Figure 18D**]. Therefore, the sensitization of the acute stress response results in a potentially pathological glucocorticoid overexposure of downstream host signaling pathways. This phenomenon of chronic stress sensitization has been frequently observed experimentally, where habituation to a chronic stressor

results in a more pronounced response to an acute stressor in comparison to the homeostatic state (26) .

**Intrinsic Ability of Adaptation *versus* relaxation:** The ability of rhythmic endogenous systems, such as the HPA axis, to synchronize to environmental, as well as internal *zeitgebers* is of critical evolutionary and adaptive significance (139). The proper synchronization of endogenous signaling systems, such as the HPA axis, to both environmental as well as internal zeitgebers is of critical adaptive significance(139). Under the entraining influence of light, the parametric subspaces shown in Figure 10 generate glucocorticoid circadian rhythms that match experimental data. However, we anticipate that underlying regulatory variability in the system will result in variability in its intrinsic entrainment properties and thus, predispose the system to differentially respond to frequency fluctuations in an entrainer depending on its regulatory constitution.

Therefore, as a measure of the adaptability of the system, we aim to determine how the entrainment properties of the system vary with putative differences in regulatory dynamics, which we suggest might occur either as a result of individual differences or as a result of regulatory adaptations to chronic stress exposure. A standard metric for evaluating the entrainment characteristics of the endogenous oscillator is to assess the range of entrainer periods for which the endogenous oscillator is phase-locked to the entrainer as a function of the coupling strength between them(140). The domain of entrainment, referred to as the Arnold tongue, is indicative of how responsive an endogenous circadian oscillator is to fluctuations in the period of an environmental zeitgeber (141-143). The intrinsic entrainment properties of the system exhibit a systematic dependence on the strength of negative feedback and adrenal sensitivity

within the HPA network. Our model of the HPA axis predicts that in the nominal condition (without chronic stress) simulated individuals with higher adrenal sensitivity tend to have wider range of entrainment for the same relative zeitgeber strength than those with lower adrenal sensitivity [**Figure 19A**] (greater flexibility in adaptation to changing environments).

Moreover, by comparing the simulated individuals with the same level of adrenal sensitivity as shown in [**Figure 19B**], the simulated individuals that are not subjected to chronic stress tend to have the widest domain of entrainment, with the Arnol'd tongue becoming smaller with increasing the levels of chronic stress (increasing the value of $k_{p1}$). This implies that despite having maintained homeostatic levels of HPA output, the system must adapt its regulatory processes in order to maintain the same adrenal sensitivity such that it compromises on its range of entrainment (ability to adapt).

A related question concerns the ability of the system to absorb perturbations as a function of the oscillator's (HPA axis) characteristics. For a periodic system, this property is quantified by the Floquet exponent, which is representative of the system's stability to amplitude perturbations (144). Our simulations show that the calculated Floquet exponents decrease with increasing adrenal sensitivity for both the unstressed as well as chronically stressed parametric subspaces, respectively. Moreover, we find that at a given level of adrenal sensitivity ($k_{p3}$) the value of the leading Floquet exponent tends to increase with the level of simulated chronic stress exposure [**Supplementary Figure S4, Table A5**]. In other words, the more easily the system is entrained, the more sensitive it becomes. In agreement with our results, Abraham et al. (142) show both theoretically using limit cycle oscillators of varying complexity as well as experimentally for circadian

oscillators in the SCN and in fibroblasts that for a given zeitgeber strength the range of entrainment of these oscillators varies inversely with the intrinsic amplitude of the oscillator [**Supplementary Figure S5**] and the rigidity of the oscillator given by its amplitude relaxation rate (inferred from the Floquet exponent).

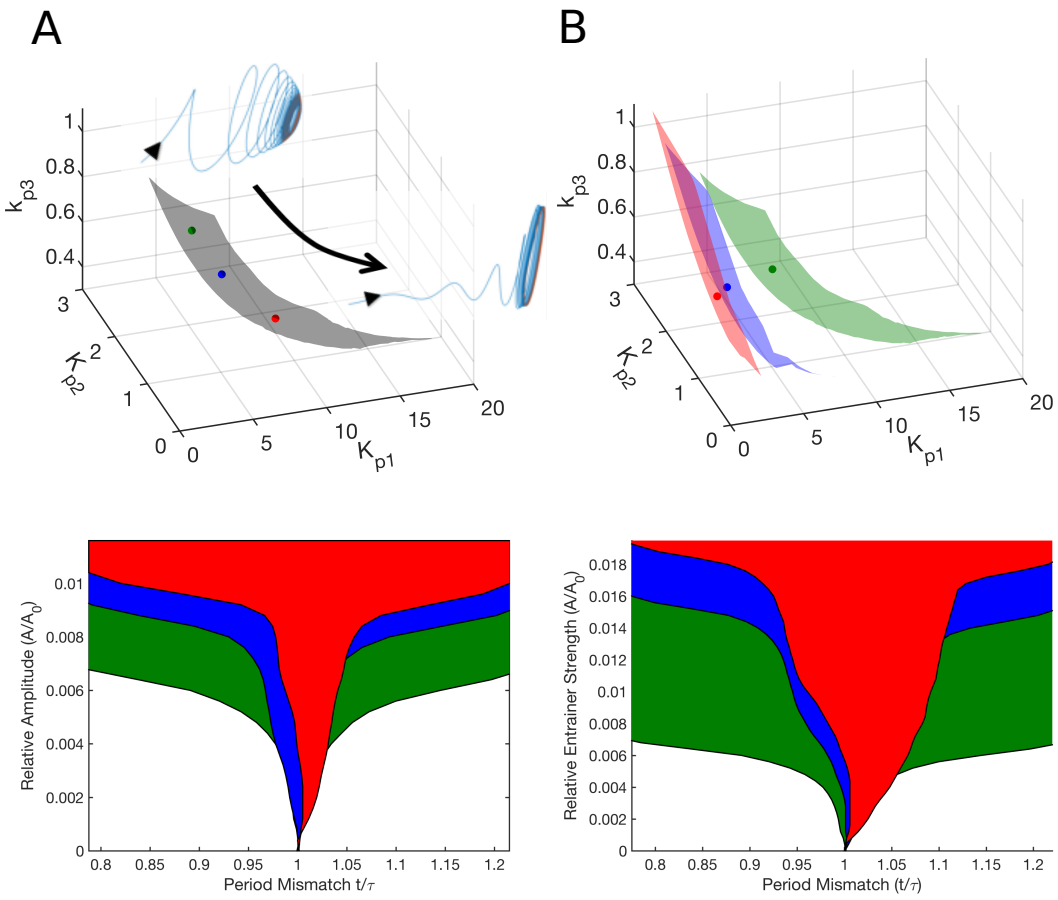


Figure 19: a) The domain of entrainment (depicted by the Arnold tongue) decreases with decreasing adrenal sensitivity. The parameter set with lowest adrenal sensitivity is depicted in red, that with intermediate adrenal sensitivity is depicted in blue and that with the highest adrenal sensitivity is depicted in green (Top). Arnold tongues are shown for the three representative parameter sets on the nominal unstressed surface with decreasing adrenal sensitivity (Bottom). This implies that simulated individuals with higher adrenal sensitivity are more flexibly entrained to changes in the zeitgeber frequency. Parameter t represents the entrainer period, while τ represents the intrinsic period of the oscillator. Furthermore, we find that the stability of the system to amplitude perturbations increases with decreasing adrenal sensitivity as depicted qualitatively by the rapid return of the system to the stable homeostatic oscillatory solution after an acute perturbation (Top). b) The domain of entrainment (depicted by the Arnold tongue) decreases with increasing levels of chronic stress for parameter sets at the same level of adrenal sensitivity. The parameter set in the nominal unstressed case is depicted in green, the parameter set in the case of intermediate stress is depicted in blue, and that in the case of high stress is depicted in red (Top). The width of Arnol'd tongue decreases with increasing levels of chronic stress when comparing parameter sets at the same level of adrenal sensitivity (Bottom). This implies that chronic stress decreases the ability of the system to be flexibly adapt to changes in the zeitgeber

frequency. t represents the entrainer period, $\tau$ represents the intrinsic period of the oscillator, A represents the amplitude of the entrainer, while $A_0$ represents the entrainer strength.

**Response to Transient and Permanent Changes in the Light-Dark Schedule:** Given that regulatory variability results in differences in the intrinsic entrainment characteristics of the HPA axis, we next sought understand the implications of these differences for the behavior of the system in response to two cases of physiologically relevant perturbations in light/dark schedule. Understanding the system's response to perturbations in the light schedule can provide improved insight into how regulatory variability might influence an individual's tolerance to shiftwork or jet lag (141).

In the first case, we tested the hypothesis that differences in the regulatory constitution of the nominal system resulted in a differential response of the HPA axis to a transient inversion (lasting 96h) of the light/dark cycle, meant to simulate the effects of shift work. Studies suggest that the maximal circadian phase-shift during shift work is an important parameter that might be predictive of tolerance to shift work schedules (145,146). Therefore, we characterized the maximal phase shift in the corticosterone circadian rhythm after a transient inversion of the light/dark cycle. The maximal phase-shift is greater for simulated individuals with greater adrenal sensitivity and hypothalamic negative feedback [**Figure 20A**].

Moreover, comparing these results to those for the domain of entrainment, we find that simulated individuals with a smaller domain of entrainment (narrower Arnold tongue) are also more resilient to changes in the phase of the corticosterone rhythm upon the transient perturbation of the light/dark schedule.

Following this, we sought to determine how the underlying regulatory diversity influences the time required for the system to re-synchronize following a permanent shift in the light-dark schedule. The time to re-synchronization is considered to be an important parameter with implications for understanding factors determining tolerance to circadian disruption during jet lag (147,148). Similar to the maximal phase perturbation following a transient perturbation in light-schedule, we find a parametric dependence of the time required for re-synchronization to the new light-dark schedule. Subjects exhibiting the maximal phase perturbation in response to a transient change in light/dark schedule also exhibit the shortest time to resynchronization upon a permanent change in light/dark schedule [**Figure 20B**]. In other words, subjects who were more susceptible to disruption were the fastest to adopt the new photoperiod schedule. Thus, our model simulations predict that simulated individuals with the greatest adrenal sensitivity and hypothalamic negative feedback take the least time for adaptation. Our results therefore highlight an interesting trade-off in that individuals that fare better in accommodating transient changes in photoperiod, (shift-work) are not able to adapt as swiftly to permanent changes in photoperiod (jet lag)

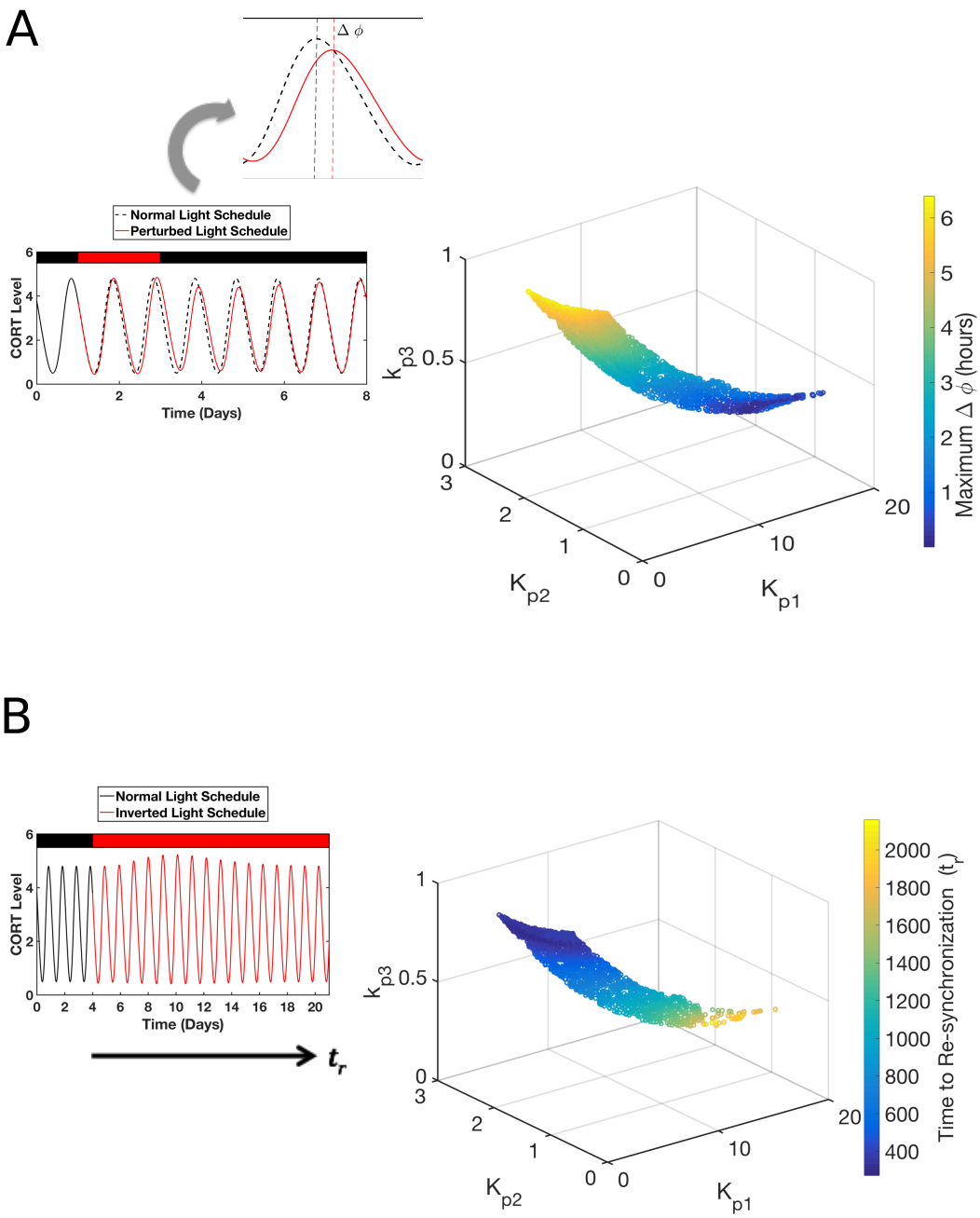


Figure 20: a): The maximal phase shift in the CORT rhythm was determined upon a transient inversion in the light/dark schedule lasting for 96 hours for the nominal surface. The maximal phase shift decreases with decreasing adrenal sensitivity. This implies that simulated individuals with lower adrenal sensitivity are more robust to transient perturbations in the light/dark cycle, such as those occurring during rapidly-rotating shift-work. b): The nominal system was subjected to an abrupt inversion of the light-dark schedule. The color depicts the time required to resynchronize to the new light-dark schedule after this abrupt change. This implies that simulated individuals with higher adrenal sensitivity adapt more easily to permanent changes in the light-dark schedule similar to those occurring during trans-meridian jet-travel, and are thus less susceptible to jet lag.

## 3.4 Discussion

A tightly controlled regulatory network is necessary for the maintenance of appropriate basal activity and responsiveness of the HPA axis (26,149). However, numerous observations of significant sex differences in the basal activity of the HPA axis as well as in its response to a variety of psychological and physiological stressors, have led investigators to suggest differential negative feedback and sensitivity of the HPA axis in male and females. The differences in the processes represented by these parameters are thought to be primarily mediated by the gonadal steroids, estrogen and testosterone. As discussed in the introduction, these differences in the activity of the HPA axis are thought to contribute to the observed disparity in the prevalence of psychiatric, infectious and autoimmune disease between males and females. Furthermore, we hypothesize that differences in the circadian rhythms of CORT would be indicative of the differential regulation of the HPA axis and might also contribute to the observed sex differences in HPA axis responsiveness. Therefore, we use a semi-mechanistic model of the HPA axis to gain insight into the processes that might be responsible for observed sex differences.

#### 3.4.1.1 Distinct Parameter Spaces Account for Sex-specific and Inter-Individual Regulatory Differences

Our model of the HPA axis confirms the hypothesis that differences in adrenal sensitivity and the strength of negative feedback can indeed account for the significant sex differences observed in the amplitude of the CORT circadian rhythm (**Figure 11**). Furthermore, **Figure 10** shows the existence of distinct parameter sub-spaces representing the multiple parameter sets that correspond to male and female CORT

profiles, respectively. Despite the existence of a wide range of male- and female-specific parameters sets, it is possible to draw certain general conclusions regarding the differences in adrenal sensitivity and autoregulatory negative feedback that contribute to the sexually dimorphic CORT profiles in our model. The majority of the parameter sets constituting the female parameter space have a greater adrenal sensitivity ($k_{p3}$) than those in the male parameter space. This finding is in agreement with a number of studies, which suggest a greater sensitivity to ACTH in the female HPA axis and is thought to contribute to the higher basal levels of CORT in females (14,131,150). Estrogen has been known to contribute to the greater adrenal sensitivity in females while testosterone has been shown to have an inhibitory influence on the HPA axis sensitivity (11,151). Furthermore, the model predicts the possibility of differential influence of GR-mediated negative feedback at the level of the pituitary ($K_{p2}$) and PVN ($K_{p1}$). In general, the model predicts a much weaker inhibition of CRH in the female HPA axis, as can be seen from **Figure 10** where ($K_{p1}$) levels for in-silico females are higher than those for in-silico males. On the other hand, there is a greater overlap between ($K_{p2}$) levels between males and females, with results indicating weaker inhibition of ACTH in males than in females. While the exact mechanisms by which negative feedback occurs at the level of the pituitary and PVN are yet to be completely elucidated (152,153), it is possible that there are differences in the strength of GR-mediated negative feedback of ACTH and CRH secretion. While, such a result has been difficult to verify experimentally (11), studies suggest that the greater neuronal activity in the limbic regions in males might contribute to a stronger inhibition of the PVN and the HPA axis in males in comparison to females

(154,155). Moreover, interestingly, estradiol has been shown to potentiate the cortisol-mediated negative feedback to the pituitary in unstressed humans (156).

Glucocorticoid circadian rhythms must be maintained within an optimal physiological range in order to maintain the proper functioning of various downstream homeostatic systems including metabolic, immune and cognitive signaling pathways and preserve the well-being of the host (8). Importantly, parameter sets within a sex-specific region qualitatively result in largely the same output CORT profile despite relatively large quantitative differences between them, as shown in **Figures 10 and 11**, where each sex-specific region spans a wide range of parameter values. We suggest that this highlights the large degree of regulatory flexibility inherent to the system. Furthermore, the latter results emphasize the existence of a unique quantitative relationship between the sex-specific parameters in our model ($K_{p1}$, $K_{p2}$ and $k_{p3}$) that is approximated graphically by the surfaces for each sex in **Figure 10**. The existence of such a relationship between the three sex-specific parameters ($K_{p1}$, $K_{p2}$ and $k_{p3}$) in our model underscores the importance of accounting for compensatory dynamics between the processes representing the parameters, such that they produce a considerably similar phenotype, the sex-specific CORT rhythm in this case. This is especially important while considering an autoregulatory network such as the HPA axis, where dynamic and reciprocal regulatory control is an important feature of the network (8,18,157).

Moreover, we suggest our results emphasize that the existence of these sex-specific parametric surfaces can viewed as accounting for the inter-individual variability inherent in the regulation of the HPA axis, arising out of differences in the three-sex specific parameters mediating negative feedback and adrenal sensitivity. A number of

studies suggest that much of the interindividual variation in the regulation of HPA axis activity can be attributed to gene polymorphisms in functional loci associated with these processes (17). Variability in the expression and ligand-binding affinity of GR , an essential modulator of glucocorticoid negative feedback in the pituitary and hypothalamus is thought to contribute to substantial differences in the HPA axis function (158,159). Similarly, significant interindividual differences in adrenal sensitivity have been attributed to functional polymorphisms in a number of genes regulating the activity of ACTH and it's downstream signaling mediators (160-162). Such functional polymorphisms are thought to contribute to the significant interindividual variation in the incidence of a number of disorders associated with HPA axis dysregulation, including PTSD and depression (163,164). Moreover, our model predicts that both CRH and ACTH exhibit significantly greater variability, as evidenced by the wide range of AUCs observed by each of these mediators, compared to that of CORT [**Figure 13 & 14**]. It has been suggested that such variation in mediators might be a result of heritable differences in the form of gene polymorphisms as well as epigenetic mechanisms due to differences in life history (165). For instance, studies have shown that polymorphisms in genes regulating CRH activity are associated with altered CORT response to stimulation despite similar baseline CORT levels (166-168). Therefore, we hypothesize that the sub-spaces within the male and female parameter regions [**Figure 10**] might represent the regulatory dynamics prevalent in specific sub-populations of interest. Accordingly, it is important that these regulatory dynamics are adequately characterized to understand both disruptions in activity as well as in devising restorative interventions (169). Thus, while we have primarily focused on a sex-specific stratification of parameters, one could

envision the existence of similar regulatory landscapes that correspond to populations of interest stratified on the bases of age, disease state, ethnicity etc. We suggest that this has broad relevance to efforts in precision and personalized medicine that seek to study sex differences as well as inter-individual differences by obtaining population-specific parameterizations of models of physiological systems (170).

In order to gain further insight into the behavior of the system and the observed relationships between the parameter sets we determined the activity of the other mediators involved in the regulation of the HPA axis; CRH, ACTH and receptor-bound glucocorticoid levels (DR(N)). **Figure 10**, shows an inverse relationship between the strength of inhibition of CRH ($1/K_{p1}$) and strength of inhibition of ACTH ($1/K_{p2}$) for both males and female parameter spaces. Interestingly, the mean ACTH levels for a given level of adrenal sensitivity ($k_{p3}$) remains nearly unchanged. This result implies that strength of inhibition of CRH ($1/K_{p1}$) and strength of inhibition of ACTH ($1/K_{p2}$) are regulated such that the CORT profile remains relatively unchanged within the males and female parameter regions, respectively. This explains the inverse relationship between the two parameters since at similar levels of adrenal sensitivity ($k_{p3}$) in-silico subjects with stronger inhibition of CRH would exhibit weaker inhibition of ACTH such that the eventual ACTH drive influencing CORT production remains relatively constant. As expected the mean levels of ACTH are inversely related to level of adrenal sensitivity [**Figure 12**]. Furthermore, results presented in **Figure 12** suggest that the mean levels of ACTH in females are lower than those in males for the majority of parameter sets. This further supports the argument that adrenal sensitivity is greater in females than in males. Experimental studies have shown that adrenal capacity for CORT secretion in response to

the same ACTH stimulus is significantly greater in females. This has been shown to be true both in vitro, using adrenal tissue homogenates and in vivo (131,171). Moreover, the study by Atkinson and Wadell on sex differences in basal HPA axis activity found that females secrete significantly higher basal levels of CORT despite no significant sex differences in immunoreactive (I) ACTH (14). Although our results indicate that ACTH levels are lower in females, notably they still suggest that females have a greater capacity for CORT secretion in response to the same (or in our case, even lower) ACTH drive. This discrepancy between our model and experiment might be because we do not explicitly account for important biochemical mechanisms relevant to the HPA signaling network, since the entire signaling cascade responsible for the ACTH stimulated de-novo synthesis of CORT is lumped into a single synthesis term in our equation for CORT production [**Equation 33**]. Moreover, the experiments by Atkinson and Waddell measured immunoreactive-(I) ACTH levels, which might not be representative of bioactive-ACTH levels (14). Indeed, the ratio of bioactive to immunoreactive ACTH levels has been shown to vary during the estrous cycle (172,173).

CRH levels generally appear to be greater in females than in males [**Figure 13**]. This is in agreement with experimental findings where CRH levels were found to be greater in the female PVN under basal conditions (174,175). This result is interesting since parameters were selected such that only CORT profiles were in qualitative agreement with experimental findings without imposing requirements on the behavior of other mediators of the HPA axis. **Figure 15** shows greater receptor-bound CORT (DR(N)) levels for in-silico females than males. This implies that, in general, glucocorticoid negative feedback in females can be thought to be weaker than in males,

since despite the higher levels of receptor-bound CORT, the CORT profile is much more pronounced in females. This is supported by experimental evidence, which suggests that estrogen might impair GR-mediated negative feedback in female rodents (95,176).

#### 3.4.1.2 Response to Bolus ACTH Injection

We simulated the in-silico response of the model to ACTH injection in order to determine whether greater adrenal sensitivity in females suggested by higher basal CORT levels also resulted in greater stimulus-driven CORT secretion. Further, this enables us to determine if the system described by the male and female parameter-spaces behave in a concerted, sex-specific manner in response to stimulation. Additionally, an important factor that is often not taken into account in most experimental studies is the possibility of time-of-day dependent responses to HPA axis stimulation. A temporal dependence of the immune response has been investigated by a number of studies (177-179). Therefore, we simulated an ACTH injection at various times during the circadian period to see whether our model exhibits a time-of-day dependent response as well as to see if this putative time-of-day dependence influences the extent to which sex differences are observed in the CORT response. Notably, model results predict a significant time-of-day dependence in CORT response to ACTH injection, with the response generally being maximal during or near the peak of the circadian rhythm irrespective of sex [**Figure 16**], indicating a significant dependence of the CORT response to ACTH injection on the dynamic state of the system. Moreover, our simulations predict that the in-silico female CORT response to ACTH is greater than that in males at all the time-points studied, suggesting a more pronounced CORT response in females over the entire circadian period. Importantly, our results are in agreement with a number of experimental

observations, which show that females respond to ACTH injections with a greater secretion of CORT with respect to baseline levels in both rodent and human studies (131,150,180). Indeed, estrogen has been shown to sensitize the adrenal response to ACTH regardless of sex in both rodents as well as in human studies (181-183). Therefore, our model predicts that the increased adrenal sensitivity and decreased negative feedback responsible for higher basal levels of CORT also result in an increased stimulated release of CORT in females. Based on the predictions from our simulations, CORT response to stimulation decreases with decreasing levels of CORT for both in-silico females and males (137,184). Thus, our model predicts a circadian variation in adrenal responsiveness to ACTH that arises out of the interacting dynamics between the HPA axis hormones. Notably, such a diurnal variation of adrenal responsiveness to ACTH has been observed experimentally, with peak responsiveness being observed close to the start of the active phase (185).

**Response to Acute Stress**

As shown in **Figure 17**, our model also predicts a time-of-day dependent sexually dimorphic acute stress response under nominal conditions without chronic stress. While in-silico females exhibit a substantially stronger response in comparison to in-silico males at time-points closer to the end of the active phase and early part of the inactive phase the sex difference in the response becomes exceedingly small towards the end of the inactive phase and the early part of the active phase. Most studies find that females respond stronger than males to acute stressors, however, in some cases there appears to be a dependence on the type of stressor used. For instance, in a study by Iwasaki-Sekino et al.(174) females exhibited a stronger CORT response to footshock, while a study by

Sterrenburg et al.(186) found males to respond more strongly to acute restraint stress. Our results deviate from experimental results in this regard likely due to the complexity of the stress response, which we are not able to capture in our model. While we consider a simplified-CRH driven stress response protocol, in reality the acute stress response involves the coordinated activation of multiple hypothalamic centers as well as the pituitary and adrenals (26). Furthermore, a variety of acute stress mediators, including many proinflammatory cytokines, are known to directly and independently activate the pituitary and adrenals, providing an alternate stress-responsive pathway (26,187).

#### 3.4.1.3 Adaptation to Chronic Stress

Allostasis proposes that in order to maintain evolutionary fitness, the regulation of critical physiological mediators, such as glucocorticoids, must optimize for the maintenance of their basal predictive functions (e.g. robust circadian rhythmicity) as well as flexibility in their reactive functions (e.g. stress response and adaptation to variation in light schedule)(135). This requires the existence of a multitude of regulatory strategies (regulatory diversity) that optimize the primary circadian phenotype of the HPA axis while balancing flexibility and adaptation in the critical operational phenotype of the HPA axis.

We hypothesize that regulatory diversity is necessary for the HPA axis to maintain homeostatic levels of its critical phenotype (i.e., tight operational glucocorticoid bounds). However, stress-induced allostatic maintenance of homeostasis, enabled through regulatory diversity, comes at a cost as the system, once adapted, needs to trade adaptation for responsiveness [**Figure 21**]. This conceptual framework is reminiscent of

the “bow-tie” architectures suggested to underline the function of a multitude of physiological systems in their attempt to conserve functionality in the presence of operational variability(188,189) exemplifying trade-offs between numerous competing requirements. We suggest that an improved understanding of the dynamics of such architectures in the context of the HPA axis can provide new insights in to its functioning in both health and disease.

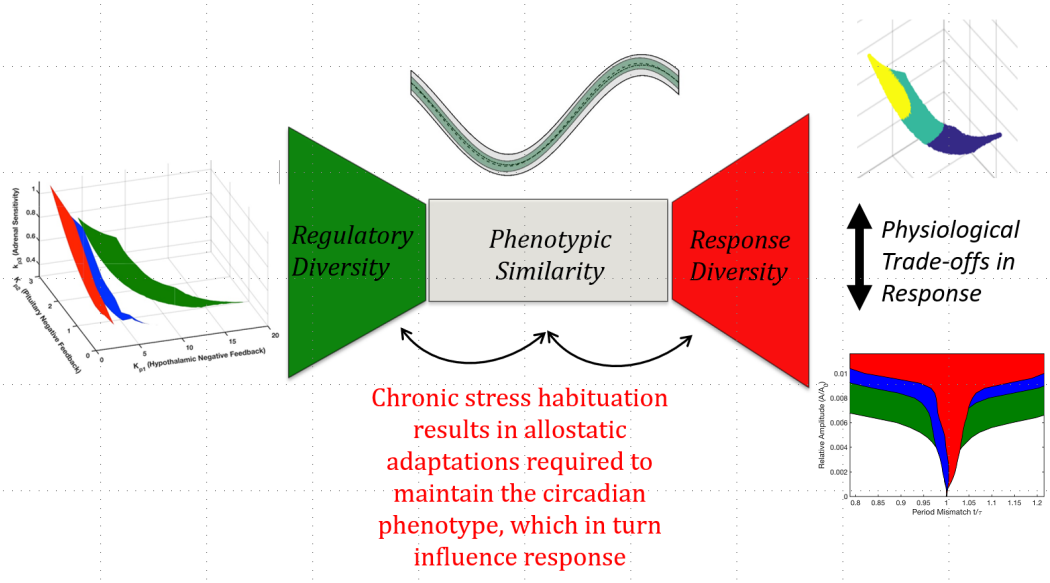


Figure 21: The variability in parametric surfaces is indicative of diverse individualized regulatory strategies thought which the host can maintain circadian glucocorticoid rhythms, a critical physiological phenotype within narrow homeostatic bounds. Furthermore, the underlying regulatory diversity results in flexibility in the response characteristics of the HPA axis, specifically its stress-responsive and entrainment properties. These features are suggestive of bow-tie architectures found in many complex physiological systems. Moreover, in order to conserve the circadian phenotype the system adjusts compensatory regulatory processes in a systematic manner that results in the existence of trade-offs between the stress-responsive and time-keeping functions of the HPA axis. Finally, allostatic habituation to chronic stress results in specific regulatory adaptations that alter the systems acute stress response and entrainment characteristics, indicative of the physiological cost (accumulation of allostatic load) associated with adaptation.

The circadian rhythmicity of endogenous glucocorticoids is partially indicative of the master circadian clock, located in the SCN, and has important implications for the homeostatic signaling of many physiological systems (1,190). Our results suggest that despite substantial regulatory diversity, the HPA axis must adjust compensatory

processes to maintain homeostatic levels of its mediators. We hypothesized that the existence of these diverse regulatory strategies to conserve the circadian phenotype will have significant consequences for the critical operational characteristics of the HPA axis, specifically its stress response and entrainment behavior.

In characterizing the entrainment properties of the system, we determined the domain of entrainment of the system (as depicted by the Arnold tongues) and the behavior of the system to physiologically relevant perturbations in the light/dark schedule. Simulated individuals with a wider domain of entrainment also exhibit the largest phase shift in response to an abrupt but transient change (lasting 96 hours) in the light-dark cycle. On the other hand, we also find that simulated individuals with largest phase disruptions are also able to re-synchronize more quickly after a permanent inversion of the light/dark schedule. These results are consistent with experimental findings, which have shown that clock with narrow entrainment ranges generally respond with smaller phase changes in response to zeitgber stimuli(191,192). Our results highlight an important trade-off for all circadian systems between the ability to be a precise time-keeping mechanism *versus* the ability to be easily entrained to a rhythmic environmental stimulus. Since, the HPA axis conveys circadian information from the central SCN to peripheral tissues such a trade-off between entrainability and robust time-keeping functions is particularly important to consider (193,194). These dynamics are of relevance towards understanding circadian disruption occurring during jet lag and shift-work. In the context of adaptation to jet lag it might beneficial for the circadian system to quickly resynchronize to a change in light schedule, thus preventing prolonged periods of internal desynchronization with the external environment (147). On the other hand,

studies on shift work have found that individuals exhibiting a high amplitude temperature circadian rhythm and a slow adjustment in the phase of the rhythm during the night-shift schedule were more tolerant to shift-work in a rapidly rotating shift system, reporting medical complaints at a lower frequency in comparison to individuals less resistant to shift-work (145,146). Therefore, model simulations predict that individuals with robust endogenous glucocorticoid rhythmicity will be more tolerant to rapid shift-work rotations, while those with a wide domain of entrainment will be able to flexibly adapt to changes in zeitgeber characteristics.

In addition to its synchronizing purpose, the HPA functions as the primary humoral stress response mechanism, with a flexible response to stressful external stimuli being essential for host fitness (97,98). We find that individuals with higher adrenal sensitivity exhibit a more robust response to an acute stressor. Moreover, given that the system adjusts compensatory regulatory processes in order to maintain the critical homeostatic circadian phenotype, we hypothesized that this might result in a systematic mutual variation of the response characteristics. Therefore, we assessed whether the regulatory mechanisms of the HPA axis vary in a manner that couples the stress-responsive and entrainment functions of the HPA axis. Our results suggest that higher adrenal sensitivity and negative feedback makes the HPA easier to entrain. Thus we predict that individuals with high adrenal sensitivity, and hence a more robust acute stress response, will more fluently adapt to jet lag, but will be more susceptible to circadian desynchrony due rapidly-rotating shift-work. Therefore, our model highlights the existence of a critical trade-off between the two primary physiological functions of the HPA axis: its ability to function as a robust timekeeper, resilient to fluctuations in an

environment zeitgeber *versus* its ability to respond to environmental stressors. It is suggested that the optimal strategy between the stress responsiveness and entrainability on one hand, and robustness of rhythmicity will depend on the differences in individual life history and exposure to variable natural habitats (135,195). We hypothesize that the regulatory diversity represents phenotypic plasticity where an individual organism is capable of modulating its phenotypic state in response to variations in its perceived environment so as to minimize transient accumulations of allostatic load (196). Thus adopting a robust phenotype might be beneficial to prevent over activation in a highly variable natural habitat with frequent exposure to stressors, while adopting a more responsive phenotype might be advantageous in a relatively predictable natural habitat (165). Therefore, the existence of diverse regulatory schemes might be reflective of multiple evolutionarily stable survival strategies in a context specific manner (135).

Our results indicate that the accumulation of allostatic load, due to chronic stress, results in a substantial increase in the strength of hypothalamic negative feedback and adrenal sensitivity, accompanied by a reduction in regulatory flexibility [**Figure 18B**]. It might be expected that the increased CRH drive to the system as a result of chronic stress must be counterbalanced by an appropriate increase in the strength of inhibition to CRH ($1/K_{p1}$). This increase in inhibitory strength predicted by the model is in general agreement with experimental findings where chronic restraint stress has been shown to result in increased branching of PFC GABAergic interneurons, suggestive of enhanced inhibition of the HPA axis (197,198). A similar enhanced negative feedback phenotype has also been observed in response to chronic stress in conditions such as PTSD (199). Counter-intuitively, however, we find that our model predicts that the host must also

increase its adrenal sensitivity in order to maintain pre-stress CORT circadian rhythms. Interestingly, such an increase in adrenal sensitivity to ACTH has been documented in rats subjected to chronic stress despite there being no significant differences in basal CORT levels between stressed and unstressed conditions (200). These results underscore the importance of considering the interdependent autoregulatory feedback of the HPA axis network in trying to understand its function in both homeostatic as well stressed situations.

Our model predicts that exposure to chronic stress results in a decrease in the variability and range of the intrinsic amplitude and period of the HPA axis. We suggest that the chronic stress-induced decrease in the variability of key regulatory features of the HPA axis results in a loss of flexibility of the system, which in turn renders the host more susceptible to subsequent environmental stressors. Natural variability in circadian parameters is known to contribute to organismal fitness by facilitating effective adaptation to locally varying environments (201,202). A number of studies suggest that natural allelic variation within the same population contributes to phenotypic variation that is thought to enable adaptive fine-tuning of the phenotype to environmental variation (202-204). Deletion of the neuropeptide Y gene (NPY), which is involved in a protective response to stress, resulted in a decrease in inter-individual variability in clock period, a shortening of the clock period, and a slower adaptive response to abrupt changes in the photoperiod (205). It has been hypothesized that maintenance of regulatory plasticity enables flexible adaptability in response to changing environmental conditions, with a loss in plasticity associated with reduced stress resilience and negative outcomes (112,196).

Moreover, we find that the adaptation to chronic stress involves a sharp decrease in the range of $K_{p1}$ levels that the system can span. This is accompanied by a decrease in the area of the surface with increasing levels of chronic stress [**Figure 18**]. As discussed previously, we suggest that the parameter sub-spaces reflect the regulatory flexibility of the system. Therefore, the decrease in the area of these surfaces implies a loss in its regulatory flexibility as the system is now constrained to a narrower region within the regulatory landscape. We propose that this loss in regulatory flexibility can be thought to occur as a result of the accumulation of alloastatic load and represents the physiological cost associated with successful habituation to chronic stress. The accumulation of allostatic load is indicative of the physiological trade-offs resulting from the chronic engagement of compensatory mechanisms involved in the adaptation to stress (110). Therefore, it is emphasized that despite the host assuming a pre-stress CORT circadian rhythm, it does not return to the "normal" physiological state due to allostatically-driven alterations in the feedback and adrenal sensitivity of HPA network. Often, however, experimental determination of such changes in regulatory flexibility is difficult.

Moreover, the detrimental effects of allostatic adaptations often become apparent only when the host is subjected to a subsequent environmental challenge (165). Accordingly, we investigate the HPA axis response to a subsequent acute stressor in order to determine the effect of the decreased regulatory flexibility within a more physiologically relevant framework. It should be noted that while in reality the initiation of the stress response is a result of a complex cascade of events that involves multiple anatomical regions, such as the PVN, BNST (bed nucleus of the stria terminalis), pituitary, and even adrenals. We consider a transient increase in CRH production to be a

simplified general representation that might simulate the effect of various acute stressors. As with the response to the ACTH injection, we find a strong time-of-day dependence of the acute stress response [**Figure 17**]. The simulated acute stress response is in general greater during the inactive (light) phase in comparison to the dark (active) phase. This is in qualitative agreement with experimental observations in rats as well as in humans, which show that the response to acute inflammatory stress is greatest in the middle of the inactive phase when hormone levels are low, while it is least-pronounced in the middle of active phase (137,178,184,206,207).

Interestingly, experimental studies show that there is a time-of-day dependent sensitization of the HPA axis to subsequent stressor upon exposure to prior chronic stress. In a study by Johnson et al., exposure to prior stress resulted in an enhanced proinflammatory stress response, upon subsequent administration of LPS in the light phase but not in the dark phase (208). Furthermore, CORT levels remained elevated for a longer duration when LPS was administered in the light phase. In qualitative agreement with experiment, the differences in acute stress response between the healthy and chronically stressed states are relatively small at most time points during the day, with response to acute stressor applied at 12-hour time-point, in the middle of the light phase, being the most significant. The reason for this can be explained by the difference in the rate of CRH synthesis [**Supplementary Figure S3**] between the unstressed and the two stressed states, wherein, the greatest difference in CRH synthesis between the three states can be observed at the 12-hour time-point. Considering the response at this time point to be the most physiologically relevant in relation to the responses at the other time points, the model predicts a sensitization of the acute stress response in chronically stressed

conditions. Notably, this phenomenon of chronic stress sensitization has been well documented in the literature. Numerous studies have found that exposure to a novel acute stressor after habituation to a homotypical chronic stressor results in a disproportionately large acute stress response in comparison to controls that have not been chronically stressed (209,210). We emphasize that this sensitization of the HPA axis stress response is further indicative of the physiological cost of allostatic adaption to the chronic stress regimen.

There is substantial evidence to suggest that individuals differ in their ability to adapt to stressful events (17). Therefore, based on our proposition, that samples within the parametric surfaces might capture the inter-individual variability in regulatory phenotypes, we sought to determine if our model could characterize possible differences in the ability to adapt to our chronic stress protocol based on the regulatory constitution of the individual subjects, as represented by their coordinates in the regulatory landscape considered in **Figure 18**. As discussed above, we specifically focus on the acute stress response at 12-hr time-point, since we consider to this to be the most physiologically relevant difference. Using symbolic representation to characterize the adaption to chronic stress, we find that individuals with higher levels of adrenal sensitivity tend to have a more pronounced acute stress response under chronic conditions [**Figure 18**]. Furthermore, individuals at comparable levels of adrenal sensitivity tend to respond more strongly to the acute stressor when subjected to increasing levels of chronic stress. These results imply that individuals with inherently higher adrenal sensitivity might exhibit a greater degree of chronic stress sensitization, while those with lower adrenal sensitivity might have the ability to exhibit a more “resilient” phenotype in response to chronic

stress. High levels of adrenal responsiveness in the form of exaggerated HPA axis reactivity to stress has often been associated with a greater probability to develop pathological psychological conditions such as PTSD and depression (17,211,212). Thus, our model results emphasize that a return to basal glucocorticoid levels upon exposure to chronic stress does not imply the system returns to a normal physiological status, underscoring the importance of using multiple metrics of HPA axis activity (e.g. basal levels and acute stress reactivity) to characterize adaptive and maladaptive stress responses (213).

Upon habituation to the chronic stress regimen we find that for the same level of adrenal sensitivity, the Arnold tongue becomes significantly narrower for increasing levels of chronic stress exposure. Furthermore, as predicted by theory (142), this decrease in the width of Arnold tongue is also accompanied by a general increase in the corresponding Floquet exponents. From the viewpoint of a faithful timekeeper such an allostatic adaptation might seem beneficial by making the system a more precise circadian clock. However, on the other hand, as was discussed above, this also implies that habituation to chronic stress requires regulatory adaptations, which make it more difficult for the system to synchronize to diurnally varying environmental signals. Such a phenomenon of lack of entrainment of the internal circadian clock to external zeitgebers corresponds to non-24 hour sleep-wake syndrome, which has been observed in both sighted and blind patients (214,215). Furthermore, this has also been observed in patients of schizophrenia(216), and in cases where subjects had experienced severe psychological stress(217).

In conclusion, our results support the hypothesis that the sex differences in CORT circadian rhythms are due to greater adrenal sensitivity and weaker negative feedback in females. In doing so, we implicitly account for the effect of gonadal steroids on the HPA axis using three tunable parameters representing the sensitivity and feedback within the network. While this approach allows us to capture the significant sex differences in HPA axis activity, a limitation of our model is that by not explicitly modeling the interactions between the gonadal steroids and the HPA axis, we might not able to exhaustively characterize the dynamics within the network. However, given the complex interactions between estradiol and testosterone, and the HPA axis, our model is a simplification as a first-step enables us to study the influence of the gonadal steroids on the essential feedback processes of the HPA network. Future modeling efforts including greater detail on the regulatory networks between the sex hormones and the HPA axis, can allow for a more comprehensive analysis of HPA axis dynamics during the course of the estrous cycle, and their evolution upon exposure to chronic stress regimens.

We identify two distinct regions of our putative sex-specific parameters that generate a family of CORT circadian profiles, which are in good agreement with experimental data. These results suggest the existence of a quantitative relationship between the putative sex-specific parameters that underscores the ability of the HPA axis to balance multiple compensatory mechanisms so as to produce a single qualitatively coherent phenotype. Moreover, the sub-spaces also emphasize the existence of multiple regulatory phenotypes, which we propose is indicative of inter-individual differences in the regulation of the HPA axis. Such differences in regulation might result in differential responses to stressors. Therefore, it becomes important to adequately characterize the

regulatory landscape to understand differences in specific populations of interest. In agreement with experimental findings, our simulations predict the HPA axis response to ACTH injection to be significantly more pronounced in females, and underscore the temporal dependence of the response. Furthermore, our model predicts specific allostatic regulatory adaptations in response to chronic stress that can lead to a phenotype of chronic stress sensitization. Moreover, model results suggest that individuals with greater HPA axis sensitivity might be more susceptible to a maladptive response to chronic stress. Taken together, these results have general relevance to approaches in personalized and precision medicine and highlight the need to quantitatively understand the complex and dynamic nature of regulation in physiological feedback systems such as the HPA axis.

# CHAPTER 4: Modeling the Pharmacological Manipulation of the Circadian Rhythms of the HPA Axis

## 4.1 Background

Natural glucocorticoids (GC) are a class of cholesterol-derived hormones secreted from the zona fasiculata of the adrenal glands (218). These hormones mediate a wide array of physiological functions with potent modulatory effects on metabolic, anti-inflammatory, immunosuppressive and cognitive signaling (218,219). The synthesis of natural glucocorticoids, primarily cortisol in humans, is regulated by the hypothalamic-pituitary-adrenal (HPA) axis, which along with the sympathetic nervous system constitutes the primary physiological stress response mechanism. HPA axis activity is mediated through a signaling cascade involving the sequential release of corticotrophin-releasing hormone (CRH), adrenocorticotropic hormone (ACTH) and cortisol (CORT). Cortisol transduces its physiological functions by binding to the glucocorticoid receptor (GR) and furthermore, regulates its own release by strongly inhibiting the release of its precursors, CRH and ACTH (8). Importantly, the basal activity of the HPA axis hormones exhibits pronounced circadian variation, with a peak in glucocorticoid secretion during the early morning hours in humans (8). Cortisol is critically involved in the appropriate synchronization of peripheral circadian clock genes, which further coordinate the functions of their residing tissues and promote homeostasis (149). Therefore, the maintenance of homeostatic cortisol circadian rhythms is critical to overall host survival (220).

Since the discovery of the immunosuppressive and anti-inflammatory properties of cortisone (a closely related natural analog of cortisol) by Hench and Kendall in 1948 (221), synthetic GCs have been extensively used in the treatment of chronic inflammatory conditions including asthma, skin infections, and rheumatoid arthritis (RA) as well as for their immunosuppressive effects in patients undergoing organ transplantation (28,52,222). Synthetic GCs are structurally similar to natural GCs and while they transduce their physiological actions by binding to GR, they can significantly differ from natural GCs in their potency and metabolic clearance (223). Despite the pharmacological benefits of synthetic GC administration, chronic use of synthetic GCs is associated with serious systemic adverse effects, especially during high-dose administration (224-227). Patients receiving synthetic GCs are at an increased risk of developing the pathological disorders associated with the supraphysiological exposure to GCs, including a higher risk of developing psychological disorders like depression, drug-induced hyperglycemia, long-term diabetes mellitus, osteoporosis, gastritis and cardiovascular disease (21,226,228-230). The incidence of these adverse effects is associated with the chronic suppression of homeostatic cortisol rhythmicity as a result of the potent negative feedback effects of the synthetic GCs on the HPA axis precursors.

Given the central regulatory function of the endogenous glucocorticoids, chronic disruption of cortisol rhythmicity is thought to result in the subsequent misalignment of peripheral circadian clocks, thus leading to the development of systemic complications (2,149). Therefore, there is a great deal of interest in the development of novel dosing regimens that can minimize the disruption of homeostatic circadian activity of cortisol, while still maintaining the pharmacological benefits of long-term synthetic GC therapy

(231). Accordingly, a number of studies have investigated the influence of administration time of exogenous GCs on the endogenous cortisol rhythm with the aim of identifying dosing regimens that minimize the disruption of the endogenous cortisol rhythm and the incidence of adrenal suppression. For example, healthy subjects administered synthetic GCs in the morning were found to exhibit the least suppression of the endogenous cortisol rhythm, while evening administration, resulted in maximal suppression of cortisol secretion and thus, found to be less physiologically compatible (222,225,232-234). Additional studies aimed to replicate the endogenous cortisol activity for patients suffering from adrenal insufficiency (235). While these studies showed that the administration time could likely be tailored to minimize disruption or to replicate the endogenous glucocorticoid rhythm in the short-term, comprehensive studies on the longer-term influences of chronic dosing of synthetic GCs are currently lacking.

Along with time-of-dosing, the influence of dose strength and different administration routes on endogenous HPA axis activity in the context of chronic exposure to synthetic GCs has yet to be elucidated. Adequately accounting for such factors in exploratory experimental studies can be exceedingly expensive as clinical designs grow in complexity and size (170). In such cases, a model-based approach can be a particularly useful tool for efficiently generating and evaluating experimentally-verifiable hypotheses related to the dose-exposure-response relationship for synthetic GCs. Through mathematical modeling, the impact of pharmacokinetics (dose, administration time, route of administration, duration of treatment, etc) in accordance with internal circadian rhythms and external environmental influences, such as light, can be thoroughly investigated (170). For example, physiologically-based modeling was previoulsy

implemented to understand how endogenous melatonin, a compound with strong circadian dependence, was influenced by the administration of exogenous melatonin and to elucidate the chronopharmacokinetics of exogenous melatonin for replication of the endogenous rhythm of melatonin (236).

In this study, we developed a mathematical model to explore the influence of exogenous GC dosing on the endogenous cortisol rhythm for a generic synthetic GC, considering both an intra-venous bolus and once-daily oral dosing. For these administration routes, we compared the HPA axis activity as indicated by changes in the cortisol rhythm due to a bolus of drug in systemic circulation with the pharmacological response following slower appearance rates in systemic circulation considering absorption after oral dosing. Furthermore, we attempt to determine how the response to short term treatment differs from that of chronic repeated dosing. As such, the goal of this study was to elucidate how long-term chronopharmacological dosing regimens influenced the basal cortisol activity using a model-based approach.

## 4.2 Approach

### 4.2.1 Description of the HPA axis model

A schematic of the model is depicted in **Figure 22**. The mediators of the HPA axis, CRH, ACTH and cortisol are represented by nonlinear ODEs that form a limit-cycle type Goodwin oscillator, such that they produce circadian (24hr) oscillations (38,134). Briefly, CRH induces the release of ACTH, which subsequently induces the release of CORT [**Equation 48-50**]. The synthesis of CRH is described by zero-order kinetics, while ACTH and CORT synthesis is described by first-order kinetics. Moreover, the

model accounts for the binding of CORT to the glucocorticoid receptor (GR) (36) as well as the pharmacodynamics of the cortisol-bound receptor complex [**Equation 51-54**], which subsequently inhibits GR mRNA transcription. **Equations 48-50** also account for inhibitor influence of the nucleated CORT-bound receptor complex on the release of CORT and ACTH. We account for the entraining influence of light on the HPA axis via the suprachiasmatic nucleus (SCN). Light is assumed to have an inductive influence on CRH in diurnal animals by inhibiting its degradation (120). Furthermore, the model considers a 1-2 hour delay between the start of light exposure and the onset of the photo-induced effects in the HPA axis, denoted by the term $light_{effect}$ (121). This delay in the photo-inductive effect on the HPA axis was modeled using a series of transit compartments [**Equation 44**]. Finally, a step function is used to model the light profile, while a Hill function is used to describe the dynamics of the phototransduction pathways [**Equation 42-47**].

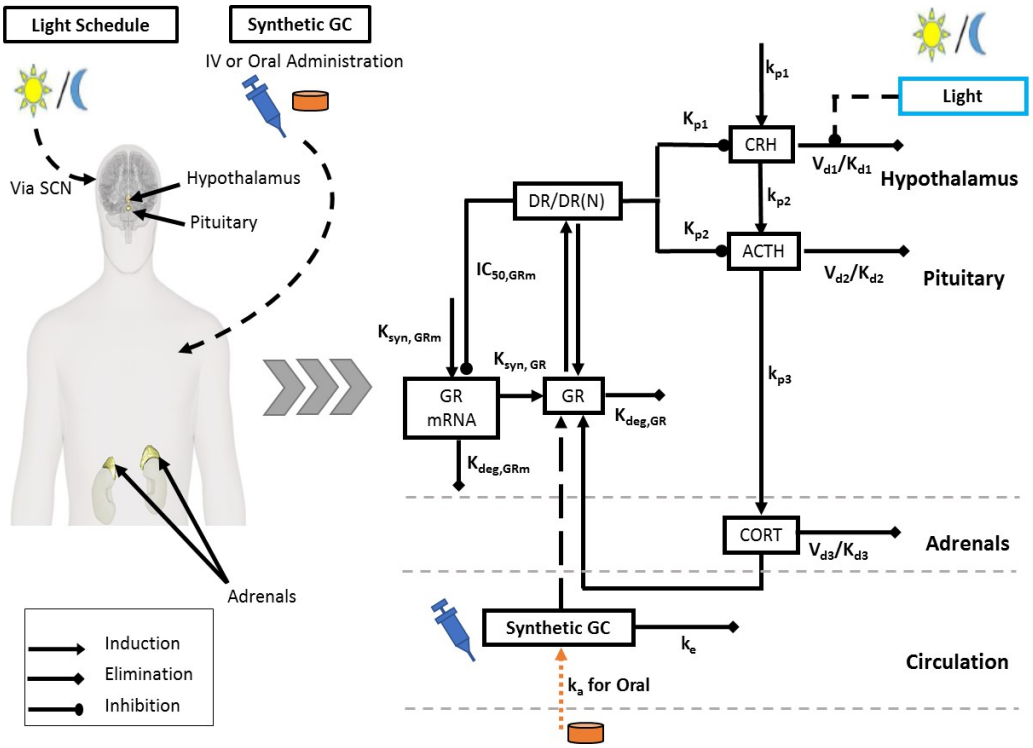

Figure 22: Model Schematic: A schematic of the model depicting the primary interactions in the hypothalamus-pituitary-adrenal (HPA) axis. The synthetic glucocorticoids (GC) competitively bind to the glucocorticoid receptor and contribute to the negative feedback arm of the HPA axis. Synthetic GCs are administered by either a bolus injection directly into systemic circulation or by oral administration. Appearance in systemic circulation following oral administration is indicated by the orange line.

#### 4.2.1.1 HPA Axis Mediators

$$light = \begin{cases} 1 & 6{:}00 \le t \le 18{:}00 \\ 0 & 18{:}00 < t < 6{:}00 \end{cases} \quad \textbf{Eq. 42}$$

$$\frac{dlight_{TCsynth1}}{dt} = k_t\left(light - light_{TCsynth1}\right) \quad \textbf{Eq. 43}$$

$$\frac{dlight_{TCsynth1\,i}}{dt} = k_t\left(light_{TCsynth\,i-1} - light_{TCsynth\,i}\right), i = \{1,2,3\} \quad \textbf{Eq. 44}$$

$$\frac{dlight_{TCdeg1}}{dt} = k_t\left(light_{deg} - light_{TCdeg1}\right) \quad \textbf{Eq. 45}$$

$$\frac{dlight_{TCdeg\,i}}{dt} = k_t\left(light_{TCdeg\,i-1} - light_{TCdeg\,i}\right); i = \{1,2,3\} \quad \textbf{Eq. 46}$$

$$\frac{dlight_{effect}}{dt} = k_{us}\frac{light^n_{TCsynth\,i}}{K^n_{M,us} + light^n_{TCsynth\,i}} - k_{deg,us}light_{effect}(1 + k_{eff}light_{TCdeg\,i}) \quad \textbf{Eq. 47}$$

$$\frac{dCRH}{dt} = \frac{k_{p1}.K_{p1}}{K_{p1} + DR(N)} - V_{d1}.\frac{CRH \cdot \left(1 - \frac{light_{effect}}{1 + light_{effect}}\right)}{K_{d1} + CRH} \quad \textbf{Eq. 48}$$

$$\frac{dACTH}{dt} = \frac{k_{p2}.K_{p2}CRH}{K_{p2} + DR(N)} - V_{d2}.\frac{ACTH}{K_{d2} + ACTH} \quad \textbf{Eq. 49}$$

$$\frac{dCORT}{dt} = k_{p3}.ACTH - V_{d3}.\frac{CORT}{K_{d3} + CORT} \quad \textbf{Eq. 50}$$

$$\frac{dGR_{mRNA}}{dt} = k_{syn_{GRm}}.\left(1 - \frac{DR(N)}{IC_{50_{GRm}} + DR(N)}\right) - k_{deg}.GR_{mRNA} \quad \textbf{Eq. 51}$$

#### 4.2.1.2 Glucocorticoid Receptor Pharmacodynamics

$$\frac{dGR}{dt} = k_{syn,GR}.GR_{mRNA} + r_f.k_{re}.DR(N) - k_{on}.(CORT).GR - k_{deg,GR}.GR \quad \textbf{Eq. 52}$$

$$\frac{dDR}{dt} = k_{on}.(CORT).GR - k_T.DR \quad \textbf{Eq. 53}$$

$$\frac{dDR(N)}{dt} = k_T.DR - r_f.k_{re}.DR(N) \quad \textbf{Eq. 54}$$

#### 4.2.1.3 Glucocorticoid Receptor Pharmacodynamics after GC Dosing

Upon dosing synthetic GCs, the equations describing the glucocorticoid receptor dynamics are modified to consider competitive binding between endogenous cortisol and the synthetic GC for the glucocorticoid receptor, resulting in increased negative feedback to the HPA axis precursors, CRH and ACTH. GR is assumed to have the same affinity for endogenous and synthetic GCs.

$$\frac{dGR}{dt} = k_{syn,GR}.GR_{mRNA} + r_f.k_{re}.DR(N) - k_{on}.(CORT + GC).GR - k_{deg,GR}.GR \quad \textbf{Eq. 55}$$

$$\frac{dDR}{dt} = k_{on}.(CORT + GC).GR - k_T.DR \quad \textbf{Eq. 56}$$

### 4.2.2 Description of pharmacokinetic models for synthetic GC administration

The influence of once-daily dosing is described using pharmacokinetic models that qualitatively captured the experimentally observed features of the drug exposure profile, such as the absorption rate and half-life, for a representative synthetic GC. While some synthetic GCs demonstrate complex pharmacokinetics due to competitive binding of the corticosteroid binding globulin (CBG) and interconversion between pharmacologically active and inactive forms by 11β-hydroxysteroid dehydrogenase type1/2 (223,225,237), linear pharmacokinetics are assumed for the representative synthetic GC with emphasis on understanding how the circadian rhythmicity of endogenous cortisol may be influenced by dosing rather than to evaluate the role of saturable processes in the dose-exposure-response relationship.

To assess how the endogenous cortisol rhythm is influenced by the rate of appearance of drug into the system, pharmacokinetic models describing an intra-venous (IV) and oral dosing are used assuming absorption and elimination follow first-order rate processes. Disposition of synthetic GCs was previously described by 1 or 2 compartment models depending on the drug, administration route and dose (223). For this preliminary dosing study, a 1-compartment model was assumed to describe drug distribution within the body. The rate of disappearance of drug from systemic circulation following an

injection is described by **Equation 57**. Disappearance from the gastrointestinal tract (GIT) after oral administration is described by **Equation 58** and the amount of drug in systemic circulation is given by **Equation 59**. These equations were simplified from those developed by Xu et al. for IV and oral dosing of prednisolone using a 1-compartment model (237), neglecting first pass extraction and interconversion between prednisolone and prednisone for this preliminary study. Since the displacement of cortisol from plasma protein, metabolic enzymes, and GR binding sites due to competition with synthetic GCs was not considered, the loss of endogenous cortisol and drug from the system are independent in this model.

The 1-compartment model [**Equation 57**] was amended to simulate extended release of an oral dose using a series of five transit compartments (TC) as shown in **Equations 60-62**. The use of transit compartments has previously been implemented to delay the absorption rate (238,239). The pharmacokinetics of synthetic GCs as described according to **Equations 60-62** will herein be referred to as slow-acting synthetic GCs whereas the behavior described by **Equation 59** will be referred to as the fast-acting synthetic GCs.

#### 4.2.2.1 IV Administration

$$\frac{dGC}{dt} = -k_E \cdot GC \qquad \textbf{Eq. 57}$$

#### 4.2.2.2 Oral Administration

$$\frac{dGC_{GIT}}{dt} = -k_a \cdot GC_{GIT} \qquad \textbf{Eq. 58}$$

$$\frac{dGC}{dt} = k_a \cdot GC_{GIT} - k_E \cdot GC \quad \textbf{Eq. 59}$$

$$dGC_{TC1} = k_{at,1} \cdot (GC_{GIT} - GC_{TC1}) \quad \textbf{Eq. 60}$$

$$dGC_{TC,i} = k_{at,i} \cdot \left(GC_{TC,i-1} - GC_{TC,i}\right), i = 2,3,4,5\} \quad \textbf{Eq. 61}$$

$$\frac{dGC}{dt} = k_a \cdot GC_{TC5} - k_E \cdot GC \quad \textbf{Eq. 62}$$

### 4.2.3 Parameterization of the Model

Since we are interested in understanding how our model predictions describe clinical data, the model is calibrated to human data such that endogenous cortisol peaked in the early morning. The model input parameters are given in the Appendix [**Table A6**].

### 4.2.4 Dosing Experiments

Several chronopharmacological dosing regimens are simulated to understand how administration time, dosing strength, administration route, and duration of treatment of synthetic GCs disrupted HPA axis activity. The administration time of the IV bolus or once-a-day oral dose of synthetic GCs varied by 1-hour intervals throughout the simulated day.

Changes in amplitude, acrophase, and area-under-the-curve (AUC) of the endogenous cortisol rhythm are used as metrics to quantify disruption of the HPA axis activity relative to the baseline activity. Amplitude and acrophase are determined when the cortisol rhythm reached a new stable oscillatory state after chronic once-daily dosing. The relative change in amplitude is calculated by **Equation 63**.

$$Relative\ Amplitude\ (\%) = \frac{Amplitude_{treatment} - Amplitude_{baseline}}{Amplitude_{baseline}} x100\% \quad \textbf{Eq. 63}$$

The AUC of the endogenous cortisol profile is determined for the 24-hour period following the first dose and after multiple doses when the cortisol rhythm reaches the new stable state. The change in 24-hour AUC for short and long term pharmacological effects is calculated by **Equation 64**.

$$Relative\ AUC\ (\%) = \frac{AUC_{[t_{dose} \rightarrow t_{dose}+24]_{treatment}} - AUC_{[t_{dose} \rightarrow t_{dose}+24]_{baseline}}}{AUC_{[t_{dose} \rightarrow t_{dose}+24]_{baseline}}} x100\% \quad \textbf{Eq. 64}$$

### 4.2.5 Responsiveness of the HPA Axis

We studied the cortisol response to in-silico CRH stimulation in order to determine whether modulating the rhythmic characteristics of cortisol through once-daily chronopharmacological dosing of synthetic GCs (at the nominal dose) also alters the responsiveness of the HPA axis. IV administration of CRH was simulated as a single pulse perturbation in the CRH rhythm, a procedure used by a number of studies in order to determine differences in the HPA axis responsiveness (27,132). We quantified the cortisol response to CRH injection by calculating the difference in AUC of the cortisol profiles between the stimulated and un-stimulated control condition for 4-hours from the application of the simulated CRH injection. Finally, we simulated the administration of

CRH at multiple time points, at 2-hour intervals throughout the simulated day, in order to quantify the time-of-day dependent response of the HPA axis to CRH stimulation.

## 4.3 Results

### 4.3.1 Pharmacokinetic Profiles for the synthetic glucocorticoid

The pharmacokinetic profiles for the representative synthetic glucocorticoid administered by IV and oral administration routes are given in **Figure 23** for the nominal dose of 1x. The faster-acting oral dose resulted in a $C_{max} \approx 40\%$ of the initial dose, $t_{max}$ = 2.75 hour, and 100% bioavailability ($AUC_{IV} = AUC_{oral}$). The slow-acting oral GC had a $C_{max} \approx 30\%$, $t_{max}$ = 8.4 hour, and 99% bioavailability.

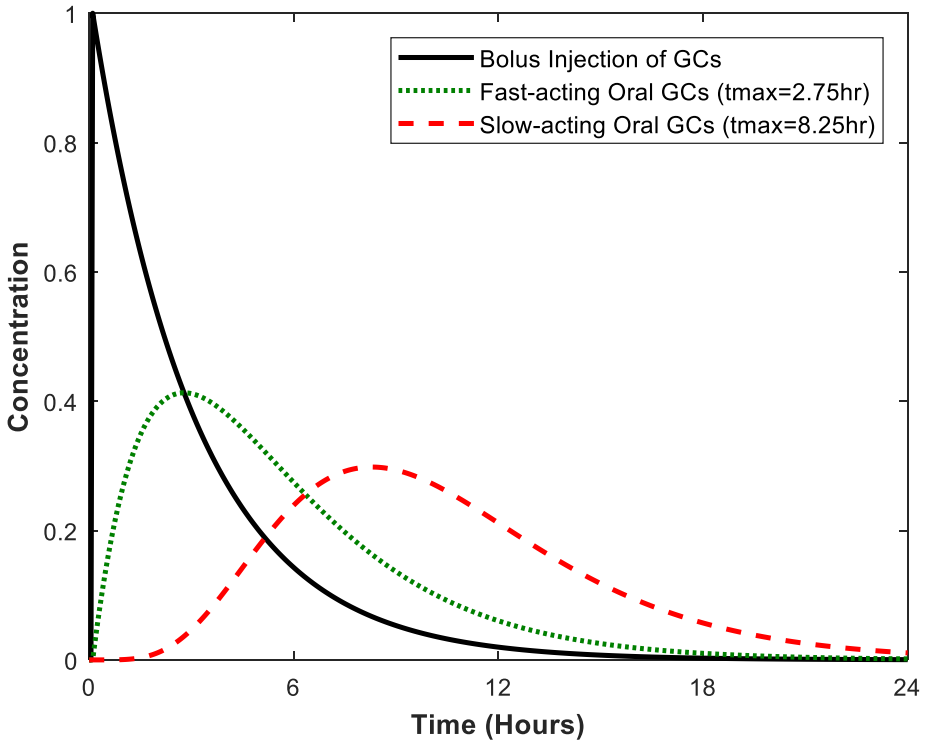


Figure 23: Pharmacokinetic profiles for synthetic glucocorticoids administered by a bolus injection, an oral dose with faster release, and an oral dose with slower, extended release. Representative profiles are shown for a nominal dose of synthetic GCs.

### 4.3.2 Influence of once-daily chronopharmacological dosing of synthetic GCs on the cortisol circadian rhythm

Once-a-day administration of synthetic GCs caused endogenous cortisol activity to evolve to a new stable, regular circadian rhythm [**Figure 24**]. Upon termination of synthetic GC intervention, the cortisol rhythm returned to the basal activity observed prior to dosing [**Supplementary Fig. S6**].

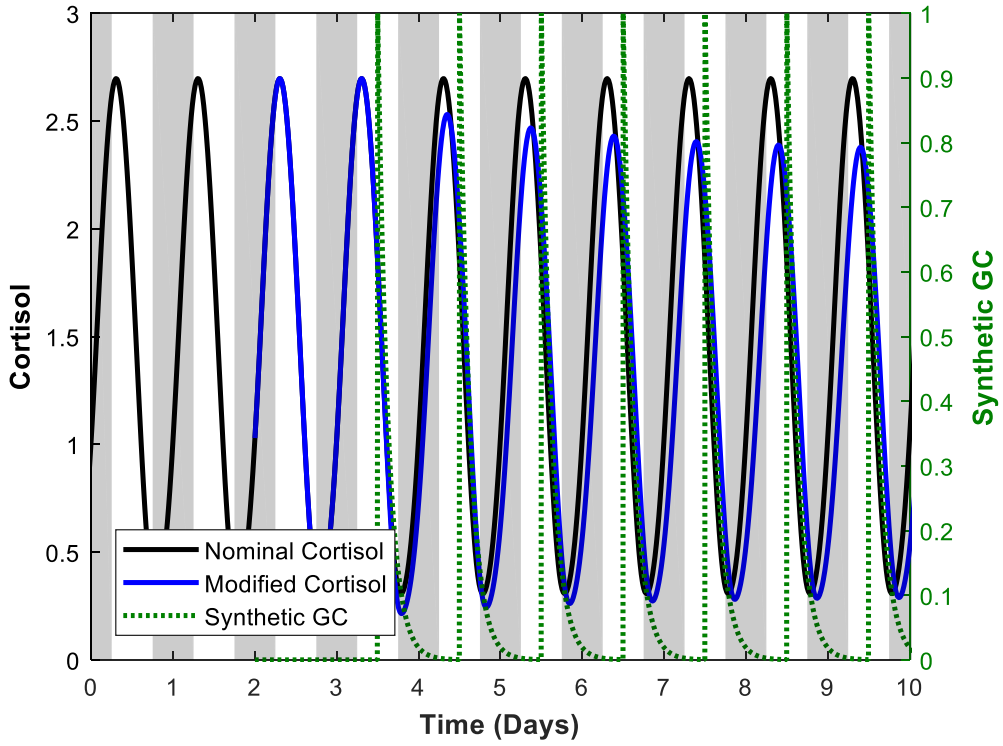


Figure 24: Modified cortisol profiles after dosing of synthetic glucocorticoids by bolus injection at the nominal amount (1x). The modified cortisol rhythm is indicated by the blue line. The black line corresponds to the nominal cortisol profile based on endogenous HPA axis activity. The pharmacokinetic profiles for the bolus injection are indicated by the dotted green line. The grey shaded areas represent the time at which the system is not exposed to light.

The amplitude and acrophase of this new stable cortisol rhythm depended on the time at which the drug was administered as shown in **Figure 25**. Amplitude generally decreased when the daily dosing of synthetic GCs by bolus injection was initiated during the declining phase of the nominal cortisol rhythm [**Figure 25a**]. The endogenous

cortisol rhythm following once-a-day administration of the fast-acting and slow-acting oral doses qualitatively showed similar changes in amplitude as the bolus injection, but with an advance in dosing times by about 2 hours and 6 hours to produce the same effect on the cortisol rhythm. The shifts roughly correlated with the time needed to reach the maximum pharmacological effect following orally administered synthetic GCs due to the absorption rates ($t_{max}$ = 2.75-hour and $t_{max}$ = 8.4-hour). Maximal suppression occurred when synthetic GCs were administered daily at 3:00 PM by bolus injection, 1:00 PM for the faster-acting oral dose, and 9:00 AM for the slow-acting oral dose. For all administration routes, certain once-daily chronopharmacological dosing regimens resulted in HPA axis induction, corresponding to an increase in amplitude of the endogenous cortisol rhythm. Maximal induction of the endogenous cortisol amplitude largely occurred when synthetic GCs were administered during the simulated night.

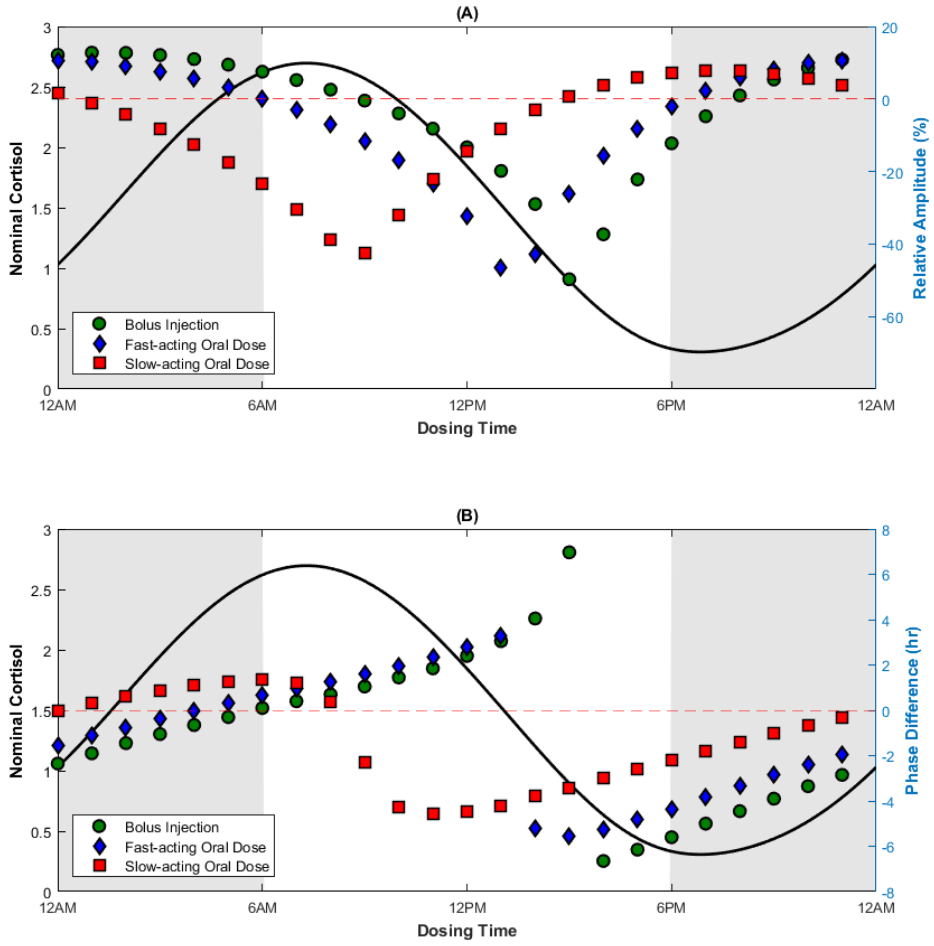


Figure 25: Amplitude and phase of the modified cortisol rhythm after once-daily chronopharmacological dosing of synthetic glucocorticoids. The relative amplitude and difference in the acrophase of the modified cortisol rhythm after a repeated once-a-day administration of a bolus injection, fast-acting oral dose, or slow-acting oral dose are shown in A and B, respectively. The nominal cortisol rhythm (indicated by the black line) is given for reference to show how dosing times align with the phase of baseline circadian rhythm. The shaded areas represent the time at which the system is not exposed to light. The change in amplitude is calculated by *Relative Amplitude (%)* = $[(Amp_{treatment} - Amp_{baseline})/Amp_{baseline}] \times 100\%$. A negative value for phase difference indicates an advance in the acrophase (i.e. peaks earlier in the simulated day relative to the nominal cortisol rhythm) while a positive value indicates a delay in the acrophase (i.e. peaks later in the simulated day).

A once-daily bolus injection introduced near the nadir or during the rising phase of the nominal cortisol rhythm predicted an advance in the acrophase of the cortisol rhythm, whereas initiating dosing near the peak or descending phase of the cortisol

rhythm resulted in a delay of the acrophase [**Figure 25b**]. For both administration routes, the change in acrophase was most sensitive when synthetic GCs were administered at dosing times associated with greatest amplitude suppression for all routes of administration. Furthermore, while the change in acrophase for the bolus injection and fast-acting oral doses exhibited a discontinuity (termed Type 0 (240)), the acrophase response varied more smoothly (continuous, termed Type 1 (240)) for the slow-acting oral dose, which had a lower maximal plasma concentration. The relationship between amplitude and phase are shown **Figure 26** for the bolus injection and the slow-acting oral dose. The fast-acting oral dose revealed similar behavior to the bolus injection (data not shown). Depending on the time of the synthetic GC administration the acrophase of the new stable rhythm was found to adopt two different values for a given change in its amplitude with the difference between acrophases increasing with greater amplitude suppression as observed for the bolus injection [**Figure 26a**]. Similar behavior was observed for the slow-acting GC, but to a lesser extent [**Figure 26b**].

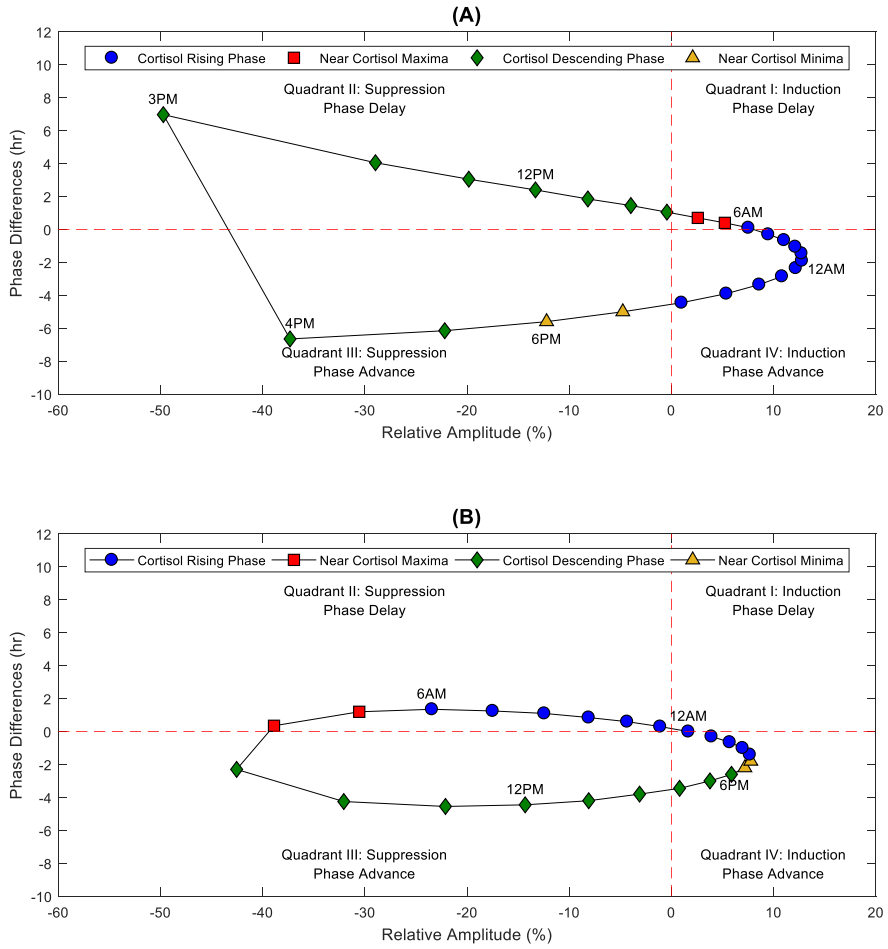


Figure 26: Relationship between the relative amplitude and phase difference of the modified cortisol rhythm after long-term once-daily chronopharmacological dosing of synthetic glucocorticoids. Amplitude and phase for the modified cortisol rhythms after chronic administration of a daily bolus injection and the slow-acting oral dose are shown in A and B, respectively. Marker labels correspond to the time of administration. Marker color indicates the administration time relative to the nominal cortisol rhythm where blue circles correspond to dosing times from 8:00 PM to 6:00 AM (ascending phase of baseline rhythm), red squares correspond to dosing times from 7:00 AM to 8:00 AM (near peak of baseline rhythm), green diamonds correspond to dosing times from 9:00 AM to 5:00 PM (descending phase of baseline rhythm), and yellow triangles correspond to dosing times from 6:00 PM to 7:00 PM (near nadir of baseline rhythm).

Importantly, our simulations indicated that specific chronopharmacological regimens of synthetic GC administration can minimize the disruption of the nominal GC rhythm. For example, daily administration of a nominal dose of synthetic GCs by bolus injection around 9:00 AM, resulted in a minimal change to the amplitude and acrophase of the cortisol rhythm relative to the basal activity, whereas a fast-acting oral dose at 6:00

AM or a slow-acting oral dose at midnight resulted in minimal change. Moreover, the amplitude change after a single dose was not indicative of the amplitude change after repeated administration [**Figure 27**] considering that several days to weeks of once-a-day dosing was needed before the endogenous cortisol stabilized to the new rhythm. Simulations predicted similar behavior following oral administration [**Supplementary Fig. S7**].

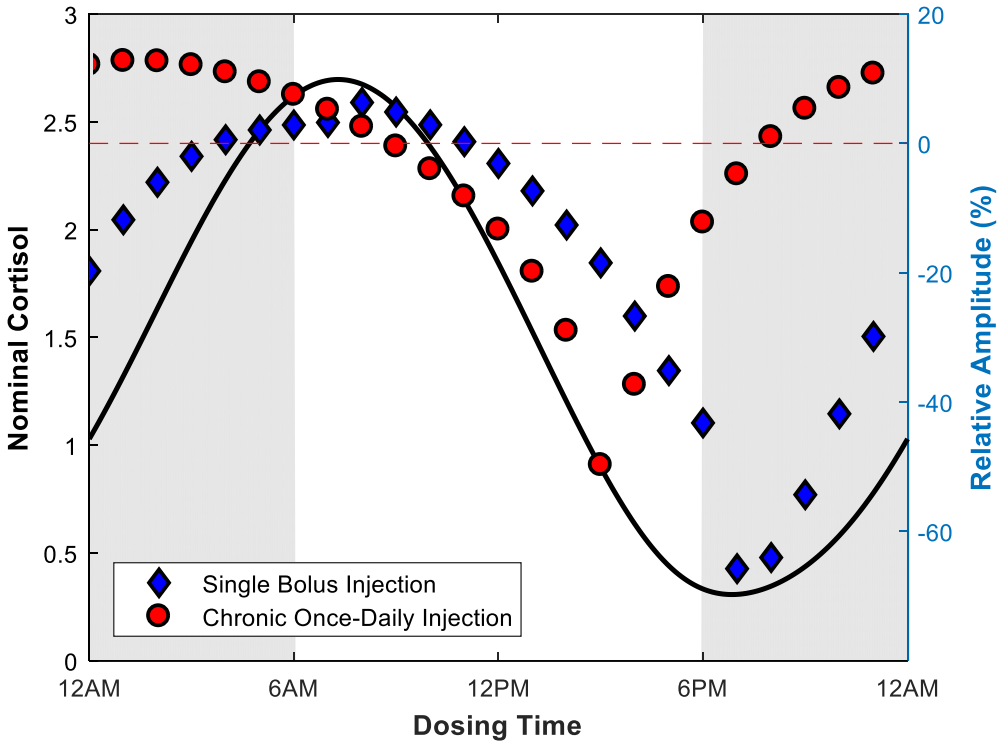


Figure 27: Amplitude of the modified cortisol rhythm after single and repeated once-daily chronopharmacological dosing of synthetic glucocorticoids by bolus injection at the nominal dose. The relative amplitude associated with the modified cortisol rhythm after a single injection and after long-term once-daily IV dosing are shown. The relative change in amplitude is calculated by *Relative Amplitude (%) = [(*$Amp_{treatment}$ - $Amp_{baseline}$*)/*$Amp_{baseline}$*] x 100%.*

### 4.3.3 Impact of synthetic GCs on the responsiveness of the HPA axis

The rhythmic characteristics of the endogenous glucocorticoids have important implications for the stress-responsiveness of the HPA axis. Therefore, we determined how alterations in the cortisol circadian rhythm as a result of chronic daily administration of synthetic GCs (at the nominal dose) influenced the responsiveness of the HPA axis. In doing so, we simulated the HPA axis response to a CRH stimulation test once the cortisol rhythm attained a new stable state following repeated administration of the synthetic GCs. Moreover, possible alterations in the time-dependent response to CRH stimulation was determined. Fig. 9 compares the change in cortisol secretion following the simulated CRH stimulation test for baseline conditions without synthetic GC administration and for the dosing regimens that led to greatest disruption of the endogenous cortisol rhythm (dosing at 3:00 PM and 1:00 AM).

A robust time-of-day dependence in the cortisol response to CRH administration was observed for all chronopharmacological dosing regimens considered (data not shown), with the maximal response occurring near the nadir of the endogenous cortisol rhythm. On the other hand, the HPA axis was minimally responsive when stimulated near the circadian maxima of the cortisol rhythm. Furthermore, the time at which the maximal response occurred was correlated to the acrophase of the cortisol rhythm. Thus, a phase advance in the cortisol rhythm as a result of the chronopharmacological dosing resulted in a phase advance in the time at which the maximal response to CRH stimulation occurred, in comparison to the nominal case in the absence of dosing [**Figure 28**]. Importantly, our simulations predicted that a suppression of the cortisol amplitude after synthetic GC administration was associated with a loss in the time-of-day dependence of

the HPA axis response to CRH stimulation. Moreover, chronopharmacological dosing regimens that largely preserved the rhythmic characteristics of the nominal cortisol profile exhibited minimal alterations in the responsiveness of the HPA axis.

## 4.4 Discussion

Recognizing the functional importance of the circadian regulation underlying the signaling dynamics of complex physiological systems, such as the HPA axis, has led to great interest in the incorporation of chronobiological principles for the development of safer and more efficacious therapies (241,242). A major concern associated with long-term therapeutic use of GCs is the suppression of endogenous HPA axis activity (149). However, chronopharmacological delivery of synthetic GCs is a promising approach to minimize the disruption of the endogenous cortisol circadian rhythmicity. In the present work, we used a semi-mechanistic mathematical model of the HPA axis to study the influence of chronic chronopharmacological intervention on endogenous HPA axis activity.

The model predicted that for all simulated routes of administration considered, the endogenous circadian activity of the HPA axis adapted to the repeated daily exposure to synthetic GCs by adopting a new stable circadian rhythm. Moreover, all three routes of administration of synthetic GCs resulted in qualitatively similar alterations of the cortisol circadian rhythm. However, due to differences in the duration for which synthetic GCs were maintained above a minimum pharmacologically active amount, both the oral administration routes considered resulted in a greater suppression of HPA axis activity in comparison to IV administration. Oral administration resulted in a comparable change in

the rhythmic characteristics of the cortisol rhythm at earlier dosing times. This shift in response to earlier dosing times was most prominent for slow-acting oral administration, for which the maximal plasma drug concentrations were delayed the longest. Therefore, our results suggested that the exposure profile of synthetic GCs might be systematically manipulated in order to optimize the dosing time as well as the pharmacodynamic effect on the cortisol rhythm. An improved characterization of the chronopharmacological influence of synthetic GCs on HPA axis activity can lead to the development of novel dosage forms in order to improve patient compliance and limiting the incidence of adverse effects while maintaining treatment efficacy (243). Indeed, modified-release (MR) prednisolone tablets that delay the release of drug up to 4 hours after administration have been developed to chronopharmacologically target the late-night (2:00 to 4:00 AM) circadian rise in proinflammatory cytokines in RA patients by enabling the dose to be administered at 10:00 PM, conveniently before the patients slept (28). The use of MR prednisolone was shown to result in an improvement in clinical symptoms while also preventing the suppression of endogenous cortisol rhythmicity. Furthermore, once-daily dosing of extended release formulations have proven effective for improved pain relief in patients with osteoarthritis of the knee (244) and in studies aiming to replicate endogenous cortisol rhythmicity in patients suffering from adrenal insufficiency (245,246), thereby replacing therapies requiring multiple doses per day. Together, these studies highlight the benefits of novel formulations with systematically manipulated exposure profiles, to aide in the development of improved chronic synthetic GC treatment options.

The maintenance of homeostatic circadian rhythms in the HPA axis is dependent on an intricate balance between the temporally-varying feedforward and feedback processes within the HPA network. Given this variation in regulatory dynamics of the HPA axis, chronopharmacological dosing can reduce the disruption of the endogenous cortisol rhythm. Indeed, our simulations suggest that once-daily administration of synthetic GCs shortly after the start of the active phase (around 6:00 AM for fast-acting oral GCs or 9:00 AM for a bolus injection, in our case) can minimize the suppression of the endogenous cortisol rhythm, by largely preserving its amplitude and acrophase. Moreover, the simulated suppression of the cortisol rhythm after the first dose is in qualitative agreement with experimental findings exploring the short-term influence of the synthetic GC administration of endogenous cortisol rhythmicity. A number of studies have found that administration of a single dose of synthetic GCs by infusion in the morning results in minimal disruption of the endogenous cortisol rhythm, while evening administration is associated with a substantial suppressive effect (232). Long-term daily administration of synthetic GCs by bolus injection or a fast-acting oral dose in the latter half of the active phase (late afternoon in humans) is predicted to result in maximal suppression of cortisol rhythm.

In addition to the changes in amplitude, there were substantial alterations in the acrophase of the cortisol rhythm upon long-term once-daily administration of synthetic GCs. The acrophase of the circadian rhythm of critical signaling hormones, such as cortisol, is tightly regulated and is thought to enable the host to optimally separate physiologically incompatible processes to different times of the day (1,9). Disruptions in the appropriate circadian activity of cortisol are associated with a number of health

problems (247). Therefore, understanding the influence of dosing on the acrophase of the endogenous cortisol rhythm is particularly important.

Interestingly, models simulations predicted that the time of dosing could be varied such that the acrophase of the cortisol rhythm adopted two different values for roughly the same change in amplitude. The acrophase of the rhythm was most sensitive for chronic dosing regimens that resulted in high plasma concentrations of synthetic GCs towards the end of active phase (late afternoon). Moreover, dosing times resulting in maximal amplitude suppression were also associated with the greatest resetting in the acrophase of the rhythm. These observations are in agreement with experimental studies on the phase-resetting behavior, in response to a light pulse, of the mammalian circadian clock in individual fibroblasts (248,249). Therefore, daily dosing of the bolus injection or fast-acting synthetic GCs near the beginning of the subjective night is predicted to be least favorable due to the maximal disruption of the endogenous cortisol rhythm.

Finally, an important indicator of HPA axis activity involves its ability to mount an appropriate response to stressors. Model simulations predict that altering the rhythmic characteristics of cortisol through chronopharmacological dosing modifies the responsiveness of the HPA axis. Decreased cortisol amplitude upon chronopharmacological dosing is predicted to result in a dampening in the time-of-day dependence of the response to CRH stimulation, while an increase in the amplitude of the cortisol circadian rhythm is associated with a more robust time-of day-dependent response to CRH stimulation. Interestingly, Kirwan et al. found that RA patients who exhibited an induction in cortisol amplitude after daily administration of MR-prednisolone also had a more robust cortisol response to CRH stimulation (27). In partial

agreement with these experimental results, our simulations predict that an increase in cortisol amplitude associated after chronopharmacological synthetic GC administration can lead to enhanced HPA responsiveness in a time-dependent manner.

While previous models have successfully studied the time-dependence of cortisol suppression after a single dose (225), our simulations can also explore the adaptability and responsiveness of the HPA axis following repeated administration. By accounting for a more physiologically relevant representation of the interactions between feedforward and feedback processes in the HPA network, our model predicts that synthetic GCs can have a complex non-trivial influence on HPA axis activity that might not be captured by simpler mathematical representations, which do not account for endogenous circadian rhythmicity. In doing so, we further emphasize the importance of using multiple metrics (circadian amplitude, acrophase, AUC and responsiveness) to comprehensively understand the alterations in HPA axis activity in response to chronopharmacological intervention. The current model may be augmented with a physiologically-based pharmacokinetic model that accounts for the nonlinear dynamics associated with some synthetic GCs. These complexities arise from competitive binding to the corticosteroid binding globulin (CBG) and to interconversion between pharmacologically active and inactive forms by 11β-hydroxysteroid dehydrogenase type1/2 for both endogenous and synthetic GCs (223,225,237). Furthermore, these proteins exhibit their own circadian rhythmicity (250,251), which can complicate the chronopharmacological relationship between dose, drug exposure, and response. The feedback mechanisms underlying dysregulation of the HPA axis are thought to be a result of the imbalance between GR and mineralocorticoid receptors (252). As such, the disruption of the HPA axis following

administration of synthetic GCs can be studied more thoroughly considering the activity of both receptors. Moreover, clinical studies have shown that differences in pharmacokinetics (i.e. clearance) are often balanced by differences in pharmacodynamics (i.e. receptor affinity) such that dose adjustment of synthetic GCs may not be needed across age, sex or ethnic subgroups (223,253). A model-based methodology may be particularly useful to explain the physiological mechanisms underlying these clinical outcomes, and to evaluate the need for therapeutic dose monitoring of chronic synthetic GC treatment considering the inherent stochasticity of physiological input parameters (170).

# CHAPTER 5: Conclusion

The circadian dynamics of the HPA axis network are critical determinants of its activity in both basal conditions as well as in response to acute and chronic stress. We propose to use semi-mechanistic mathematical models of the HPA axis that might provide insight into the mechanisms contributing to pathological and basal differences in HPA axis rhythms. The goal of Chapter 2 was to understand how a chronic elevation of proinflammatory cytokines might result in a disrupted pathological glucocorticoid circadian rhythm that is frequently observed in patients with severe RA as well as in animal models of RA. We considered two alternative hypothetical mechanisms for the onset of adrenal insufficiency, which yield qualitatively similar changes in glucocorticoid rhythms. The model provides a foundation for further work on the significance of circadian rhythms in neuroendocrine-immune signaling in chronic inflammatory diseases by incorporating more detailed descriptions of the dynamics of proinflammatory cytokines, and the sympathetic nervous system.

Chapter 3 provided further insight into the key network processes that contribute to sex differences in basal circadian activity. We postulated that these processes also contribute to sex differences in the HPA axis stress response. Moreover, we find that significant individual variability might exist in the processes contributing to negative feedback and adrenal sensitivity of the HPA network even when the CORT profile between individuals is qualitatively similar. Our results predict the existence of a trade-off between the stress-responsiveness of the HPA axis and its ability to be a faithful time-keeping mechanism that is robust to noise in environmental conditions. Moreover, we specifically highlight allostatic regulatory adaptations upon chronic stress habituation that

influence the stress-responsiveness and entrainment properties of the HPA axis. Our models suggest that by adapting to chronic stress in a way that homeostatic glucocorticoid rhythms are maintained, the system is forced to compromise either its entrainment characteristics (adaptation) or its responsiveness to external stimuli, or in many cases both. An improved understanding of the regulatory dynamics of the HPA axis can provide new insights into its functioning in both health and disease and are relevant for the development of improved approaches to personalized and precision medicine.

Finally, in Chapter 4, we developed a mathematical model to explore the influence of chronic exogenous GC dosing on the endogenous cortisol rhythm for a generic synthetic GC, considering both an intra-venous bolus and once-daily oral dosing. Interestingly, model results predicted that the changes in cortisol rhythmicity upon acute chronopaharmacological exposure to synthetic GCs is not necessarily indicative of the influence of chronic once-daily dosing on HPA axis activity. Moreover, model results predict that certain chronopharmacological dosing regimens preserve the nominal cortisol circadian rhythm. Taken together, our results provide a framework for understanding physiological plasticity in the circadian dynamics of the HPA axis and the implications of these regulatory mechanisms in the incidence of pathology and for the development of effective therapeutic strategies.

# Acknowledgement of publications

This dissertation contains significant portions of the following publications:

Rao R, DuBois D, Almon R, Jusko WJ, Androulakis IP. Mathematical modeling of the circadian dynamics of the neuroendocrine-immune network in experimentally induced arthritis. Am J Physiol Endocrinol Metab 2016; 311:E310-324

Rao RT, Androulakis IP. Modeling the Sex Differences and Interindividual Variability in the Activity of the Hypothalamic-Pituitary-Adrenal Axis. Endocrinology 2017; 158:4017-4037

Note: This work has also been submitted to *Chronobiology International* and *Stress: The International Journal on the Biology of Stress*. The candidate is the original author of the material

# References


**1.** Buijs RM, van Eden CG, Goncharuk VD, Kalsbeek A. The biological clock tunes the organs of the body: timing by hormones and the autonomic nervous system. J Endocrinol 2003; 177:17-26

**2.** Dibner C, Schibler U, Albrecht U. The mammalian circadian timing system: organization and coordination of central and peripheral clocks. Annu Rev Physiol 2010; 72:517-549

**3.** Partch CL, Green CB, Takahashi JS. Molecular architecture of the mammalian circadian clock. Trends Cell Biol 2014; 24:90-99

**4.** Gekakis N, Staknis D, Nguyen HB, Davis FC, Wilsbacher LD, King DP, Takahashi JS, Weitz CJ. Role of the CLOCK Protein in the Mammalian Circadian Mechanism. Science 1998; 280:1564-1569

**5.** Schibler U, Gotic I, Saini C, Gos P, Curie T, Emmenegger Y, Sinturel F, Gosselin P, Gerber A, Fleury-Olela F, Rando G, Demarque M, Franken P. Clock-Talk: Interactions between Central and Peripheral Circadian Oscillators in Mammals. Cold Spring Harb Symp Quant Biol 2015; 80:223-232

**6.** Kalsbeek A, van der Spek R, Lei J, Endert E, Buijs RM, Fliers E. Circadian rhythms in the hypothalamo-pituitary-adrenal (HPA) axis. Mol Cell Endocrinol 2012; 349:20-29

**7.** Straub RH, Cutolo M, Buttgereit F, Pongratz G. Energy regulation and neuroendocrine–immune control in chronic inflammatory diseases. Journal of Internal Medicine 2010; 267:543-560

**8.** Spiga F, Walker JJ, Terry JR, Lightman SL. HPA Axis-Rhythms. In: Terjung R, ed. Comprehensive Physiology. Hoboken, NJ, USA: John Wiley & Sons, Inc.; 2014:1273-1298.

**9.** Sukumaran S, Almon RR, DuBois DC, Jusko WJ. Circadian rhythms in gene expression: Relationship to physiology, disease, drug disposition and drug action. Adv Drug Deliv Rev 2010; 62:904-917

**10.** Kalsbeek A, Palm IF, La Fleur SE, Scheer FA, Perreau-Lenz S, Ruiter M, Kreier F, Cailotto C, Buijs RM. SCN outputs and the hypothalamic balance of life. Journal of biological rhythms 2006; 21:458-469

**11.** Goel N, Workman JL, Lee TT, Innala L, Viau V. Sex differences in the HPA axis. Compr Physiol 2014; 4:1121-1155

**12.** Seale JV, Wood SA, Atkinson HC, Bate E, Lightman SL, Ingram CD, Jessop DS, Harbuz MS. Gonadectomy reverses the sexually diergic patterns of circadian and stress-induced hypothalamic-pituitary-adrenal axis activity in male and female rats. J Neuroendocrinol 2004; 16:516-524

**13.** Bailey M, Silver R. Sex differences in circadian timing systems: implications for disease. Front Neuroendocrinol 2014; 35:111-139

**14.** Atkinson HC, Waddell BJ. Circadian variation in basal plasma corticosterone and adrenocorticotropin in the rat: sexual dimorphism and changes across the estrous cycle. Endocrinology 1997; 138:3842-3848

**15.** Angele MK, Schwacha MG, Ayala A, Chaudry IH. Effect of gender and sex hormones on immune responses following shock. Shock 2000; 14:81-90

**16.** Figueiredo HF, Ulrich-Lai YM, Choi DC, Herman JP. Estrogen potentiates adrenocortical responses to stress in female rats. American journal of physiology Endocrinology and metabolism 2007; 292:E1173-1182

**17.** Ebner K, Singewald N. Individual differences in stress susceptibility and stress inhibitory mechanisms. Current Opinion in Behavioral Sciences 2017; 14:54-64

**18.** Kudielka BM, Wust S. Human models in acute and chronic stress: assessing determinants of individual hypothalamus-pituitary-adrenal axis activity and reactivity. Stress 2010; 13:1-14

**19.** Becker-Krail D, McClung C. Implications of circadian rhythm and stress in addiction vulnerability. F1000Res 2016; 5:59

**20.** Spies CM, Straub RH, Cutolo M, Buttgereit F. Circadian rhythms in rheumatology--a glucocorticoid perspective. Arthritis Res Ther 2014; 16 Suppl 2:S3

**21.** Oster H, Challet E, Ott V, Arvat E, Ronald de Kloet E, Dijk DJ, Lightman S, Vgontzas A, Van Cauter E. The Functional and Clinical Significance of the 24-Hour Rhythm of Circulating Glucocorticoids. Endocr Rev 2017; 38:3-45

**22.** Cutolo M, Villaggio B, Otsa K, Aakre O, Sulli A, Seriolo B. Altered circadian rhythms in rheumatoid arthritis patients play a role in the disease's symptoms. Autoimmunity Reviews 2005; 4:497-502

**23.** Kouri V-P, Olkkonen J, Kaivosoja E, Ainola M, Juhila J, Hovatta I, Konttinen YT, Mandelin J. Circadian Timekeeping Is Disturbed in Rheumatoid Arthritis at Molecular Level. PLoS ONE 2013; 8

**24.** Rao RT, Pierre KK, Schlesinger N, Androulakis IP. The Potential of Circadian Realignment in Rheumatoid Arthritis. Critical Reviews™ in Biomedical Engineering 2016; 44

**25.** Herman JP. Neural control of chronic stress adaptation. Front Behav Neurosci 2013; 7:61

**26.** Herman JP, McKlveen JM, Ghosal S, Kopp B, Wulsin A, Makinson R, Scheimann J, Myers B. Regulation of the Hypothalamic-Pituitary-Adrenocortical Stress Response. Compr Physiol 2016; 6:603-621

**27.** Kirwan JR. Targeting the time of day for glucocorticoid delivery in rheumatoid arthritis. International Journal of Clinical Rheumatology 2011; 6:273-279

**28.** Kirwan JR, Clarke L, Hunt LP, Perry MG, Straub RH, Jessop DS. Effect of novel therapeutic glucocorticoids on circadian rhythms of hormones and cytokines in rheumatoid arthritis. Ann N Y Acad Sci 2010; 1193:127-133

**29.** Rao RT, Scherholz ML, Hartmanshenn C, Bae S-A, Androulakis IP. On the analysis of complex biological supply chains: From process systems engineering to quantitative systems pharmacology. Computers & Chemical Engineering 2017; 107:100-110

**30.** McInnes IB, Schett G. The Pathogenesis of Rheumatoid Arthritis. New England Journal of Medicine 2011; 365:2205-2219

**31.** Straub RH, Cutolo M. Circadian rhythms in rheumatoid arthritis: Implications for pathophysiology and therapeutic management. Arthritis & Rheumatism 2007; 56:399-408

**32.** Harbuz M. Neuroendocrine function and chronic inflammatory stress. Exp Physiol 2002; 87:519-525

**33.** Straub RH, Paimela L, Peltomaa R, Scholmerich J, Leirisalo-Repo M. Inadequately low serum levels of steroid hormones in relation to interleukin-6 and tumor necrosis factor in untreated patients with early rheumatoid arthritis and reactive arthritis. Arthritis Rheum 2002; 46:654-662

**34.** Meyer-Hermann M, Figge MT, Straub RH. Mathematical modeling of the circadian rhythm of key neuroendocrine-immune system players in rheumatoid arthritis: a systems biology approach. Arthritis Rheum 2009; 60:2585-2594

**35.** Sriram K, Rodriguez-Fernandez M, Doyle FJ. Modeling Cortisol Dynamics in the Neuro-endocrine Axis Distinguishes Normal, Depression, and Post-traumatic Stress Disorder (PTSD) in Humans. PLoS Computational Biology 2012; 8

**36.** Ramakrishnan R, DuBois DC, Almon RR, Pyszczynski NA, Jusko WJ. Fifth-generation model for corticosteroid pharmacodynamics: application to steady-state receptor down-

regulation and enzyme induction patterns during seven-day continuous infusion of methylprednisolone in rats. J Pharmacokinet Pharmacodyn 2002; 29:1-24

**37.** Earp JC, Dubois DC, Molano DS, Pyszczynski NA, Almon RR, Jusko WJ. Modeling corticosteroid effects in a rat model of rheumatoid arthritis II: mechanistic pharmacodynamic model for dexamethasone effects in Lewis rats with collagen-induced arthritis. J Pharmacol Exp Ther 2008; 326:546-554

**38.** Mavroudis PD, Corbett SA, Calvano SE, Androulakis IP. Mathematical modeling of light-mediated HPA axis activity and downstream implications on the entrainment of peripheral clock genes. Physiological Genomics 2014; 46:766-778

**39.** Gonze D, Bernard S, Waltermann C, Kramer A, Herzel H. Spontaneous synchronization of coupled circadian oscillators. Biophys J 2005; 89:120-129

**40.** Kalsbeek A, van der Vliet J, Buijs RM. Decrease of endogenous vasopressin release necessary for expression of the circadian rise in plasma corticosterone: a reverse microdialysis study. J Neuroendocrinol 1996; 8:299-307

**41.** Kow LM, Pfaff DW. Vasopressin excites ventromedial hypothalamic glucose-responsive neurons in vitro. Physiol Behav 1986; 37:153-158

**42.** Dunn AJ. Cytokine Activation of the HPA Axis. Annals of the New York Academy of Sciences 2000; 917:608-617

**43.** Harbuz MS, Rees RG, Eckland D, Jessop DS, Brewerton D, Lightman SL. Paradoxical responses of hypothalamic corticotropin-releasing factor (CRF) messenger ribonucleic acid (mRNA) and CRF-41 peptide and adenohypophysial proopiomelanocortin mRNA during chronic inflammatory stress. Endocrinology 1992; 130:1394-1400

**44.** Jessop DS, Harbuz MS, Lightman SL. CRH in chronic inflammatory stress. Peptides 2001; 22:803-807

**45.** Aguilera G, Jessop DS, Harbuz MS, Kiss A, Lightman SL. Differential regulation of hypothalamic pituitary corticotropin releasing hormone receptors during development of adjuvant-induced arthritis in the rat. J Endocrinol 1997; 153:185-191

**46.** Brady LS, Page SW, Thomas FS, Rader JL, Lynn AB, Misiewicz-Poltorak B, Zelazowski E, Crofford LJ, Zelazowski P, Smith C. 1,1'-Ethylidenebis[L-tryptophan], a contaminant implicated in L-tryptophan eosinophilia myalgia syndrome, suppresses mRNA expression of hypothalamic corticotropin-releasing hormone in Lewis (LEW/N) rat brain. Neuroimmunomodulation 1994; 1:59-65

**47.** Chover-Gonzalez AJ, Tejedor-Real P, Harbuz MS, Gibert-Rahola J, Larsen PJ, Jessop DS. A differential response to stress is not a prediction of susceptibility or severity in adjuvant-induced arthritis. Stress 1998; 2:221-226

**48.** Turnbull AV, Rivier CL. Regulation of the hypothalamic-pituitary-adrenal axis by cytokines: actions and mechanisms of action. Physiological Reviews 1999; 79:1-71

**49.** Earp JC, DuBois DC, Molano DS, Pyszczynski NA, Keller CE, Almon RR, Jusko WJ. Modeling Corticosteroid Effects in a Rat Model of Rheumatoid Arthritis I: Mechanistic Disease Progression Model for the Time Course of Collagen-Induced Arthritis in Lewis Rats. J Pharmacol Exp Ther 2008; 326:532-545

**50.** Straub RH, Harle P, Sarzi-Puttini P, Cutolo M. Tumor necrosis factor-neutralizing therapies improve altered hormone axes: an alternative mode of antiinflammatory action. Arthritis Rheum 2006; 54:2039-2046

**51.** Luedde T, Heinrichsdorff J, de Lorenzi R, De Vos R, Roskams T, Pasparakis M. IKK1 and IKK2 cooperate to maintain bile duct integrity in the liver. PNAS 2008; 105:9733-9738

**52.** Edwards C. Sixty years after Hench--corticosteroids and chronic inflammatory disease. J Clin Endocrinol Metab 2012; 97:1443-1451

**53.** Sharma A, Jusko WJ. Characteristics of indirect pharmacodynamic models and applications to clinical drug responses. Br J Clin Pharmacol 1998; 45:229-239

**54.** Foteinou PT, Calvano SE, Lowry SF, Androulakis IP. Modeling endotoxin-induced systemic inflammation using an indirect response approach. Math Biosci 2009; 217:27-42

**55.** Kokkonen H, Soderstrom I, Rocklov J, Hallmans G, Lejon K, Rantapaa Dahlqvist S. Up-regulation of cytokines and chemokines predates the onset of rheumatoid arthritis. Arthritis Rheum 2010; 62:383-391

**56.** Scheff JD, Calvano SE, Lowry SF, Androulakis IP. Modeling the influence of circadian rhythms on the acute inflammatory response. Journal of Theoretical Biology 2010; 264:1068-1076

**57.** Yao Z, DuBois DC, Almon RR, Jusko WJ. Modeling circadian rhythms of glucocorticoid receptor and glutamine synthetase expression in rat skeletal muscle. Pharm Res 2006; 23:670-679

**58.** Buttgereit F, Burmester GR, Straub RH, Seibel MJ, Zhou H. Exogenous and endogenous glucocorticoids in rheumatic diseases. Arthritis Rheum 2011; 63:1-9

**59.** Da Silva JA, Jacobs JW, Kirwan JR, Boers M, Saag KG, Ines LB, de Koning EJ, Buttgereit F, Cutolo M, Capell H, Rau R, Bijlsma JW. Safety of low dose glucocorticoid treatment in rheumatoid arthritis: published evidence and prospective trial data. Ann Rheum Dis 2006; 65:285-293

**60.** Bijlsma JW. Disease control with glucocorticoid therapy in rheumatoid arthritis. Rheumatology (Oxford) 2012; 51 Suppl 4:iv9-13

**61.** Neeck G, Federlin K, Graef V, Rusch D, Schmidt KL. Adrenal secretion of cortisol in patients with rheumatoid arthritis. J Rheumatol 1990; 17:24-29

**62.** Dekkers JC, Geenen R, Godaert GL, van Doornen LJ, Bijlsma JW. Diurnal rhythm of salivary cortisol levels in patients with recent-onset rheumatoid arthritis. Arthritis Rheum 2000; 43:465-467

**63.** Straub RH, Buttgereit F, Cutolo M. Alterations of the hypothalamic-pituitary-adrenal axis in systemic immune diseases - a role for misguided energy regulation. Clin Exp Rheumatol 2011; 29:S23-31

**64.** Wolff C, Krinner K, Schroeder JA, Straub RH. Inadequate corticosterone levels relative to arthritic inflammation are accompanied by altered mitochondria/cholesterol breakdown in adrenal cortex: a steroid-inhibiting role of IL-1β in rats. Ann Rheum Dis 2014:annrheumdis-2013-203885

**65.** Sarlis NJ, Chowdrey HS, Stephanou A, Lightman SL. Chronic activation of the hypothalamo-pituitary-adrenal axis and loss of circadian rhythm during adjuvant-induced arthritis in the rat. Endocrinology 1992; 130:1775-1779

**66.** Chowdrey HS, Larsen PJ, Harbuz MS, Jessop DS, Aguilera G, Eckland DJ, Lightman SL. Evidence for arginine vasopressin as the primary activator of the HPA axis during adjuvant-induced arthritis. Br J Pharmacol 1995; 116:2417-2424

**67.** Mason D. Genetic variation in the stress response: susceptibility to experimental allergic encephalomyelitis and implications for human inflammatory disease. Immunol Today 1991; 12:57-60

**68.** Shanks N, Moore PM, Perks P, Lightman SL. Alterations in hypothalamic-pituitary-adrenal function correlated with the onset of murine SLE in MRL +/+ and lpr/lpr mice. Brain Behav Immun 1999; 13:348-360

**69.** Gibbs JE, Ray DW. The role of the circadian clock in rheumatoid arthritis. Arthritis Research & Therapy 2013; 15

**70.** Narasimamurthy R, Hatori M, Nayak SK, Liu F, Panda S, Verma IM. Circadian clock protein cryptochrome regulates the expression of proinflammatory cytokines. Proceedings of the National Academy of Sciences 2012; 109:12662-12667

**71.** Voigt RM, Forsyth CB, Green SJ, Mutlu E, Engen P, Vitaterna MH, Turek FW, Keshavarzian A. Circadian disorganization alters intestinal microbiota. PLoS ONE 2014; 9:e97500

**72.** Cardinali DP, Esquifino AI. Circadian disorganization in experimental arthritis. Neurosignals 2003; 12:267-282

**73.** Seres J, Herichova I, Roman O, Bornstein S, Jurcovicova J. Evidence for Daily Rhythms of the Expression of Proopiomelanocortin, Interleukin-1-Beta and Interleukin-6 in Adenopituitaries of Male Long-Evans Rats: Effect of Adjuvant Arthritis. Neuroimmunomodulation 2004; 11:316-322

**74.** Cutolo M, Straub RH. Circadian rhythms in arthritis: Hormonal effects on the immune/inflammatory reaction. Autoimmunity Reviews 2008; 7:223-228

**75.** Straub RH, Pongratz G, Cutolo M, Wijbrandts CA, Baeten D, Fleck M, Atzeni F, Grunke M, Kalden JR, Scholmerich J, Lorenz HM, Tak PP, Sarzi-Puttini P. Increased cortisol relative to adrenocorticotropic hormone predicts improvement during anti-tumor necrosis factor therapy in rheumatoid arthritis. Arthritis Rheum 2008; 58:976-984

**76.** Ehrhart-Bornstein M, Hinson JP, Bornstein SR, Scherbaum WA, Vinson GP. Intraadrenal interactions in the regulation of adrenocortical steroidogenesis. Endocr Rev 1998; 19:101-143

**77.** Herrmann M, Scholmerich J, Straub RH. Influence of cytokines and growth factors on distinct steroidogenic enzymes in vitro: a short tabular data collection. Ann N Y Acad Sci 2002; 966:166-186

**78.** Cutolo M, Masi AT. Circadian Rhythms and Arthritis. Rheumatic Disease Clinics of North America 2005; 31:115-129

**79.** Li S, Lu A, Li B, Wang Y. Circadian rhythms on hypothalamic–pituitary–adrenal axis hormones and cytokines of collagen induced arthritis in rats. J Autoimmun 2004; 22:277-285

**80.** Straub RH, Cutolo M. Circadian rhythms in rheumatoid arthritis: implications for pathophysiology and therapeutic management. Arthritis Rheum 2007; 56:399-408

**81.** Nguyen KD, Fentress SJ, Qiu Y, Yun K, Cox JS, Chawla A. Circadian gene Bmal1 regulates diurnal oscillations of Ly6C(hi) inflammatory monocytes. Science 2013; 341:1483-1488

**82.** Spengler ML, Kuropatwinski KK, Comas M, Gasparian AV, Fedtsova N, Gleiberman AS, Gitlin II, Artemicheva NM, Deluca KA, Gudkov AV, Antoch MP. Core circadian protein CLOCK is a positive regulator of NF-κB–mediated transcription. Proceedings of the National Academy of Sciences 2012; 109:E2457-E2465

**83.** Bevaart L, Vervoordeldonk MJ, Tak PP. Evaluation of therapeutic targets in animal models of arthritis: how does it relate to rheumatoid arthritis? Arthritis Rheum 2010; 62:2192-2205

**84.** Mussener A, Litton MJ, Lindroos E, Klareskog L. Cytokine production in synovial tissue of mice with collagen-induced arthritis (CIA). Clin Exp Immunol 1997; 107:485-493

**85.** Steiner G, Tohidast-Akrad M, Witzmann G, Vesely M, Studnicka-Benke A, Gal A, Kunaver M, Zenz P, Smolen JS. Cytokine production by synovial T cells in rheumatoid arthritis. Rheumatology (Oxford) 1999; 38:202-213

**86.** Ingpen ML. The quantitative measurement of joint changes in rheumatoid arthritis. Ann Phys Med 1968; 9:322-327

**87.** Kowanko IC, Knapp MS, Pownall R, Swannell AJ. Domiciliary self-measurement in the rheumatoid arthritis and the demonstration of circadian rhythmicity. Ann Rheum Dis 1982; 41:453-455

**88.** Kowanko IC, Pownall R, Knapp MS, Swannell AJ, Mahoney PG. Circadian variations in the signs and symptoms of rheumatoid arthritis and in the therapeutic effectiveness of flurbiprofen at different times of day. Br J Clin Pharmacol 1981; 11:477-484

**89.** Bellamy N, Sothern RB, Campbell J, Buchanan WW. Circadian rhythm in pain, stiffness, and manual dexterity in rheumatoid arthritis: relation between discomfort and disability. Ann Rheum Dis 1991; 50:243-248

**90.** Loubaris N, Cros G, Serrano JJ, Boucard M. Circadian and circannual variation of the carrageenin inflammatory effect in rat. Life Sci 1983; 32:1349-1354

**91.** Labrecque G, Dore F, Belanger PM. Circadian variation of carrageenan-paw edema in the rat. Life Sci 1981; 28:1337-1343

**92.** Chrousos GP. Stress and sex versus immunity and inflammation. Sci Signal 2010; 3:pe36

**93.** Young EA. Sex differences in response to exogenous corticosterone: a rat model of hypercortisolemia. Mol Psychiatry 1996; 1:313-319

**94.** Viau V, Sawchenko PE. Hypophysiotropic neurons of the paraventricular nucleus respond in spatially, temporally, and phenotypically differentiated manners to acute vs. repeated restraint stress: rapid publication. J Comp Neurol 2002; 445:293-307

**95.** Burgess LH, Handa RJ. Chronic estrogen-induced alterations in adrenocorticotropin and corticosterone secretion, and glucocorticoid receptor-mediated functions in female rats. Endocrinology 1992; 131:1261-1269

**96.** Riede SJ, van der Vinne V, Hut RA. The flexible clock: predictive and reactive homeostasis, energy balance and the circadian regulation of sleep-wake timing. J Exp Biol 2017; 220:738-749

**97.** Johnson EO, Kamilaris TC, Chrousos GP, Gold PW. Mechanisms of stress: A dynamic overview of hormonal and behavioral homeostasis. Neuroscience & Biobehavioral Reviews 1992; 16:115-130

**98.** Chrousos GP. Stress and disorders of the stress system. Nat Rev Endocrinol 2009; 5:374-381

**99.** Chung S, Son GH, Kim K. Circadian rhythm of adrenal glucocorticoid: Its regulation and clinical implications. Biochimica et Biophysica Acta (BBA) - Molecular Basis of Disease 2011; 1812:581-591

**100.** Scheer FAJL, Hilton MF, Mantzoros CS, Shea SA. Adverse metabolic and cardiovascular consequences of circadian misalignment. Proceedings of the National Academy of Sciences 2009; 106:4453-4458

**101.** Koch CE, Leinweber B, Drengberg BC, Blaum C, Oster H. Interaction between circadian rhythms and stress. Neurobiol Stress 2017; 6:57-67

**102.** Dick TE, Molkov YI, Nieman G, Hsieh YH, Jacono FJ, Doyle J, Scheff JD, Calvano SE, Androulakis IP, An G, Vodovotz Y. Linking Inflammation, Cardiorespiratory Variability, and Neural Control in Acute Inflammation via Computational Modeling. Front Physiol 2012; 3:222

**103.** McEwen BS, Wingfield JC. What is in a name? Integrating homeostasis, allostasis and stress. Horm Behav 2010; 57:105-111

**104.** Peters A, McEwen BS. Introduction for the allostatic load special issue. Physiol Behav 2012; 106:1-4

**105.** McEwen BS. Interacting mediators of allostasis and allostatic load: towards an understanding of resilience in aging. Metabolism 2003; 52:10-16

**106.** Sterling P. Homeostasis vs allostasis: Implications for brain function and mental disorders. JAMA Psychiatry 2014; 71:1192-1193

**107.** Cannon WB. Organization for physiological homeostasis. Phys Reviews 1929; IX:399-431

**108.** Gross CG. Claude Bernard and the Constancy of the Internal Environment. The Neuroscientist 1998; 4:380-385

**109.** Sterling P. Allostasis: A model of predictive regulation. Physiology & Behavior 2012; 106:5-15

**110.** McEwen BS, Gianaros PJ. Central role of the brain in stress and adaptation: links to socioeconomic status, health, and disease. Ann N Y Acad Sci 2010; 1186:190-222

**111.** Juster RP, McEwen BS, Lupien SJ. Allostatic load biomarkers of chronic stress and impact on health and cognition. Neurosci Biobehav Rev 2010; 35:2-16

**112.** McEwen BS, Gray J, Nasca C. Recognizing Resilience: Learning from the Effects of Stress on the Brain. Neurobiol Stress 2015; 1:1-11

**113.** Karatsoreos IN, McEwen BS. Psychobiological allostasis: resistance, resilience and vulnerability. Trends Cogn Sci 2011; 15:576-584

**114.** Grissom N, Bhatnagar S. Habituation to repeated stress: get used to it. Neurobiol Learn Mem 2009; 92:215-224

**115.** Peters A, McEwen BS. Stress habituation, body shape and cardiovascular mortality. Neurosci Biobehav Rev 2015; 56:139-150

**116.** McEwen BS, Gianaros PJ. Stress- and allostasis-induced brain plasticity. Annu Rev Med 2011; 62:431-445

**117.** Romero LM, Dickens MJ, Cyr NE. The Reactive Scope Model - a new model integrating homeostasis, allostasis, and stress. Horm Behav 2009; 55:375-389

**118.** Acevedo A, Androulakis IP. Allostatic breakdown of cascading homeostat systems: A computational approach. Heliyon 2017; 3:e00355

**119.** Rao RT, Androulakis IP. Modeling the Sex Differences and Interindividual Variability in the Activity of the Hypothalamic-Pituitary-Adrenal Axis. Endocrinology 2017; 158:4017-4037

**120.** Kalsbeek A, Fliers E, Hofman MA, Swaab DF, Buijs RM. Vasopressin and the output of the hypothalamic biological clock. J Neuroendocrinol 2010; 22:362-372

**121.** Jung CM, Khalsa SB, Scheer FA, Cajochen C, Lockley SW, Czeisler CA, Wright KP, Jr. Acute effects of bright light exposure on cortisol levels. J Biol Rhythms 2010; 25:208-216

**122.** Zamora-Sillero E, Hafner M, Ibig A, Stelling J, Wagner A. Efficient characterization of high-dimensional parameter spaces for systems biology. BMC Syst Biol 2011; 5:142

**123.** von Dassow G, Meir E, Munro EM, Odell GM. The segment polarity network is a robust developmental module. Nature 2000; 406:188-192

**124.** Zhang J, Yuan Z, Li HX, Zhou T. Architecture-dependent robustness and bistability in a class of genetic circuits. Biophys J 2010; 99:1034-1042

**125.** Antonov IA, Saleev V. An economic method of computing LP τ-sequences. USSR Computational Mathematics and Mathematical Physics 1979; 19:252-256

**126.** Press WH, Teukolsky SA, Vetterling WT, Flannery BP. Numerical recipes in C. Vol 2: Cambridge university press Cambridge.

**127.** Bratley P, Fox BL. Algorithm 659: Implementing Sobol's quasirandom sequence generator. ACM Transactions on Mathematical Software (TOMS) 1988; 14:88-100

**128.** Joe S, Kuo FY. Remark on algorithm 659: Implementing Sobol's quasirandom sequence generator. ACM Transactions on Mathematical Software (TOMS) 2003; 29:49-57

**129.** Hong HS, Hickernell FJ. Algorithm 823: Implementing scrambled digital sequences. ACM Transactions on Mathematical Software (TOMS) 2003; 29:95-109

**130.** Jiri, Matousek. On the L2-discrepancy for anchored boxes. J Complex 1998; 14:527-556

**131.** Osborn JA, Kim CK, Yu W, Herbert L, Weinberg J. Fetal ethanol exposure alters pituitary-adrenal sensitivity to dexamethasone suppression. Psychoneuroendocrinology 1996; 21:127-143

**132.** Markovic VM, Cupic Z, Vukojevic V, Kolar-Anic L. Predictive modeling of the hypothalamic-pituitary-adrenal (HPA) axis response to acute and chronic stress. Endocr J 2011; 58:889-904

**133.** Lin J, Keogh E, Lonardi S, Chiu B. A Symbolic Representation of Time Series, with Implications for Streaming Algorithms. 2003, 2003

**134.** Rao R, DuBois D, Almon R, Jusko WJ, Androulakis IP. Mathematical modeling of the circadian dynamics of the neuroendocrine-immune network in experimentally induced arthritis. Am J Physiol Endocrinol Metab 2016; 311:E310-324

**135.** Korte SM, Koolhaas JM, Wingfield JC, McEwen BS. The Darwinian concept of stress: benefits of allostasis and costs of allostatic load and the trade-offs in health and disease. Neurosci Biobehav Rev 2005; 29:3-38

**136.** Goldstein DS, McEwen B. Allostasis, homeostats, and the nature of stress. Stress 2002; 5:55-58

**137.** Fonken LK, Weber MD, Daut RA, Kitt MM, Frank MG, Watkins LR, Maier SF. Stress-induced neuroinflammatory priming is time of day dependent. Psychoneuroendocrinology 2016; 66:82-90

**138.** Fekedulegn DB, Andrew ME, Burchfiel CM, Violanti JM, Hartley TA, Charles LE, Miller DB. Area under the curve and other summary indicators of repeated waking cortisol measurements. Psychosom Med 2007; 69:651-659

**139.** Albrecht U. Timing to Perfection: The Biology of Central and Peripheral Circadian Clocks. Neuron 2012; 74:246-260

**140.** Gerard C, Goldbeter A. Entrainment of the mammalian cell cycle by the circadian clock: modeling two coupled cellular rhythms. PLoS Comput Biol 2012; 8:e1002516

**141.** Erzberger A, Hampp G, Granada AE, Albrecht U, Herzel H. Genetic redundancy strengthens the circadian clock leading to a narrow entrainment range. J R Soc Interface 2013; 10:20130221

**142.** Abraham U, Granada AE, Westermark PO, Heine M, Kramer A, Herzel H. Coupling governs entrainment range of circadian clocks. Mol Syst Biol 2010; 6:438

**143.** Bordyugov G, Abraham U, Granada A, Rose P, Imkeller K, Kramer A, Herzel H. Tuning the phase of circadian entrainment. J R Soc Interface 2015; 12:20150282

**144.** Granada AE, Cambras T, Díez-Noguera A, Herzel H. Circadian desynchronization. Interface Focus 2011; 1:153-166

**145.** Andlauer P, Reinberg A, Fourre L, Battle W, Duverneuil G. Amplitude of the oral temperature circadian rhythm and the tolerance to shift-work. J Physiol (Paris) 1979; 75:507-512

**146.** Reinberg A, Andlauer P, Guillet P, Nicolai A, Vieux N, Laporte A. Oral temperature, circadian rhythm amplitude, ageing and tolerance to shift-work. Ergonomics 1980; 23:55-64

**147.** Kiessling S, Eichele G, Oster H. Adrenal glucocorticoids have a key role in circadian resynchronization in a mouse model of jet lag. J Clin Invest 2010; 120:2600-2609

**148.** Samel A, Wegmann HM. Bright light: a countermeasure for jet lag? Chronobiol Int 1997; 14:173-183

**149.** Nicolaides NC, Charmandari E, Kino T, Chrousos GP. Stress-Related and Circadian Secretion and Target Tissue Actions of Glucocorticoids: Impact on Health. Front Endocrinol (Lausanne) 2017; 8:70

**150.** Kitay JI. Sex differences in adrenal cortical secretion in the rat. Endocrinology 1961; 68:818-824

**151.** Young EA. Sex differences and the HPA axis: implications for psychiatric disease. J Gend Specif Med 1998; 1:21-27

**152.** Kageyama K, Suda T. Regulatory mechanisms underlying corticotropin-releasing factor gene expression in the hypothalamus. Endocr J 2009; 56:335-344

**153.** Drouin J, Bilodeau S, Vallette S. Of old and new diseases: genetics of pituitary ACTH excess (Cushing) and deficiency. Clin Genet 2007; 72:175-182

**154.** Figueiredo HF, Dolgas CM, Herman JP. Stress activation of cortex and hippocampus is modulated by sex and stage of estrus. Endocrinology 2002; 143:2534-2540

**155.** Goel N, Plyler KS, Daniels D, Bale TL. Androgenic influence on serotonergic activation of the HPA stress axis. Endocrinology 2011; 152:2001-2010

**156.** Sharma AN, Aoun P, Wigham JR, Weist SM, Veldhuis JD. Estradiol, but not testosterone, heightens cortisol-mediated negative feedback on pulsatile ACTH secretion and ACTH approximate entropy in unstressed older men and women. Am J Physiol Regul Integr Comp Physiol 2014; 306:R627-635

**157.** Tsigos C, Chrousos GP. Hypothalamic-pituitary-adrenal axis, neuroendocrine factors and stress. J Psychosom Res 2002; 53:865-871

**158.** Briassoulis G, Damjanovic S, Xekouki P, Lefebvre H, Stratakis CA. The glucocorticoid receptor and its expression in the anterior pituitary and the adrenal cortex: a source of variation in hypothalamic-pituitary-adrenal axis function; implications for pituitary and adrenal tumors. Endocr Pract 2011; 17:941-948

**159.** Gross KL, Lu NZ, Cidlowski JA. Molecular mechanisms regulating glucocorticoid sensitivity and resistance. Mol Cell Endocrinol 2009; 300:7-16

**160.** Quax RA, Manenschijn L, Koper JW, Hazes JM, Lamberts SW, van Rossum EF, Feelders RA. Glucocorticoid sensitivity in health and disease. Nat Rev Endocrinol 2013; 9:670-686

**161.** Lappalainen S, Utriainen P, Kuulasmaa T, Voutilainen R, Jaaskelainen J. ACTH receptor promoter polymorphism associates with severity of premature adrenarche and modulates hypothalamo-pituitary-adrenal axis in children. Pediatr Res 2008; 63:410-414

**162.** Slawik M, Reisch N, Zwermann O, Maser-Gluth C, Stahl M, Klink A, Reincke M, Beuschlein F. Characterization of an adrenocorticotropin (ACTH) receptor promoter polymorphism leading to decreased adrenal responsiveness to ACTH. J Clin Endocrinol Metab 2004; 89:3131-3137

**163.** Cornelis MC, Nugent NR, Amstadter AB, Koenen KC. Genetics of post-traumatic stress disorder: review and recommendations for genome-wide association studies. Curr Psychiatry Rep 2010; 12:313-326

**164.** Gragnoli C. Hypothesis of the neuroendocrine cortisol pathway gene role in the comorbidity of depression, type 2 diabetes, and metabolic syndrome. Appl Clin Genet 2014; 7:43-53

**165.** Taff CC, Vitousek MN. Endocrine Flexibility: Optimizing Phenotypes in a Dynamic World? Trends Ecol Evol 2016; 31:476-488

**166.** Chong RY, Oswald L, Yang X, Uhart M, Lin PI, Wand GS. The mu-opioid receptor polymorphism A118G predicts cortisol responses to naloxone and stress. Neuropsychopharmacology 2006; 31:204-211

**167.** Sheikh HI, Kryski KR, Smith HJ, Hayden EP, Singh SM. Corticotropin-releasing hormone system polymorphisms are associated with children's cortisol reactivity. Neuroscience 2013; 229:1-11

**168.** Ventura-Junca R, Symon A, Lopez P, Fiedler JL, Rojas G, Heskia C, Lara P, Marin F, Guajardo V, Araya AV, Sasso J, Herrera L. Relationship of cortisol levels and genetic polymorphisms to antidepressant response to placebo and fluoxetine in patients with major depressive disorder: a prospective study. BMC Psychiatry 2014; 14:220

**169.** Aschbacher K, Adam EK, Crofford LJ, Kemeny ME, Demitrack MA, Ben-Zvi A. Linking disease symptoms and subtypes with personalized systems-based phenotypes: a proof of concept study. Brain Behav Immun 2012; 26:1047-1056

**170.** Hartmanshenn C, Scherholz M, Androulakis IP. Physiologically-based pharmacokinetic models: approaches for enabling personalized medicine. J Pharmacokinet Pharmacodyn 2016; 43:481-504

**171.** Malendowicz LK. Sex differences in adrenocortical structure and function. III. The effects of postpubertal gonadectomy and gonadal hormone replacement on adrenal

cholesterol sidechain cleavage activity and on steroids biosynthesis by rat adrenal homogenates. Endokrinologie 1976; 67:26-35

**172.** GOVERDE HJ, PESMAN GJ, SMALS AG. The bioactivity of immunoreactive adrenocorticotrophin in human blood is dependent on the secretory state of the pituitary gland. Clinical endocrinology 1989; 31:255-265

**173.** Buckingham JC, Dohler KD, Wilson CA. Activity of the pituitary-adrenocortical system and thyroid gland during the oestrous cycle of the rat. J Endocrinol 1978; 78:359-366

**174.** Iwasaki-Sekino A, Mano-Otagiri A, Ohata H, Yamauchi N, Shibasaki T. Gender differences in corticotropin and corticosterone secretion and corticotropin-releasing factor mRNA expression in the paraventricular nucleus of the hypothalamus and the central nucleus of the amygdala in response to footshock stress or psychological stress in rats. Psychoneuroendocrinology 2009; 34:226-237

**175.** Lu J, Wu XY, Zhu QB, Li J, Shi LG, Wu JL, Zhang QJ, Huang ML, Bao AM. Sex differences in the stress response in SD rats. Behav Brain Res 2015; 284:231-237

**176.** Viau V, Meaney MJ. Variations in the hypothalamic-pituitary-adrenal response to stress during the estrous cycle in the rat. Endocrinology 1991; 129:2503-2511

**177.** Keller M, Mazuch J, Abraham U, Eom GD, Herzog ED, Volk H-D, Kramer A, Maier B. A circadian clock in macrophages controls inflammatory immune responses. Proceedings of the National Academy of Sciences 2009; 106:21407-21412

**178.** Pollmacher T, Mullington J, Korth C, Schreiber W, Hermann D, Orth A, Galanos C, Holsboer F. Diurnal variations in the human host response to endotoxin. J Infect Dis 1996; 174:1040-1045

**179.** Alamili M, Bendtzen K, Lykkesfeldt J, Rosenberg J, Gogenur I. Pronounced inflammatory response to endotoxaemia during nighttime: a randomised cross-over trial. PLoS ONE 2014; 9:e87413

**180.** Arnetz L, Rajamand Ekberg N, Brismar K, Alvarsson M. Gender difference in adrenal sensitivity to ACTH is abolished in type 2 diabetes. Endocr Connect 2015; 4:92-99

**181.** Lund TD, Munson DJ, Haldy ME, Handa RJ. Dihydrotestosterone may inhibit hypothalamo-pituitary-adrenal activity by acting through estrogen receptor in the male mouse. Neurosci Lett 2004; 365:43-47

**182.** Nowak KW, Neri G, Nussdorfer GG, Malendowicz LK. Effects of sex hormones on the steroidogenic activity of dispersed adrenocortical cells of the rat adrenal cortex. Life Sci 1995; 57:833-837

**183.** Kirschbaum C, Schommer N, Federenko I, Gaab J, Neumann O, Oellers M, Rohleder N, Untiedt A, Hanker J, Pirke KM, Hellhammer DH. Short-term estradiol treatment enhances pituitary-adrenal axis and sympathetic responses to psychosocial stress in healthy young men. J Clin Endocrinol Metab 1996; 81:3639-3643

**184.** Fonken LK, Frank MG, Kitt MM, Barrientos RM, Watkins LR, Maier SF. Microglia inflammatory responses are controlled by an intrinsic circadian clock. Brain Behav Immun

**185.** Oster H, Damerow S, Kiessling S, Jakubcakova V, Abraham D, Tian J, Hoffmann MW, Eichele G. The circadian rhythm of glucocorticoids is regulated by a gating mechanism residing in the adrenal cortical clock. Cell Metab 2006; 4:163-173

**186.** Sterrenburg L, Gaszner B, Boerrigter J, Santbergen L, Bramini M, Roubos EW, Peeters BW, Kozicz T. Sex-dependent and differential responses to acute restraint stress of corticotropin-releasing factor-producing neurons in the rat paraventricular nucleus, central amygdala, and bed nucleus of the stria terminalis. J Neurosci Res 2012; 90:179-192

**187.** Bethin KE, Vogt SK, Muglia LJ. Interleukin-6 is an essential, corticotropin-releasing hormone-independent stimulator of the adrenal axis during immune system activation. Proc Natl Acad Sci U S A 2000; 97:9317-9322

**188.** Csete M, Doyle J. Bow ties, metabolism and disease. Trends Biotechnol 2004; 22:446-450

**189.** Csete ME, Doyle JC. Reverse engineering of biological complexity. Science 2002; 295:1664-1669

**190.** Buijs RM, Escobar C. Corticosterone and activity: the long arms of the clock talk back. Endocrinology 2007; 148:5162-5164

**191.** Aschoff J, Pohl H. Phase relations between a circadian rhythm and its zeitgeber within the range of entrainment. Naturwissenschaften 1978; 65:80-84

**192.** Brown SA, Kunz D, Dumas A, Westermark PO, Vanselow K, Tilmann-Wahnschaffe A, Herzel H, Kramer A. Molecular insights into human daily behavior. Proc Natl Acad Sci U S A 2008; 105:1602-1607

**193.** van der Veen DR, Riede SJ, Heideman PD, Hau M, van der Vinne V, Hut RA. Flexible clock systems: adjusting the temporal programme. Philos Trans R Soc Lond B Biol Sci 2017; 372

**194.** Hasegawa Y, Arita M. Circadian clocks optimally adapt to sunlight for reliable synchronization. J R Soc Interface 2014; 11:20131018

**195.** Ramsay DS, Woods SC. Clarifying the roles of homeostasis and allostasis in physiological regulation. Psychol Rev 2014; 121:225-247

**196.** Raubenheimer D, Simpson SJ, Tait AH. Match and mismatch: conservation physiology, nutritional ecology and the timescales of biological adaptation. Philos Trans R Soc Lond B Biol Sci 2012; 367:1628-1646

**197.** Girotti M, Pace TW, Gaylord RI, Rubin BA, Herman JP, Spencer RL. Habituation to repeated restraint stress is associated with lack of stress-induced c-fos expression in primary sensory processing areas of the rat brain. Neuroscience 2006; 138:1067-1081

**198.** McMillan PJ, Wilkinson CW, Greenup L, Raskind MA, Peskind ER, Leverenz JB. Chronic cortisol exposure promotes the development of a GABAergic phenotype in the primate hippocampus. J Neurochem 2004; 91:843-851

**199.** Sherin JE, Nemeroff CB. Post-traumatic stress disorder: the neurobiological impact of psychological trauma. Dialogues Clin Neurosci 2011; 13:263-278

**200.** Ulrich-Lai YM, Figueiredo HF, Ostrander MM, Choi DC, Engeland WC, Herman JP. Chronic stress induces adrenal hyperplasia and hypertrophy in a subregion-specific manner. American journal of physiology Endocrinology and metabolism 2006; 291:E965-973

**201.** Michael TP, Salome PA, Yu HJ, Spencer TR, Sharp EL, McPeek MA, Alonso JM, Ecker JR, McClung CR. Enhanced fitness conferred by naturally occurring variation in the circadian clock. Science 2003; 302:1049-1053

**202.** de Montaigu A, Giakountis A, Rubin M, Toth R, Cremer F, Sokolova V, Porri A, Reymond M, Weinig C, Coupland G. Natural diversity in daily rhythms of gene expression contributes to phenotypic variation. Proc Natl Acad Sci U S A 2015; 112:905-910

**203.** Salmela MJ, Greenham K, Lou P, McClung CR, Ewers BE, Weinig C. Variation in circadian rhythms is maintained among and within populations in Boechera stricta. Plant Cell Environ 2016; 39:1293-1303

**204.** Kubota A, Shim JS, Imaizumi T. Natural variation in transcriptional rhythms modulates photoperiodic responses. Trends Plant Sci 2015; 20:259-261

**205.** Harrington M, Molyneux P, Soscia S, Prabakar C, McKinley-Brewer J, Lall G. Behavioral and neurochemical sources of variability of circadian period and phase: studies of circadian rhythms of npy-/- mice. Am J Physiol Regul Integr Comp Physiol 2007; 292:R1306-1314

**206.** Mavroudis PD, Scheff JD, Calvano SE, Androulakis IP. Systems biology of circadian-immune interactions. J Innate Immun 2013; 5:153-162

**207.** Retana-Marquez S, Bonilla-Jaime H, Vazquez-Palacios G, Dominguez-Salazar E, Martinez-Garcia R, Velazquez-Moctezuma J. Body weight gain and diurnal differences of corticosterone changes in response to acute and chronic stress in rats. Psychoneuroendocrinology 2003; 28:207-227

**208.** Johnson JD, O'Connor KA, Hansen MK, Watkins LR, Maier SF. Effects of prior stress on LPS-induced cytokine and sickness responses. Am J Physiol Regul Integr Comp Physiol 2003; 284:R422-432

**209.** Akana SF, Dallman MF, Bradbury MJ, Scribner KA, Strack AM, Walker CD. Feedback and facilitation in the adrenocortical system: unmasking facilitation by partial inhibition of the glucocorticoid response to prior stress. Endocrinology 1992; 131:57-68

**210.** Marti O, Gavalda A, Gomez F, Armario A. Direct evidence for chronic stress-induced facilitation of the adrenocorticotropin response to a novel acute stressor. Neuroendocrinology 1994; 60:1-7

**211.** Del Giudice M, Ellis BJ, Shirtcliff EA. The Adaptive Calibration Model of stress responsivity. Neurosci Biobehav Rev 2011; 35:1562-1592

**212.** Franklin TB, Saab BJ, Mansuy IM. Neural mechanisms of stress resilience and vulnerability. Neuron 2012; 75:747-761

**213.** Stephens MA, Wand G. Stress and the HPA axis: role of glucocorticoids in alcohol dependence. Alcohol Res 2012; 34:468-483

**214.** Lockley SW, Skene DJ, James K, Thapan K, Wright J, Arendt J. Melatonin administration can entrain the free-running circadian system of blind subjects. J Endocrinol 2000; 164:R1-6

**215.** McArthur AJ, Lewy AJ, Sack RL. Non-24-hour sleep-wake syndrome in a sighted man: circadian rhythm studies and efficacy of melatonin treatment. Sleep 1996; 19:544-553

**216.** Wulff K, Porcheret K, Cussans E, Foster RG. Sleep and circadian rhythm disturbances: multiple genes and multiple phenotypes. Curr Opin Genet Dev 2009; 19:237-246

**217.** Kamgar-Parsi B, Wehr TA, Gillin JC. Successful treatment of human non-24-hour sleep-wake syndrome. Sleep 1983; 6:257-264

**218.** Arlt W, Stewart PM. Adrenal corticosteroid biosynthesis, metabolism, and action. Endocrinol Metab Clin North Am 2005; 34:293-313, viii

**219.** Fietta P, Fietta P, Delsante G. Central nervous system effects of natural and synthetic glucocorticoids. Psychiatry Clin Neurosci 2009; 63:613-622

**220.** Smith SM, Vale WW. The role of the hypothalamic-pituitary-adrenal axis in neuroendocrine responses to stress. Dialogues Clin Neurosci 2006; 8:383-395

**221.** Hench PS, Kendall EC, Slocumb CH, Polley HF. The effect of a hormone of the adrenal cortex (17-hydroxy-11-dehydrocorticosterone: compound E) and of pituitary adrenocortical hormone in arthritis: preliminary report. Ann Rheum Dis 1949; 8:97-104

**222.** Fisher LE, Ludwig EA, Wald JA, Sloan RR, Middleton E, Jr., Jusko WJ. Pharmacokinetics and pharmacodynamics of methylprednisolone when administered at 8 am versus 4 pm. Clin Pharmacol Ther 1992; 51:677-688

**223.** Czock D, Keller F, Rasche FM, Haussler U. Pharmacokinetics and pharmacodynamics of systemically administered glucocorticoids. Clin Pharmacokinet 2005; 44:61-98

**224.** Beltrametti SP, Ianniello A, Ricci C. Chronotherapy with low-dose modified-release prednisone for the management of rheumatoid arthritis: a review. Ther Clin Risk Manag 2016; 12:1763-1776

**225.** Xu J, Winkler J, Sabarinath SN, Derendorf H. Assessment of the impact of dosing time on the pharmacokinetics/pharmacodynamics of prednisolone. AAPS J 2008; 10:331-341

**226.** Curtis JR, Westfall AO, Allison J, Bijlsma JW, Freeman A, George V, Kovac SH, Spettell CM, Saag KG. Population-based assessment of adverse events associated with long-term glucocorticoid use. Arthritis Rheum 2006; 55:420-426

**227.** Rhen T, Cidlowski JA. Antiinflammatory action of glucocorticoids--new mechanisms for old drugs. N Engl J Med 2005; 353:1711-1723

**228.** Fardet L, Petersen I, Nazareth I. Suicidal behavior and severe neuropsychiatric disorders following glucocorticoid therapy in primary care. Am J Psychiatry 2012; 169:491-497

**229.** Hwang JL, Weiss RE. Steroid-induced diabetes: a clinical and molecular approach to understanding and treatment. Diabetes Metab Res Rev 2014; 30:96-102

**230.** Moghadam-Kia S, Werth VP. Prevention and treatment of systemic glucocorticoid side effects. International journal of dermatology 2010; 49:239-248

**231.** Cutolo M. Glucocorticoids and chronotherapy in rheumatoid arthritis. RMD Open 2016; 2:e000203

**232.** Haus E, Sackett-Lundeen L, Smolensky MH. Rheumatoid arthritis: circadian rhythms in disease activity, signs and symptoms, and rationale for chronotherapy with corticosteroids and other medications. Bull NYU Hosp Jt Dis 2012; 70 Suppl 1:3-10

**233.** Kirwan JR. Targeting the time of day for glucocorticoid delivery in rheumatoid arthritis. Int J Clin Rheumatol 2011; 6:273-279

**234.** Haus E, Sackett-Lundeen L, Smolensky MH. Rheumatoid arthritis: circadian rhythms in disease activity, signs and symptoms, and rationale for chronotherapy with corticosteroids and other medications. Bull NYU Hosp Jt Dis 2012; 70 Suppl 1:3-10

**235.** Newell-Price J, Whiteman M, Rostami-Hodjegan A, Darzy K, Shalet S, Tucker GT, Ross RJ. Modified-release hydrocortisone for circadian therapy: a proof-of-principle study in dexamethasone-suppressed normal volunteers. Clin Endocrinol (Oxf) 2008; 68:130-135

**236.** Peng HT, Bouak F, Vartanian O, Cheung B. A physiologically based pharmacokinetics model for melatonin--effects of light and routes of administration. Int J Pharm 2013; 458:156-168

**237.** Xu J, Winkler J, Derendorf H. A pharmacokinetic/pharmacodynamic approach to predict total prednisolone concentrations in human plasma. J Pharmacokinet Pharmacodyn 2007; 34:355-372

**238.** Mould DR, Upton RN. Basic concepts in population modeling, simulation, and model-based drug development-part 2: introduction to pharmacokinetic modeling methods. CPT Pharmacometrics Syst Pharmacol 2013; 2:e38

**239.** Cirincione B, Edwards J, Mager DE. Population Pharmacokinetics of an Extended-Release Formulation of Exenatide Following Single- and Multiple-Dose Administration. AAPS J 2017; 19:487-496

**240.** Johnson CH. Phase response curves: what can they tell us about circadian clocks. Circadian clocks from cell to human 1992:209-249

**241.** Smolensky MH, Peppas NA. Chronobiology, drug delivery, and chronotherapeutics. Adv Drug Deliv Rev 2007; 59:828-851

**242.** Ballesta A, Innominato PF, Dallmann R, Rand DA, Levi FA. Systems Chronotherapeutics. Pharmacol Rev 2017; 69:161-199

**243.** Levi F, Schibler U. Circadian Rhythms: Mechanisms and Therapeutic Implications. Annual Review of Pharmacology and Toxicology 2007; 47:593-628

**244.** Bodick N, Lufkin J, Willwerth C, Kumar A, Bolognese J, Schoonmaker C, Ballal R, Hunter D, Clayman M. An intra-articular, extended-release formulation of triamcinolone acetonide prolongs and amplifies analgesic effect in patients with osteoarthritis of the knee: a randomized clinical trial. J Bone Joint Surg Am 2015; 97:877-888

**245.** Johannsson G, Bergthorsdottir R, Nilsson AG, Lennernas H, Hedner T, Skrtic S. Improving glucocorticoid replacement therapy using a novel modified-release hydrocortisone tablet: a pharmacokinetic study. Eur J Endocrinol 2009; 161:119-130

**246.** Forss M, Batcheller G, Skrtic S, Johannsson G. Current practice of glucocorticoid replacement therapy and patient-perceived health outcomes in adrenal insufficiency - a worldwide patient survey. BMC Endocr Disord 2012; 12:8

**247.** Potter GD, Skene DJ, Arendt J, Cade JE, Grant PJ, Hardie LJ. Circadian Rhythm and Sleep Disruption: Causes, Metabolic Consequences, and Countermeasures. Endocr Rev 2016; 37:584-608

**248.** Pulivarthy SR, Tanaka N, Welsh DK, De Haro L, Verma IM, Panda S. Reciprocity between phase shifts and amplitude changes in the mammalian circadian clock. Proc Natl Acad Sci U S A 2007; 104:20356-20361

**249.** Spoelstra K, Albrecht U, van der Horst GT, Brauer V, Daan S. Phase responses to light pulses in mice lacking functional per or cry genes. J Biol Rhythms 2004; 19:518-529

**250.** Malisch JL, Breuner CW, Gomes FR, Chappell MA, Garland T, Jr. Circadian pattern of total and free corticosterone concentrations, corticosteroid-binding globulin, and physical activity in mice selectively bred for high voluntary wheel-running behavior. Gen Comp Endocrinol 2008; 156:210-217

**251.** Angeli A, Frajria R, Bisbocci D, Ceresa F. Temporal changes in plasma transcortin (CBG) binding capacity during the menstrual cycle. Biological Rhythm Research 1977; 8:237-242

**252.** Harris AP, Holmes MC, de Kloet ER, Chapman KE, Seckl JR. Mineralocorticoid and glucocorticoid receptor balance in control of HPA axis and behaviour. Psychoneuroendocrinology 2013; 38:648-658

**253.** Magee MH, Blum RA, Lates CD, Jusko WJ. Prednisolone pharmacokinetics and pharmacodynamics in relation to sex and race. J Clin Pharmacol 2001; 41:1180-1194

# Appendix

## Table A1

CIA Model Parameter Values

| | Parameter | Value (Mechanism A) | Values (Mechanism B) | Description |
|---|---|---|---|---|
| 1 | $k_{p1}$ | 0.418 | 0.418 | Rate of CRH production, estimated |
| 2 | $K_{p1}$ | 2.6377 | 2.6377 | Dissociation constant for CRH production, estimated |
| 3 | $V_{d1}$ | 0.2232 | 0.2232 | Rate of CRH enzymatic degradation, estimated |
| 4 | $K_{d1}$ | 4.3503 | 4.3503 | Michaelis-Menten constant of CRH enzymatic degradation, estimated |
| 5 | $k_{p2}$ | 0.4691 | 0.4691 | Rate of ACTH production, estimated |
| 6 | $V_{d2}$ | 0.8642 | 0.8642 | Rate of ACTH enzymatic degradation, estimated |
| 7 | $K_{d2}$ | 1.061 | 1.061 | Michaelis-Menten constant of ACTH enzymatic degradation, estimated |
| 8 | $k_{p3}$ | 0.6203 | 0.6203 | Rate of $CORT_{HPA}$ production, estimated |
| 9 | $V_{d3}$ | 0.4011 | 0.4011 | Rate of $CORT_{HPA}$ enzymatic degradation, estimated |
| 10 | $K_{d3}$ | 0.007511 | 0.007511 | Michaelis-Menten constant of $CORT_{HPA}$enzymatic degradation, estimated |
| 11 | $k_{syn_{GRm}}$ | 2.9 | 2.9 | Rate of synthesis of GR mRNA, (36) |
| 12 | $IC_{50,GRm}$ | 26.2 | 26.2 | Concentration of DR(N) at which GR mRNA synthesis drops to half it's maximal value |

| | | | | |
|---|---|---|---|---|
| | | | | (36) |
| 13 | $k_{deg}$ | 0.1124 | 0.1124 | Rate of degradation of GR mRNA (36) |
| 14 | $k_{syn,GR}$ | 1.1987 | 1.1987 | Rate of synthesis of GR, (36) |
| 15 | $k_{re}$ | 0.57 | 0.57 | Rate of receptor recycling from nucleus to cytoplasm (36) |
| 16 | $r_f$ | 0.49 | 0.49 | Fraction of CORT-GR complex recycled (36) |
| 17 | $k_{on}$ | 0.00329 | 0.00329 | Second order rate constant for CORT-GR binding (36) |
| 18 | $k_{deg,GR}$ | 0.0572 | 0.0572 | Rate of degradation of GR (36) |
| 19 | $k_T$ | 0.63 | 0.63 | Rate of receptor (36)translocation from cytoplasm to nucleus |
| 20 | $\tau_{CORT,HPA}$ | 0.1401 | 0.1401 | Transduction coefficient for CORT from the adrenal to periphery (38) |
| 21 | $K_{p2}$ | 3.29716 | 3.29716 | Dissociation constant for the ACTH production, estimated |
| 22 | $K_{dm}$ | 2.1147 | 10 | Michaelis-Menten constant of tolerance mediator, M, enzymatic degradation, estimated |
| 23 | $k_{pcyt\_ACTH}$ | 0.22 | 0.176 | Rate of ACTH production due to proinflammatory cytokines release, estimated |
| 24 | $K_{pcyt}$ | 12 | 11 | Dissociation constant for the ACTH production due to cytokines, estimated |
| 25 | $\gamma 2$ | 2 | 2 | Hill coefficient for inhibition of cytokine-dependent production of ACTH by DR(N), estimated |
| 26 | $k_{pm}$ | 45 | 45 | Dissociation constant for the M production, estimated |

| | | | | |
|---|---|---|---|---|
| 27 | γcyt | 4 | 4 | Hill coefficient for cytokine-dependent production of M, estimated |
| 28 | $k_{out}$ | 0.1 | 0.1 | Rate of degradation of the tolerance mediator, estimated |
| 29 | $k_{GR_{cyt}}$ | 0.4 | 0.46 | Rate of production of GR mRNA due to proinflammatory cytokines in HPA, estimated |
| 30 | γ3h | 4 | 4 | Hill coefficient for cytokine-dependent production of GR mRNA in the HPA, estimated |
| 31 | $k_{pGR_{cyt}}$ | 45 | 45 | Dissociation constant for GR mRNA cytokine-dependent production in HPA, estimated |
| 32 | γ3p | 4 | 4 | Hill coefficient for cytokine-dependent production of GR mRNA in the periphery, estimated |
| 33 | $k_{GR_{cyt}}$ | 0.4 | 0.46 | Rate of production of GR mRNA due to proinflammatory cytokines in periphery, estimated |
| 34 | $k_{pGR_{cyt}}$ | 45 | 45 | Dissociation constant for GR mRNA cytokine-dependent production in periphery, estimated |
| 35 | $k_{TC_{Cyt}}$ | 0.1 | 0.08 | Rate of production of cytokines during ongoing chronic inflammation, estimated, estimated |
| 36 | $k_{out_{Cyt\_mRNA}}$ | 1.24 | 1.24 | Rate of degradation of cytokine mRNA in the periphery, (37) |
| 37 | $k_{in_{Cyt\_per}}$ | 1.2 | 1.2 | Rate of synthesis of cytokine protein in the periphery |
| 38 | $k_{cyt\_in}$ | 0.0015 | 0.0015 | Rate of paw edema production to proinflammatory cytokines, estimated |

| | | | | |
|---|---|---|---|---|
| 39 | $k_{growth}$ | 0.01297 | 0.01297 | Natural growth rate of paw, (37) |
| 40 | $PAW_0$ | 81.68 | 81.68 | Initial value of paw size, (37) |
| 41 | $k_{m1}$ | 0.14 | 0.14 | Rate of production of tolerance mediator M, due to elevated cytokine levels, estimated |
| 42 | $\tau_{cyt}$ | 0.168 | 0.168 | Transduction coefficient for cytokines from the periphery to the HPA axis, estimated |
| 43 | $V_{dm}$ | 1 | 5 | Effectiveness factor for hypothetical tolerance mediator M |
| 44 | $\gamma m$ | 4 | 3 | Hill coefficient for tolerance mediator dependent action on ACTH (mechanism A) and CORT (mechanism B), respectively. |
| 45 | $k_{out_{Cyt_{per}}}$ | 1 | 1 | Rate of degradation of cytokine protein in the periphery, estimated |
| 46 | $\gamma 1$ | 1 | 1 | Hill coefficient for inhibition of CRH-dependent production of ACTH by DR(N), estimated |
| 47 | $k_{in_{Cyt\_mRNA}}$ | 24.82 | 24.82 | Rate of synthesis of cytokine mRNA, (37) |
| 48 | $IC_{50_{Cyt}}$ | 32.55 | 32.55 | Concentration of DR(N) at which proinflammatory cytokine synthesis constant drops to half it's maximal value (36) |
| 49 | $k_{t_{Cyt}}$ | 0.0345 | 0.0345 | Transduction coefficient for cytokines, (37) |
| 50 | $k_{dis\_Cyt}$ | 70.11 | 70.11 | Steady-state cytokine levels during disease conditions, (37) |

## Table A2

Cosinor Analysis of Simulated Waveforms

| Mediator | Mesor | | Amplitude | | Period | | Acrophase | |
|---|---|---|---|---|---|---|---|---|
| | Healthy | Arthritic | Healthy | Arthritic | Healthy | Arthritic | Healthy | Arthritic |
| Mechanism A | | | | | | | | |
| CORT in periphery | 1.3439 | 2.0902 | 0.8683 | 0.1436 | 24.004 | 24.00 | 16.226 | 5.3478 |
| ACTH | 0.6416 | 0.64421 | 0.3666 | 0.06064 | 24.003 | 24.00 | 10.142 | 23.2164 |
| Peripheral Cytokines | 21.665 | 59.2882 | 1.1068 | 0.16749 | 24.0043 | 24.00 | 9.1094 | 22.2180 |
| GR mRNA in HPA | 22.926 | 23.871 | 0.5994 | 0.0887 | 24.005 | 24.00 | 11.689 | 1.37 |
| GR in HPA | 462.244 | 471.386 | 2.6114 | 0.44573 | 24.005 | 24.00 | 10.607 | 23.2681 |
| Mechanism B | | | | | | | | |
| CORT in the periphery | 1.2268 | 2.026 | 0.9207 | 0.145 | 24.000 | 24.000 | 16.598 | 6.972 |
| ACTH | 0.6405 | 0.486 | 0.3880 | 0.0459 | 23.999 | 24.000 | 10.541 | 0.801 |
| Peripheral Cytokines | 21.832 | 51.599 | 1.2085 | 0.171 | 23.999 | 24.000 | 9.5125 | 23.845 |
| GR mRNA in HPA | 23.173 | 23.898 | 0.6589 | 0.0924 | 24.000 | 24.000 | 12.098 | 2.489 |
| GR in HPA | 468.771 | 472.73 | 2.796 | 0.4452 | 24.000 | 24.000 | 11.099 | 0.987 |

## Table A3

Experimental Cosinor Parameters and Simulated Cosinor Error Criteria

| Scaled Experimental Cosinor Parameters | | |
|---|---|---|
| $f(t) = M_{exp} + A_{exp}\cos\left(2\pi\frac{(\mathrm{t} - \theta_{exp})}{24}\right)$ | | |
| Feature | Male | Female |
| Mean ($M_{exp}$) | 1 ± 0.2 | 2.40 ± 0.14 |
| Amplitude ($A_{exp}$) | 1.01 ± 0.19 | 2.2 ± 0.42 |
| Phase ($\theta_{exp}$) | 21.3 ± 0.3 | 20.7 ± 0.9 |
| Error Criteria for Simulated Cosinor Parameters | | |
| Mean ($M_{sim}$) | $M_{exp} - \sigma_M \leq M_{sim} \leq M_{exp} + \sigma_M$ | |
| Amplitude ($A_{sim}$) | $A_{exp} - \sigma_A \leq A_{sim} \leq A_{exp} + \sigma_A$ | |
| Phase ($\theta_{sim}$) | $\theta_{exp} - \sigma_\theta \leq \theta_{sim} \leq \theta_{exp} + \sigma_\theta$ | |
| Sampling Bounds for Sex-Specific Parameters | | |
| Parameter | Lower bound | Upper bound |
| $K_{p1}$ | 0 | 6 |
| $K_{p2}$ | 0 | 20 |
| $k_{p3}$ | 0 | 1.5 |

# Table A4

List of Parameters Common to Both Sexes

| Parameter | Value | Description |
|---|---|---|
| $k_{p1}$ | 0.3819 | Estimated, zero order synthesis rate constant of CRH |
| $V_{d1}$ | 0.3492 | Estimated, first order rate constant for CRH degradation |
| $K_{d1}$ | 4.3875 | Estimated, Michaelis-Menten constant for CRH degradation |
| $k_{p2}$ | 0.4561 | Estimated, first order rate constant for synthesis of ACTH |
| $V_{d2}$ | 1.0015 | Estimated, first order rate constant for degradation of ACTH |
| $K_{d2}$ | 0.8488 | Estimated, Michaelis-Menten constant for ACTH degradation |
| $V_{d3}$ | 0.7245 | Estimated, first order rate constant for CORT degradation |
| $K_{d3}$ | 0.1807 | Estimated, Michaelis-Menten constant for CORT degradation |
| $GR(0)$ | 540.7 | Initial GR content, (36) |
| $GR_{mRNA}(0)$ | 25.8 | Initial GR mRNA content, (36) |
| $k_{syn_{GRm}}$ | 2.9 | Zero order rate constant for synthesis of GR mRNA, (36) |
| $r_f$ | 0.49 | GR recycle fraction from nucleus to cytoplasm, |

| | | |
|---|---|---|
| | | (36) |
| $k_{re}$ | 0.57 | Rate of GR recycling from nucleus to cytoplasm, (36) |
| $k_{on}$ | 0.00329 | Second-order rate constant for CORT-GR binding, (36) |
| $k_{deg,GRm}$ | $k_{syn_{GRm}}/GR_{mRNA}(0)$ | First-order rate constant for degradation of GR mRNA, (36) |
| $k_{deg,GR}$ | 0.0572 | First order rate constant for degradation of GR, (36) |
| $k_{syn,GR}$ | $GR(0).k_{deg,GR}$ / $GR_{mRNA}(0)$ | First order rate constant for synthesis of GR, (36) |
| $k_T$ | 0.63 | Rate of GR translocation from cytoplasm to nucleus, (36) |
| $k_{imp}$ | 0.5 | Strength of ACTH impulse |
| $k_{stress.out}$ | 6.79 | Rate constant for clearance of stressor |
| $k_s$ | 40 | Strength of induction of CRH production by stressor |

## Table A5

Multi-linear regression analysis to assess the dependence of the leading Floquet exponent ($\hat{y}$) on the parameters representing the negative feedback ($K_{p1}$, $K_{p2}$) and adrenal sensitivity ($k_{p3}$) in our model.

| Regression Model: $\widehat{\boldsymbol{y}} = b_0 + b_1.\boldsymbol{K_{p1}} + b_2.\boldsymbol{K_{p2}} + b_3.\boldsymbol{k_{p3}}$ | | | | |
|---|---|---|---|---|
| Condition | $b_0$ [95% CI] | $b_1$ [95% CI] | $b_2$ [95% CI] | $b_3$ [95% CI] |

| | | | | |
|---|---|---|---|---|
| Nominal | 0.1897 [0.1892 0.1902] | 0.00106 [0.00103 0.00109] | 0.0115 [0.0112 0.0118] | -0.1311 [-0.1321 - 0.1302] |
| Intermediate Stress | 0.1825 [0.1812 0.1837] | 0.0005 [0.0002 0.0008] | 0.0052 [0.0045 0.0060] | -0.0809 [-0.0830 - 0.0787] |
| High Stress | 0.1783 [0.1764 0.1801] | -0.0009 [-0.0018 - 0.00005] | 0.0014 [0.0002 0.0026] | -0.0565 [-0.0591 - 0.0539] |

## Table A6

List of Parameters Common for diurnal HPA axis model

| Parameter | Value | Description |
|---|---|---|
| $k_{p1}$ | 0.3819 $\mu Mh^{-1}$ | Estimated, zero order synthesis rate constant of CRH |
| $V_{d1}$ | 0.3492 $\mu Mh^{-1}$ | Estimated, first order rate constant for CRH degradation |
| $K_{d1}$ | 4.3875 µM | Estimated, Michaelis-Menten constant for CRH degradation |
| $k_{p2}$ | 0.4561 $\mu Mh^{-1}$ | Estimated, first order rate constant for synthesis of ACTH |
| $V_{d2}$ | 1.0015 $\mu Mh^{-1}$ | Estimated, first order rate constant for degradation of ACTH |
| $K_{d2}$ | 0.8488 µM | Estimated, Michaelis-Menten constant for ACTH degradation |
| $V_{d3}$ | 0.7245 $\mu Mh^{-1}$ | Estimated, first order rate constant for CORT |

| | | |
|---|---|---|
| | | degradation |
| $K_{d3}$ | 0.1807 µM | Estimated, Michaelis-Menten constant for CORT degradation |
| $GR(0)$ | 540.7 nmol $L^{-1}$ mg protein$^{-1}$ | Initial GR content, (36) |
| $GR_{mRNA}(0)$ | 25.8 fmol$g^{-1}$ | Initial GR mRNA content, (36) |
| $k_{syn_{GRm}}$ | 2.9 fmol$g^{-1}$ $h^{-1}$ | Zero order rate constant for synthesis of GR mRNA, (36) |
| $r_f$ | 0.49 | GR recycle fraction from nucleus to cytoplasm, (36) |
| $k_{re}$ | 0.57 $h^{-1}$ | Rate of GR recycling from nucleus to cytoplasm, (36) |
| $k_{on}$ | 0.00329 L $nmol^{-1}$ $h^{-1}$ | Second-order rate constant for CORT-GR binding, (36) |
| $k_{deg,GRm}$ | $k_{syn_{GRm}}/GR_{mRNA}(0)$ | First-order rate constant for degradation of GR mRNA, (36) |
| $k_{deg,GR}$ | 0.0572 $h^{-1}$ | First order rate constant for degradation of GR, (36) |
| $k_{syn,GR}$ | $GR(0).k_{deg,GR}$ / $GR_{mRNA}(0)$ | First order rate constant for synthesis of GR, (36) |
| $k_T$ | 0.63 $h^{-1}$ | Rate of GR translocation from cytoplasm to nucleus, (36) |
| $k_{imp}$ | 0.5 | Strength of ACTH impulse |
| $k_{stress.out}$ | 6.79 $h^{-1}$ | Rate constant for |

| | | |
|---|---|---|
| | | clearance of stressor |
| $k_s$ | 40 | Strength of induction of CRH production by stressor |
| $k_a$ | 0.42 $hr^{-1}$ | First-order absorption rate constant for PNL (237) |
| $k_e$ | 0.33 $hr^{-1}$ | First-order elimination rate constant for PNL (237) |
| $k_{t1}$,$k_{t2}$,$k_{t3}$,$k_{t4}$,$k_{t5}$ | 1 $hr^{-1}$ | Rate constants for transfer between transit compartments |

# Supplementary Figures

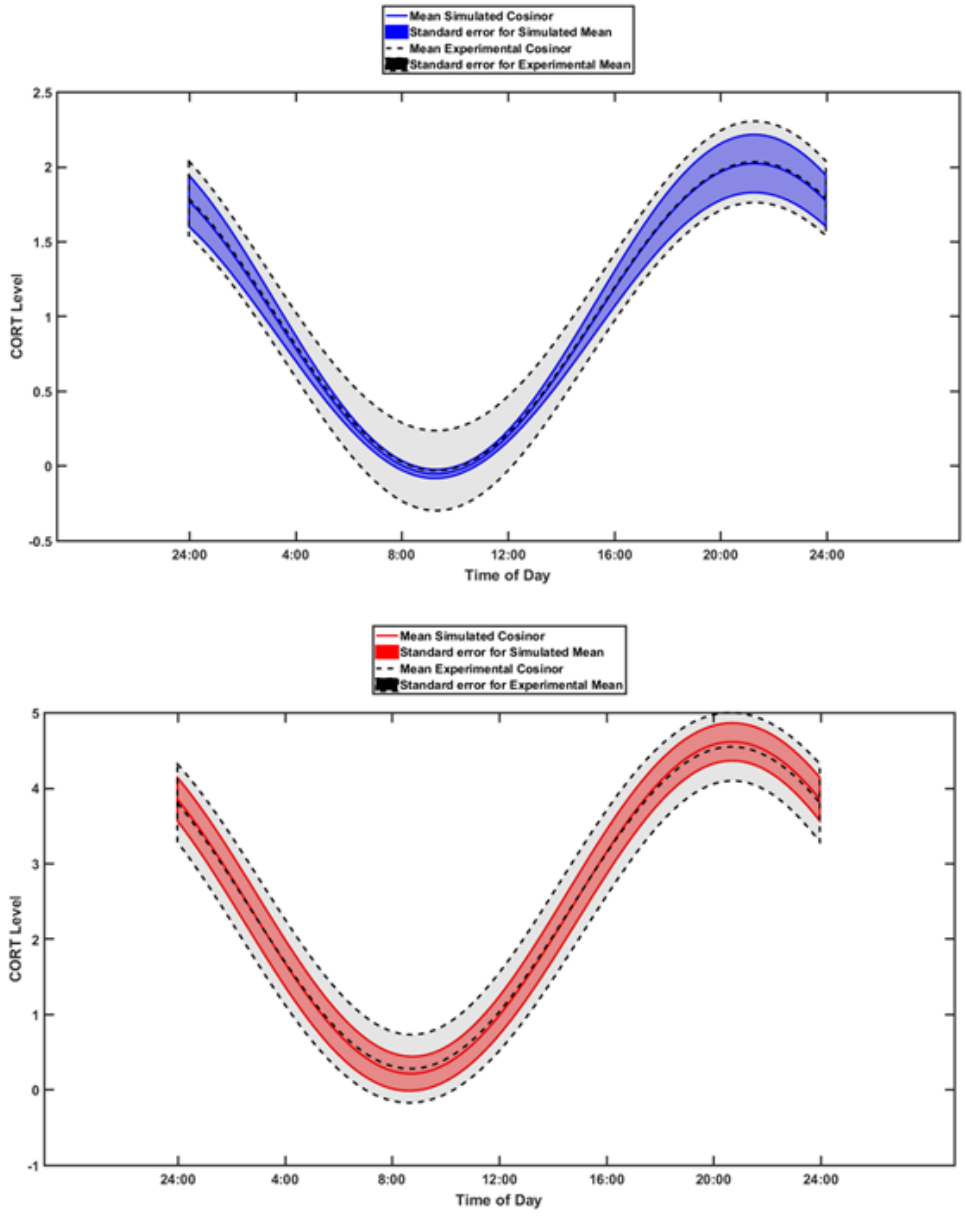


Supplementary Figure S1: Representative circadian CORT profiles generated by the parameter sets within each parameter space generated with $kp_I$=1.5× i.e. intermediate chronic stress. The blue solid line (top) represents the mean of CORT circadian profiles generated by the male parameters, while the red solid line (bottom) represents the mean of the CORT circadian profiles generated by the female parameters. The blue (top) and red (bottom) shaded areas represent the standard deviation of the male and female simulated CORT circadian profiles, respectively. The black dashed lines represent the experimental cosinor for male (top) and female (bottom), respectively. The gray shaded areas represent the standard deviation of the male (top) and female (bottom) experimental CORT cosinors, respectively.

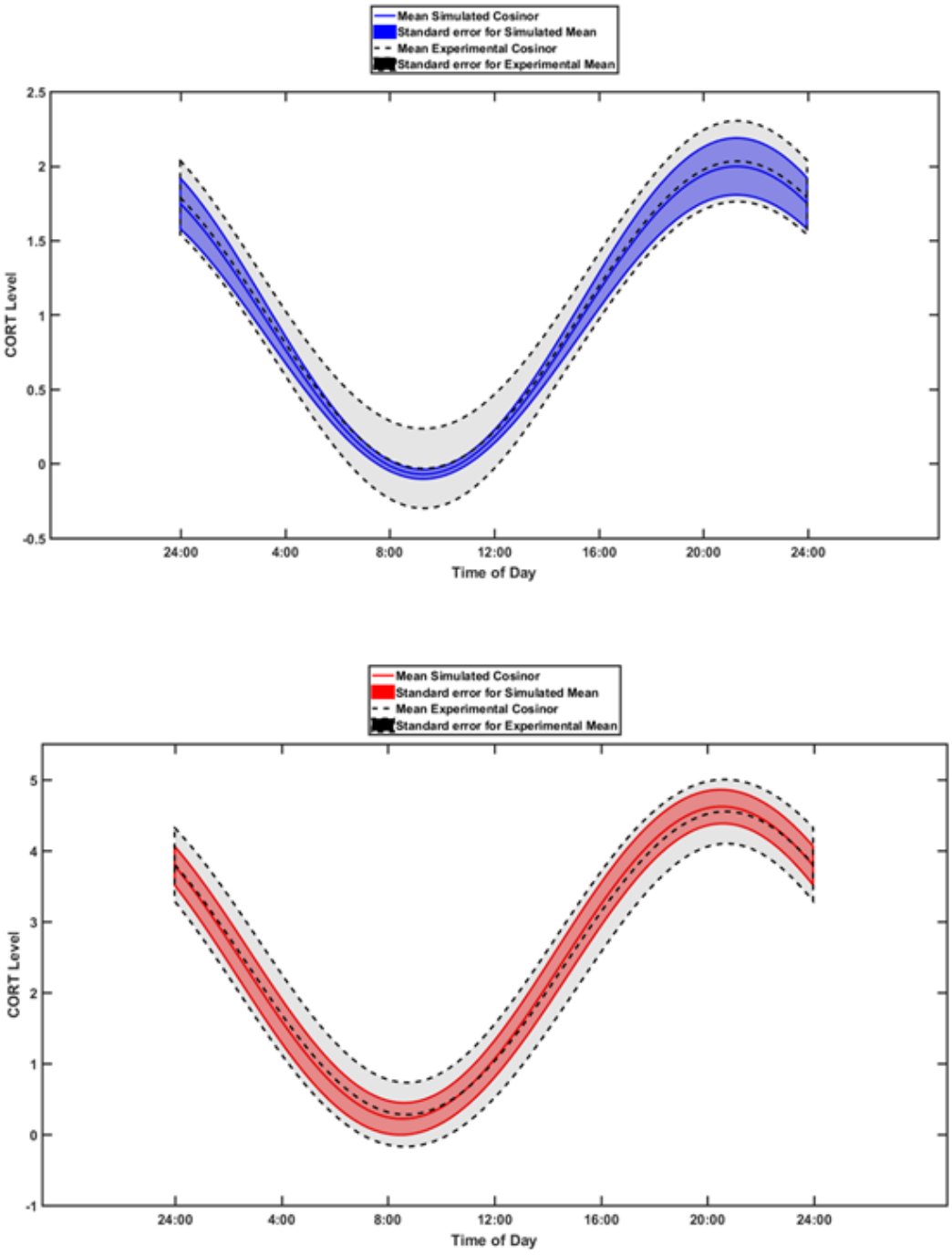


Supplementary Figure S2: Representative circadian CORT profiles generated by the parameter sets within each parameter space generated with $kp_1$=2× i.e. high chronic stress. The blue solid line (top) represents the mean of CORT circadian profiles generated by the male parameters, while the red solid line (bottom) represents the mean of the CORT circadian profiles generated by the female parameters. The blue (top) and red (bottom) shaded areas represent the standard deviation of the male and female simulated CORT circadian profiles, respectively. The black dashed lines

represent the experimental cosinor for male (top) and female (bottom), respectively. The gray shaded areas represent the standard deviation of the male (top) and female (bottom) experimental CORT cosinors, respectively.

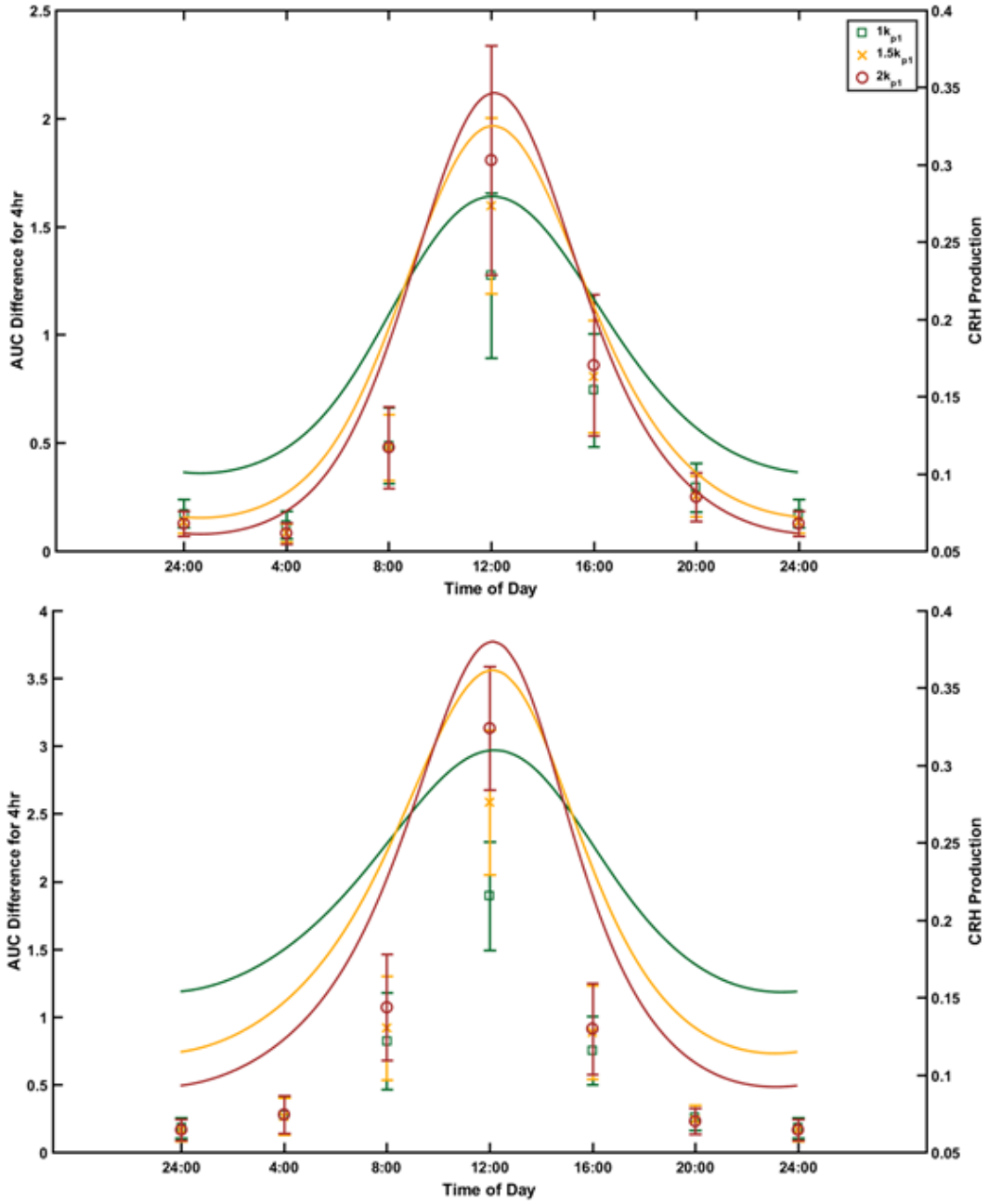


Supplementary Figure S3: Time-of-day dependent acute stress response for the three chronically stressed parameter surfaces, characterized as the difference in AUC between stimulated and nominal profiles within the first 4 hours after stimulation, for both male (top) and female (bottom). The markers (squares, crosses and circles) with the error bars indicate the difference in AUC for 4 hours from

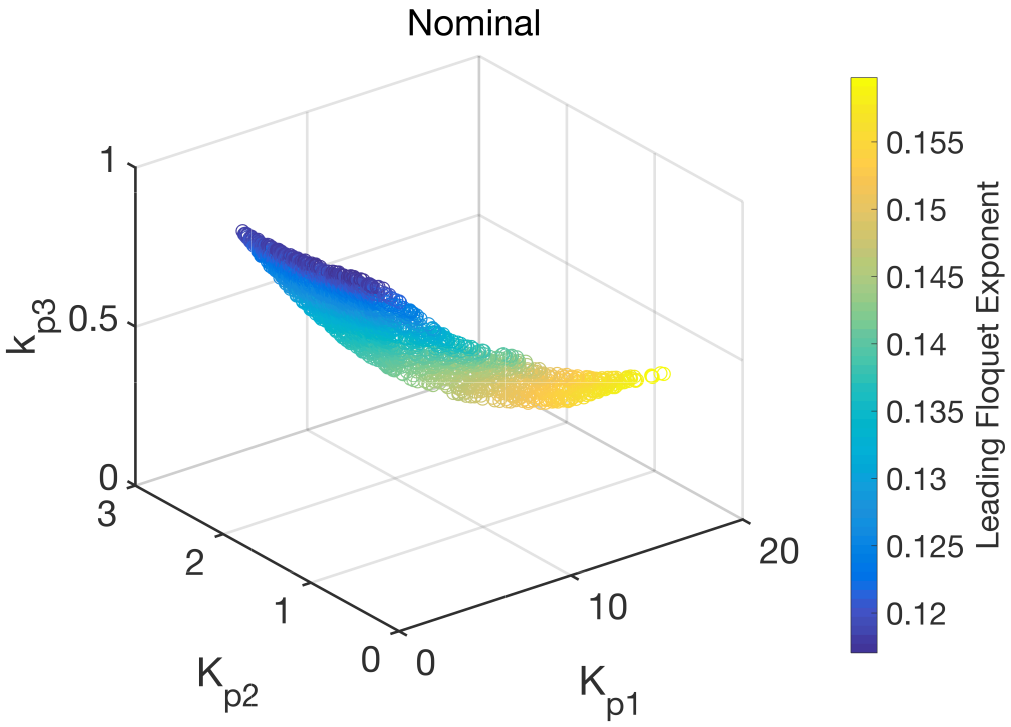


Supplementary Figure S4: The Floquet exponent, indicative of the stability of the system to amplitude perturbation, increases with decreasing adrenal sensitivity, sensitivity for the nominal condition with no chronic stress. This implies that individuals with higher adrenal sensitivity are less stable to amplitude perturbation. The color denotes the Floquet exponent of the unentrained system, with blue denoting the minimum Floquet exponent, while yellow denoting the maximum Floquet exponent.

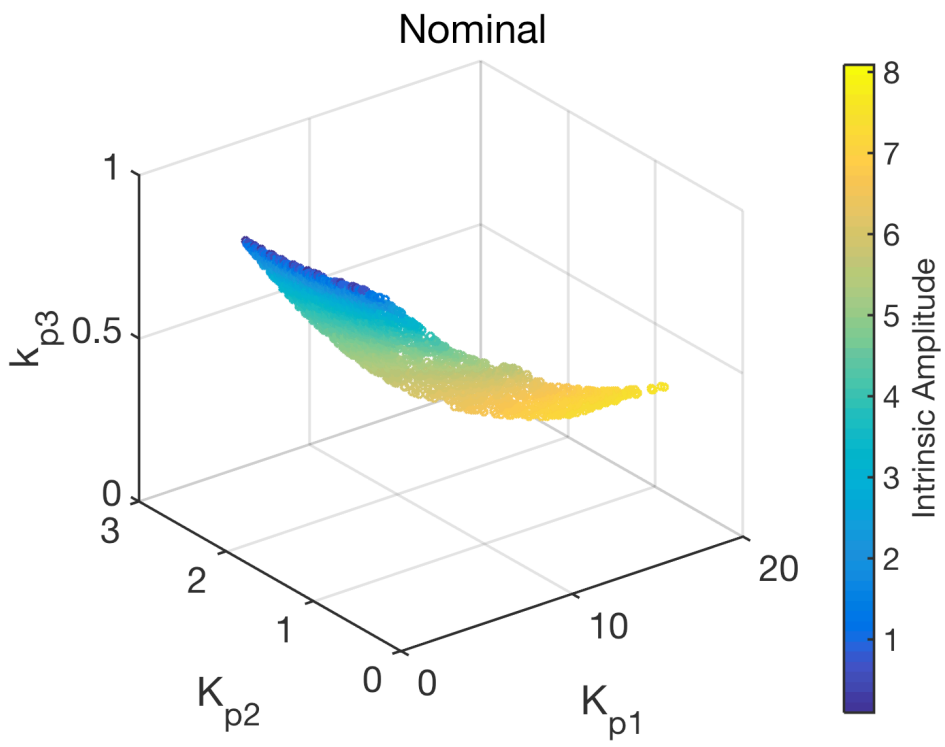


Supplementary Figure S5: The intrinsic amplitude of the unentrained system increases with decreasing levels of adrenal sensitivity sensitivity. The color denotes the intrinsic amplitude of the unentrained system, with blue denoting the minimum amplitude, while yellow denoting the maximum amplitude.

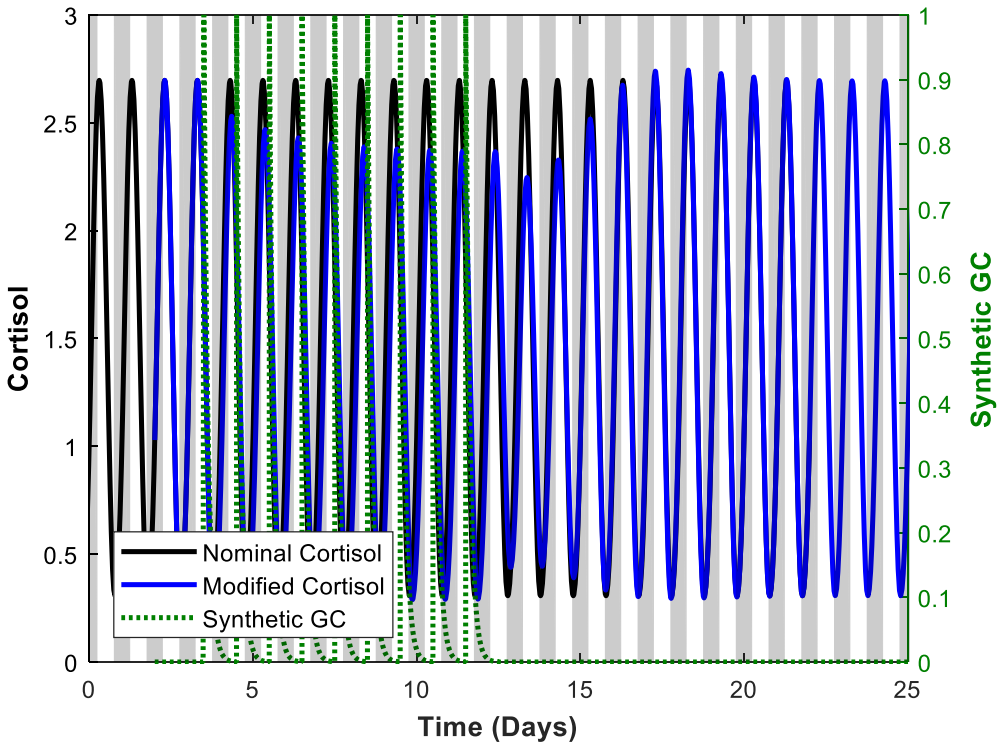


Supplementary Figure S6: Modified cortisol profile after dosing of synthetic glucocorticoids by bolus injection at the nominal amount (1x) returns to baseline when dosing ceases

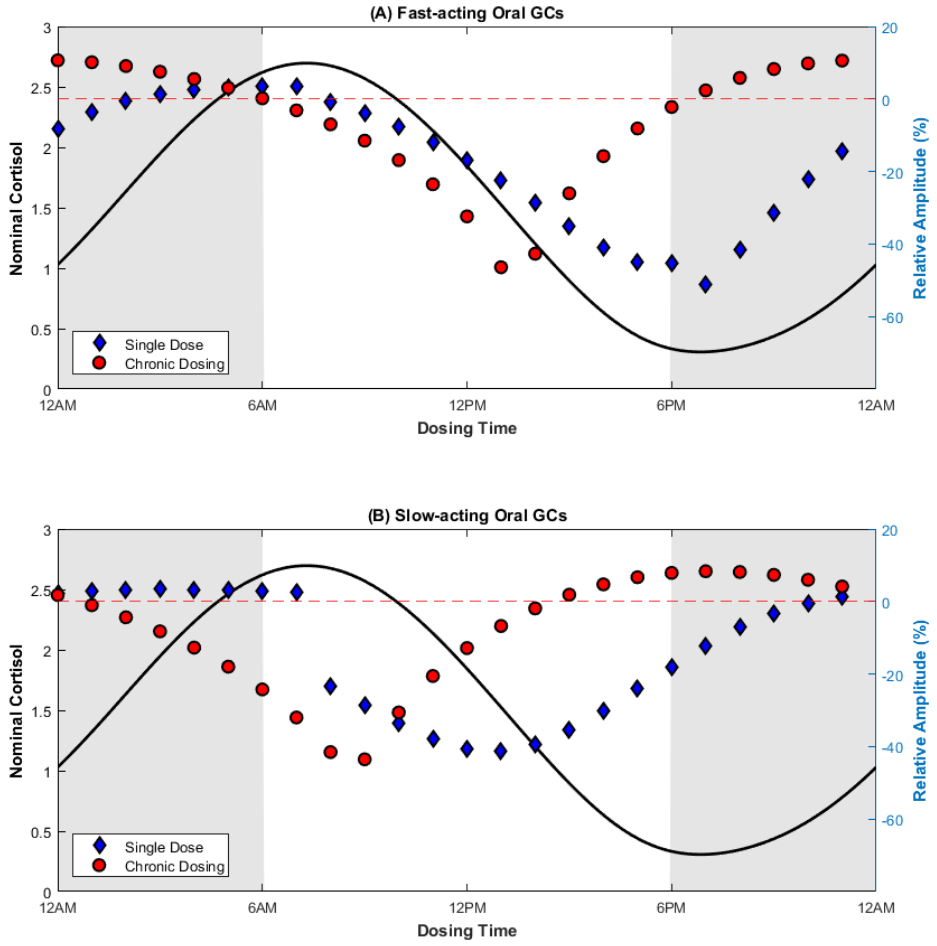


Supplementary Figure S7: Amplitude change associated with chronopharmacological dosing regimens of fast-acting and slow-acting oral glucocorticoids